Doctoral Dissertation
Doctoral Program in Chemical Engineering (32th Cycle)

Biotechnological approaches for green-based bioplastic production

Beatrice Mongili
* * * * * *

Supervisors
Prof. Debora Fino
Eng. Tonia Tommasi

Politecnico di Torino
March 09, 2020

I hereby declare that, the contents and organisation of this dissertation constitute my own original work and does not compromise in any way the rights of third parties, including those relating to the security of personal data.

Beatrice Mongili
Turin, March 09 2020

Summary

Poly-3-hydroxybutyrate (PHB) is a biodegradable and biocompostable plastic produced by a wide variety of microorganisms as carbon reserve and electron sink. PHB presents physical and mechanical properties similar to fossil-based plastic, as polypropylene. Thanks to these features, PHB became a valuable alternative to plastic in several sectors, from packaging to medical applications. Nowadays, its production at industrial scale is slightly diffused, and the research is mainly focused on the optimization of its production process, and on the discovery of new and more sustainable fermentation routes.

In this context, this work dealt with the investigation on three main problems related with PHB fermentation: the application of a waste, such as carbon monoxide, as feedstock for the fermentation; the optimization of PHB production by a variation of fermentation parameters; the implementation of a greener and more cost-effective extraction protocols for the biopolymer. To achieve these goals, specific bacterial strains were selected and studied in this investigation.

Firstly, the fermentation conditions were developed to allow the growth of the wild type strain of *Rhodospirillum rubrum*, studying the influence of carbon monoxide concentration on the bacterial growth in 30 mL of culture. In the absence of light and sole CO as the primary carbon source, this strain needed a preliminary acclimation step, which strongly influenced the growth trend of subsequent fermentation. Because of the low solubility of the gaseous substrate, a pressurized fermentation was set in a dedicated 2L reactor. And, bacterial growth and PHB production at ambient and overpressure conditions (up to 8 atm) were compared. The application of overpressure did not change the biomass growth, but a consistent increase of PHB accumulation inside the cell was registered, passing from 13% in the absence of pressure, to 37% in the pressurized system.

On the other side, the strain *Azotobacter vinelandii* OP, characterized by a high specific growth rate and a higher percentage of PHB accumulation (up to 80%), was exploited for the optimization of PHB productivity based on the variation of the gas transfer rate in a fed-batch configuration. The investigation highlighted a strong correlation between the gas transfer rate, the specific growth rate and the PHB accumulation. Therefore, the optimal agitation conditions, matching the highest volumetric productivity, were defined at a gas mass transfer constant (k_La) of 100 h^{-1}.

Finally, it was investigated a protocol for the extraction of the biopolymer from the cell. Using a genetically modified *Escherichia coli* as bacterial strain, wet and dry not-pre-treated biomass were exposed to a green-based solvent (*i.e.* dimethyl carbonate) to define the PHB extraction yield and the biopolymer purity. From this case-study, a highly pure PHB was extracted with a 70% of extraction yield, proving that this green-based approach could be a real alternative to the standard PHB extraction procedures.

Acknowledgement

This research was supported by CELBICON project in EU framework program Horizon 2020 (grant agreement number: 679050). It received the financial support from Compagnia di San Paolo, by the grant for VALPO4CYRCULAR ECONOMY.
A particular thanks to Umberto Rossi that financed the author's PhD course in Chemical Engineering.

I would like to acknowledge my supervisors Prof. **Debora Fino** and Eng. **Tonia Tommasi** for trusting on my capacities and following me in my experimental progresses. I would like to thank Dr **Auxiliadora Prieto** and her guys of CSIC (Madrid, Spain), for teaching me the delicate equilibrium around PNS bacteria. And, a sincere thank to Prof. **Àlzaro Díaz-Barrera,** Prof. **Carminna Ottone** and all the guys of Escula de Ingeniería Bioquímica of PUCV (Valparaiso, Chile), which hosted me offering all their support in the study of aerobic PHB producing bacteria.

I would like to express all my gratitude to **Manuel**, **Alberto**, and **Claudio**. I enjoyed a lot the work experience shared and our meetings, which helped me to think outside the box.

This work experience not only was a significant part of my carrier, but also it represented a substantial part of my life, which contributed to my personal growth. Thanks to all the people that I have met, to the challenges and new opportunities that I discovered. In particular, the work experience spent within the projects CELBICON and VALPO4CIRCULA ECONOMY were essential on the development of my technical and soft skills.
Thanks to all the professors and technicians with which I worked, in particular thanks to Dr **Simelys Hernandez**, Dr **Sergio Bocchini** and **Marco Del Favero** for the collaboration received during my first European project CELBICON.

A special thanks to all my colleagues working at Politecnico di Torino, because more than colleagues they became friends and anchors in the daily rough sea of

PhD-life. In particular, thanks to **Sorani**, **Viviana**, **Simone A.**, **Simone S.**, **Emanuele**, **Alessandro** for guiding me during the first period of my path, for introducing me in the world of engineering and for the knowledge shared around the design and realization of lab plants.

Thanks to **Annalisa**, your passion, dedication to work and friendship were precious qualities in the development of a workplace entirely dedicated to fermentations.

Thanks to all the people with which I share my workdays. Your unique personalities contributed to the creation of a respectful and lively work environment. Thanks a lot for all the experiences, the assignments, the delusion and successes shared. Thanks to **Silvia**, **Esperanza**, **Loredana**, **Giulio**, **Elahe**, **Giulia**, **Peppe, Roberto, Alex**, **Freddy**, **Hilmar, Alexandru**, **Melodj**, **Giulio**, **Peppe**, **Giulia**, **Alessia**, **Maddalena**, **Francesca, Fabio, Enrico, Miguel**, **Ferenc, Luca, Mohosen** and **Giuseppe**.

A great embrace to **Enrico**, a dear friend and reliable colleague during my academic experiences. To **Francesca**, **Simona** and **Giulia**, that always got in touch despite the distance.

Finally, thanks to my dear **family** that supported me in this enriching path, and to **Giovanni** that always remember me the art of smiling.

Contents

List of Tables

List of Figures

Chapter 1

Poly-3-hydroxybutirrate (PHB): applications, markets & biotech production

1.1. Introduction

Plastic is one of the most used material in the modern lifestyle due to its versatile properties, which quickly spread its production and consumption over the markets, characterizing the related industrial sector by a positive and constant growth (European Bioplastic, 2017). Even if it has been forecast that consumers' requests will increase in the next decades, the use of plastic objects has been denounced by a significant number of environmental agencies, on the base of related pollution problems, especially addressing plastic end-of-life. Indeed, 90% of plastic objects are designed for having a single-use destiny. Only a 10% is recycled, and the remaining part is delivered as hazardous wastes in the environment (Rochman et al., 2013) (Jambeck et al., 2015) (Patel et al., 2001). On the other side, plastic is a valuable material, and, it also conquered markets for its good advantages on distribution and consumption chains. For instance, this plastic material can preserve food from early deterioration or contamination; or thanks to its light weight, it reduces the amount of fuel required during the transport in comparison of other packaging solutions, when it is used as packaging material (Brody et al., 2008)(McArthur et al., 2016).

To overcome these issues and satisfy market requests at the same time, research is boosting the investigation on the production of biodegradable polymers coming from renewable feedstock that host similar material features of conventional plastic (Bátori et al., 2018). All those biopolymers are characterized by a lower carbon and environmental footprint in comparison of fossil-based plastic (Nature Comm. 2018). Among them, the poly-3-hydroxybutyrate (PHB) is an entirely biodegradable and

biocompostable plastic-like material, showing similar characteristics of polypropylene. PHB is naturally produced by several microbial species, which converts excess of carbon and energy units as storing granules ready-to-use for further famine periods (Oliveira et al., 2017). Consequently, it is the right candidate for being a valuable substitute for conventional plastic.

Up to now, some example of the PHB production under pilot and industrial plants have been faced the market. However, some critical drawbacks mainly related to its manufacturing and to processing costs are slowing down a massive diffusion of PHB.

1.2. Poly-3-hydroxybutyrate: chemical features and applications

Poly-3-hydroxybutyrate (PHB) is a biopolymer, belonging to the big class poly-hydroxyalkanoates (PHAs). As anticipated, this class of natural polyester are synthesised by several kinds of microorganisms, which exploit it as a source of carbon and energy stored in forms of molecular chains. Depending on the structure of the monomeric unit, PHAs are divided into short-chain length (*scl*) or medium chain length (*mcl*), two categories that differ for chemical and physical properties, such as glass transition temperature, crystallinity, melting temperature or degree of polymerisation, for instance.

Inside the cell, PHA chains are synthesized as an amorphous polymer organized into helixes of two-fold screw axis stabilized by van der Waals and hydrogen bonds, which form macromolecular complexes called *carbonosomes*. They are water-soluble cytoplasmatic granules, with a little-drops-like shape, in which PHAs are stored covered by a layer of proteins and phospholipids. Even if some authors questioned the presence of the phospholipid around carbonosomes structure (Bresan et al., 2016).

The kind of PHA and its molar mass is strongly dependent on the producing microorganism, on the fermentation or environmental conditions applied, on the substrate fed, and also on the extraction and purification method adopted. In general, the molecular mass of natural PHAs can range from 2 kDa to 2000 kDa on average, with a unit repetition ranging from 600 to 35000. However, some variation is reported for recombinant microorganisms, in which the molecular mass can overcome 20 MDa (Kusaka et al., 1997).

The chemical properties of PHAs depend on the composition and organization of the polymer chains, therefore, on the chain length and on the substitutional groups presented in the structure of the polyester, as shown in Figure 1.1 (Kanna and Srivastava, 2005)

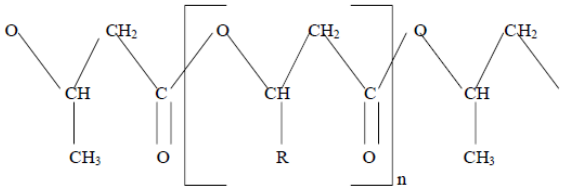

n varies from 600 to 35000

R= hydrogen	Poly(3-hydroxypropionate)
R=methyl	Poly(3-Hydroxybutyrate)
R=ethyl	Poly(3-hydroxyvalerate)
R=propyl	Poly(3-hydroxyhexanoate)
R=pentyl	Poly(3-hydroxyoctanoate)
R=nonyl	Poly(3-hydroxydodecanoate)

Figure 1-1 General structure of PHA and examples of different side-chain substitutions.
(Source: Kanna and Srivastava, 2005)

Mainly, those microorganisms that can synthesize PHAs can produce more than one biopolymer type, giving as a final product a bioplastic material characterized by chemical and mechanical properties embracing the sum of the features of the different monomers produced.

There are two main strategies for the synthesis of the biopolymer. On one side, PHAs can be produced under an excess of C-sources and a limitation of other nutrients, such as a lack of N, P or Mg. While on the other side, PHAs can be accumulated during the entire cellular growth, without the presence of triggering inputs.

As described in Figure 1.1, poly-3-hydroxybutyrate is a PHA characterized by a 3-C carbon backbone hosting a methyl substitution in position 3. It is a stable thermoplastic, with a melting point going from 168 to 182 °C. It is a solid and rigid material, characterized by a density of 1.18 – 1.26 g cm^{-3}, a glass transition temperature around 4°C and an elongation to break presented between 5-8% (Georgios et al., 2016). Due to these features, PHB found a wide range of applications. Widely, it is used in the packaging and agricultural sector, for covering and supporting crops during winter seasons. It finds application in the biomedical industry, as surgical devices, as a mediator in controlled drug release, or it is suitable as a scaffolding tissue during regeneration bioprocesses. As well as, PHB is also applied for daily-use plastic goods. Besides, for improving its range of versatility, PHB can also be modified as part of a blend with conventional plastic or with natural or inorganic fibres, or it can also be chemically modified by synthetic functional groups, returning a material with a new range of properties, as a consequence (Yeo et al., 2018).

1.3. PHB production at industrial, pilot and bench level

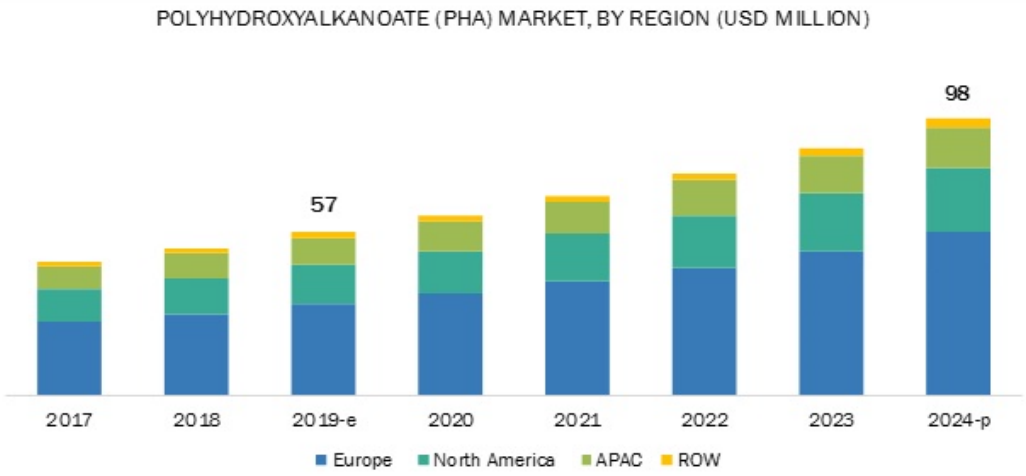

Figure 1-2 Projection of PHAs market growth.
(Source: www.marketsandmarkets.com)

Nowadays, the production of PHB *via* biotechnological routes represents a lively industrial sector, characterized by a compound annual growth rate (CARG) of 11.2%, with market size projection of USD 98 million by 2024 (Figure 1-2). Such a demand is increasing quickly for the satisfaction of the packaging sector, where PHB takes a significant role in food and beverage area, in the form of bags, sheets and disposable cutlery, principally supported by the increasing economic development of the Asia Pacific and Latin America countries (www.marketsandmarkets.com).
As Figure 1-3 reports, the major companies working on PHB production are spread all over the world, in which the production of PHAs or PHB is pushed to 10000 t/a.

Under pilot or industrial scale, the bioplastic production is mainly based on sugar-based fermentations, where single or mixed cultures convert sucrose or fatty acids into this biopolymer. There are also other examples of PHB production that deviate from the traditional fermentation systems. For instance, a pioneer U.S.A. company takes care of PHAs resin synthesis obtained *via* enzyme-based reactions (www.newlight.com). However, the most common route remains the application of bacterial strains, such as the exploitation of *Ralstonia euthropha* (also known under the name of *Cupriavidus necator*) or *Alcaligens* spp. Because of these species can accumulate up to 80% of their cell dry weight as PHAs, guaranteeing high biomass yields at the same time.

In this scenario, due to the urgent environmental needs, the investigation is pushing the development of PHAs fermentation strategies relay on circular economy principles, with the scope of reducing the environmental and money costs of this production line. As a consequence, it is encouraging the development of fermentation lines based on the utilization of wastes. Accordingly to this, laboratory-scale PHB productions are proceeding for developing PHB fermentation based on the recycling of industrial waste, as food waste, up to the application of waste gasses (Passanha et al., 2013)(Drzyzga et al., 2015)(Getachew et al., 2016)(Do et al., 2007).

Name of Company	Product (Trademark)	Substrate	Biocatalyst	Production Capacity
Biomatera, Canada	PHA resins (Biomatera)	Renewable raw materials	Non-pathogenic, non-transgenic bacteria isolated from soil	
Biomer, Germany	PHB pellets (Biomer®)	Sugar (sucrose)		
Bio-On Srl., Italy	PHB, PHBV spheres (minerv®-PHA)	Sugar beets	*Cupriavidus necator*	10,000 t/a
BluePHA, China	Customized PHBVHHx, PHV, P3HP3HB, P3HP4HB, P3HP, P4HB synthesis		Development of microbial strains via synthetic biology	
Danimer Scientific, USA	mcl-PHA (Nodax® PHA)	Cold pressed canola oil		
Kaneka Corporation, Japan	PHB-PHHx (AONILEX®)	Plant oils		3500 t/a
Newlight Technologies LLC, USA	PHA resins (AirCarbon™)	Oxygen from air and carbon from captured methane emissions	Newlight's 9X biocatalyst	
PHB Industrial S.A., Brazil	PHB, PHBV (BIOCYCLE®)	Saccharose	*Alcaligenes* sp.	3000 t/a
PolyFerm, Canada	mcl-PHA (VersaMer™ PHA)	Sugars, vegetable oils	Naturally selected microorganisms	
Shenzhen Ecomann Biotechnology Co. Ltd., China	PHA pellets, resins, microbeads (AmBio®)	Sugar or glucose		5000 t/a
SIRIM Bioplastics Pilot Plant, Malaysia	Various types of PHA	Palm oil mill effluent (POME), crude palm kernel oil		2000 t/a
TianAn Biologic Materials Co. Ltd., China	PHB, PHBV (ENMAT™)	Dextrose deriving from corn of cassava grown in China	*Ralstonia eutropha*	10,000 t/a, 50,000 t/a by 2020
Tianjin GreenBio Material Co., China	P (3, 4HB) films, pellets/foam pellets (Sogreen®)	Sugar		10,000 t/a

PHB, P3HB: poly(3-hydroxybutyrate); PHBV: poly(3-hydroxybutyrate-co-3-hydroxyvalerate); PHBVHHx: poly(3-hydroxybutyrate-co-3-hydroxyvalerate-co-3-hydroxyhexanoate); PHV: poly-3-hydroxyvalerate; P3HP3HB: poly(3-hydroxypropionate-co-3-hydroxybutyrate); P3HP4HB: poly(3-hydroxypropionate-co-4-hydroxybutyrate); P3HP: poly(3-hydroxypropionate); P4HB: poly(4-hydroxybutyrate); mcl-PHA: medium-chain length PHA; P(3,4HB): poly(3-hydroxybutyrate-co-4-hydroxybutyrate).

Figure 1-3 PHAs and PHB pilot and industrial plant.
(Source: Kourmentza et al., 2017).

1.3.1. PHB biosynthesis from gas substrates

Gas-to-liquid fermentations enclose all those processes in which a gas substrate, such as CO, CO_2, H_2, CH_4, is fed to a microbial strain as a nutrient. In this way, the producing strain can exploit it as a source of energy and carbon, for its life cycle, and for the production of a valuable product (as ethanol, butanol, acetic acid, butyric acid, 2,3-butandiol, methane, hydrogen or biopolymers). Sometimes, these gasses could not be enough for cell metabolism; therefore, these gas-based fermentations can be coupled with other sources of nutrients or energy. Hence, an advanced cultivation strategy is the coupling of gas-fermentation with electrochemical cells, or with light irradiation, for instance (Figure 1.4) (Haas et al., 2018).

Primary sources for these C-based gas feedstocks are related to anthropogenic emissions. Therefore, they can be found in steel mills and ferroalloy industries fumes, petrochemical gaseous wastes, or gas emissions coming from municipal solid wastes and pyrolysis plants (Cordero, et al. 2019) (Do et al., 2007).

As can be imagined, the application of these waste gasses includes considerable physical and engineering issues. For instance, the connections between industrial chimneys and fermentation tanks require an additional step of gas cleaning, necessary for the removal of pollutant compounds (as sulphur oxides), that could negatively affect microbial performances. Besides these technical issues, another significant

problem is represented by gas-mass transfer, preventing the feeding of the gaseous nutrient to the cell. In this case, it could be overcome by the application of high-pressure ranges or high-dense cultures. Such strategies are combined with specific bioreactor geometries in some particular cases (Amos, 2004).
However, even if these limitations represent a real barrier for a fast development of gas-based conversion technology, proof of concept tests and pilot plants are already available. At the beginning of 2018, LanzaTech announced the launch of the first commercial facility working on the conversion of industrial emission, containing a high amount of H_2 and CO, in ethanol *via* a gas-fermentation process (Zhu 2019).

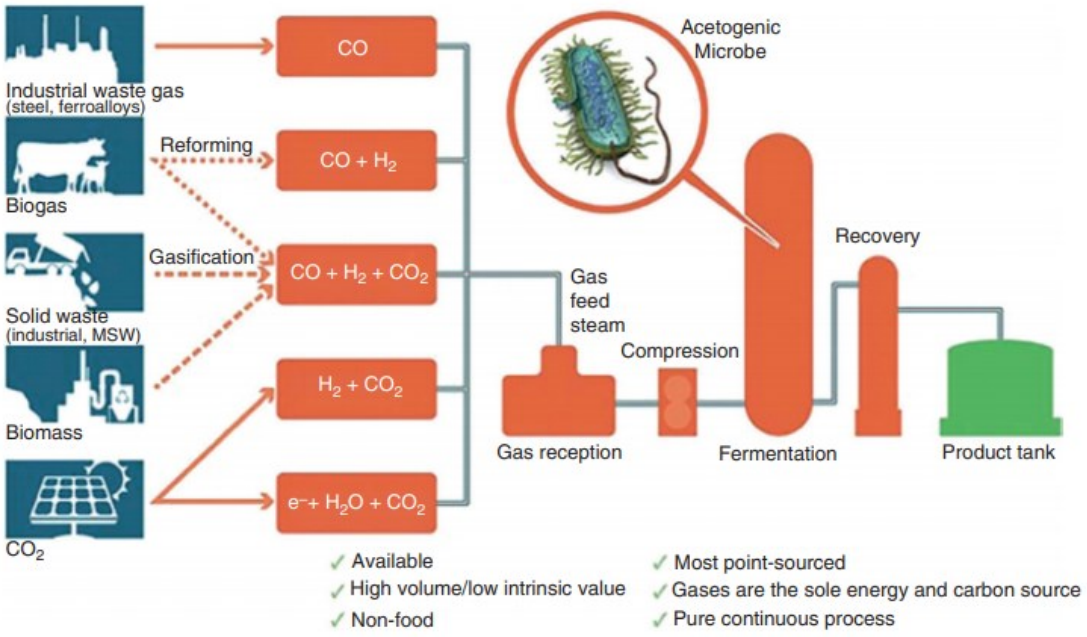

Figure 1-4 The philosophy of gas-based fermentations as interpreted by LanzaTech.
(Source: Zhu 2019).

In the case of bioplastic production, it was demonstrated that PHAs biosynthesis could occur from the conversion of pure carbon-based gasses or syngas, which give a contribution as sources of electrons and carbon units to the cellular metabolic cycles. Generally, the species taking advantages from waste gasses for PHA production are chemolithotrophic or photosynthetic, reducing CO_2 *via* Calvin-Benson-Bahassam cycle or equivalent reducing metabolic routes. As purple non-sulphur *Rhodospirillacae* spp., that consume syngas for sustaining PHB production (Tabita, 1995) (Ragsdale, 2004). Or, the model organism *Cupriavidus necator*, a H_2-oxidizing specie, that in the presence of a mixture of CO_2, H_2 and O_2 can autotrophically produce a high amount of PHB (Garcia-Gonzales et al., 2018) (Pohlmann et al., 2006). Besides them, there are also photosynthetic microorganisms as some cyanobacteria like *Synechocystis* and *Synechococcus* spp. that synthesise PHAs from CO_2 (Troschl et al., 2017). Cyanobacteria offer the advantage to be cultured in pour media as wastewaters. However, the molecular weight of produced PHAs is generally low in this kind microorganisms, maybe due to little cell biomass (0.5 – 2 μm) (Troschl et al., 2018) (Balaji et al., 2013). For this reason, cyanobacteria are usually adopted for further

genetic modification or in co-culture with other microbial species (Troschl et al., 2017).

1.3.2. Common metabolic routes for PHB production

Independently from the microbial species and the gas exploited, the synthesis of PHB proceed by a single and common biosynthetic pathway composed in three main steps by a β-ketothiolase (PhaA), NADPH-linked acetoacetyl-CoA reductase (PhaB) and a PHB synthase (PhaC), as shows in Figure 1-5 (Verlinden et al., 2007). The first step of the PHB biosynthesis is mediated by PhaA that condensates two molecules of acetyl-CoA in Aceto-Acetyl-CoA. Successively, the reductase PhaB catalyses an NADPH-dependent reduction for the synthesis of 3-hydroxybutyrril-CoA. This molecule is the monomer unit of the biopolymer, that will be enlarged by a successive condensation reaction made by the PhaC. Among them, PhaB is the limiting factor in this metabolic branch, because it depends on the availability of reducing power molecules (NADPH) (Jin et al., 2014).

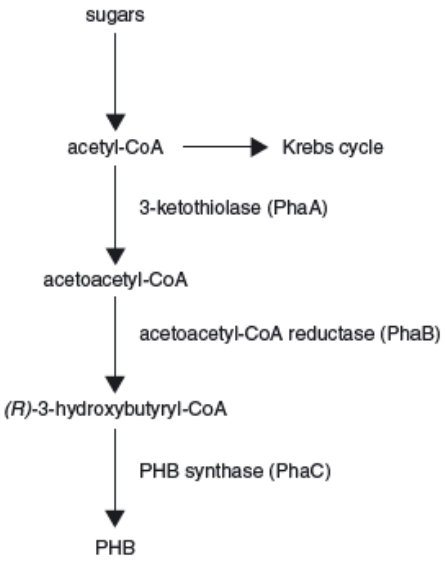

Figure 1-5 Metabolic pathway in PHB production.
(Source: Verlinden et al., 2007)

1.3.3 Model organisms studied for PHB production

Rhodospirillum rubrum

Rhodospirillum rubrum is a gram-negative, facultative aerobe bacterium belonging to the family Rhodospirillaceae. Phenotypically, this specie has a rod spiral-shape (0.5 -1 μm). Under light cultivation, it appears purple coloured, a feature that characterizes its colonies in ponds and little lakes, where it naturally lives. *R. rubrum*

is a phototactic bacterium, presenting a motile polar flagellum stimulated by light exposure (Harayama et al., 1984). It has a photosynthetic membrane organised in vesicles, lamellae and stacks, which host a large type of cytochrome c_2 and pigments, as bacteriochlorophylls and other carotenoids causing its characteristic bright purple colour and allowing the further exploitation of electron units (Imhoff et al., 1984),(Munk et al., 2001) (Figure 1-6).

Figure 1-6 *Rhodospirillum rubrum* after a Gram staining.
The image was captured in our labs.

One of the main features of this specie is that it has a very versatile metabolism (Koku et al., 2002). It can grow using sugar in anaerobiosis, or it can perform aerobic respiration, using oxygen as the final electron acceptor, or it can fixes carbon dioxide by CBB cycle in photo-auto or heterotrophic conditions, and it can grow in autotrophy under darkness, taking energy from carbon monoxide. Whenever, the selected metabolic routes depend on the energy available, on the oxidation state of carbon sources, and on the way used for dissipating the electron flow in excess, such as H_2, sulphide or organic compounds as PHAs.

For its ability to grow under CO, *R. rubrum* early became a model organism for the study of gas conversion systems during the '70s (Slater and Morris, 1973). In recent years it acquired more attention in bioremediation (for its ability to absorb heavy metals absorption such as Nickel and Cobalt), and in the production of poly-hydroxybutyrate *via* the conversion of syngas. Even it was also studied for the synthesis of Q_{10} coenzyme (Xu et al., 2015) (Tian et al., 2010) (Najafpour et al., 2003).

CO conversion and PHB biosynthesis

R. rubrum presents two main routes for assimilating gaseous carbon sources, as CO_2 and CO. The first way is represented by CBB cycle, where CO_2 is added on 3-phosphoglycerate. While, the second is composed by the conversion of carbon monoxide into carbon dioxide, which is successively reduced or add to another molecular specie (Godoy et al., 2017) (Revelles et al., 2016) (Hadicke et al., 2011). The reaction that converts the carbon monoxide into CO_2 is energetically favourited, having a $\Delta G°$ of – 20 kJ mol^{-1}(Dadak et al., 2016) (Bonam et al., 1984). It is catalysed by a carbon monoxide dehydrogenases (CODH), acting the reversible reaction known

as *water-gas shift reaction*, in which a couple of electrons and a couple of H^+ are released, thanks to the presence of Ni-Fe-S clusters in its catalytic pocket (Drennan et al., 2001):

$$CO + H_2O \rightarrow CO_2 + 2H^+ + 2e^- \quad \text{Eq. 1}$$

Even if the entire mechanism of CO conversion is not entirely understood, the leading theory claims the presence of a chemiosmotic gradient (a transmembrane proton gradient derived from the water-gas-shift reaction) across the cell membrane, which guides ADP phosphorylation reactions by a membrane ATP synthase channel (Maness et al., 2005). Therefore, a big membrane-bound protein complex composed by CODH, an accessory electron transport protein equipped with a Fe-S centre, a membrane CO-induced hydrogenase and an ATP-synthase should co-orchestrate an electron transport chain promoting both: *i)* proton pumping and *ii)* proton reduction coupled with ATP synthesis activity (Ensign et al., 1991) (Maness et al., 2002) (Fox et al., 1996). Within this mechanism, the cell should be able to dissipate the excess of electrons content and to provide ATP during dark fermentation.

Under a gas-based fermentation, the presence of carbon monoxide strictly regulates the genes expression linked to CO metabolism by a transcriptional factor called CooA. CooA acts as CO-sensor, improving the expression levels of CODH, CO-induced hydrogenases and other proteins involved in carboxylation reactions because it is activated by carbon monoxide (Wawrousek et al., 2014)(Shelver et al., 1997)(Revelles et al., 2016). Moreover, even if CO is the preferred substrate in the absence of other carbon and energy sources, it is not clear if it could negatively affect *R. rubrum* growth as an inhibitor (Kerby et al., 1995)(Klasson et al., 1993). Despite this, it is generally recognized that this microorganism needs an acclimation time on CO, before achieving a CO-limited growth.

PHB biosynthesis in *Rhodospirillum rubrum*

The production of PHA in *R. rubrum* is dependent on fermentation conditions in which the bacterium is exposed. Therefore, high concentration of carbon units, availability of reducing equivalents and stressing growth environment stimulate and could improve the production of this biopolymer, which is composed of 99% of polyhydroxybutyrate (PHB) and 1-2% of poly-3-hydroxyvalerate (PHV). This proportion is widely conserved during the biopolymer synthesis. However, it is also reported that an improvement of PHV ratio can increase the tensile and the impact strength of the polymer (Heinrich et al., 2015).

The PHB biosynthetic pathway is constituted by the three main enzymes PhaA, Phab and PhaC, among which PhaB determines the reaction bottleneck. However, in *R. rubrum*, its activity depends on the cellular NADPH supply, that is in general provided by a transmembrane pyridine transhydrogenase, operating under anaerobic condition and by the turnover of Kreb's cycle (Grammel et al., 2003). Indeed, it was proved that

even if high amounts of NADPH are guaranteed, the PHB production does not improve, because of the precursor of PHB, acetyl-CoA, is addressed to the for the energetic balance of the cell (Heinrich et al., 2015).

Azotobacter vinelandii OP

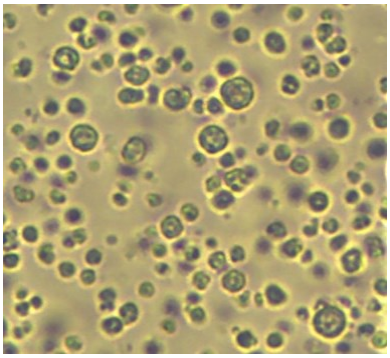

Figure 1-7 An image of *A. vinelandii* OP.
The image was captured in laboratories of Escuela de Engenieria Bioquimica, PUCV, Valparaiso, Chile.

Azotobacter vinelandii is a strictly aerobic Gram-negative nitrogen-fixing specie, which naturally synthesizes two industrial relevant biopolymers: alginate and poly-hydroxybutyrate (Noar et al., 2018). It is a soil bacterium, basically studied as a model organism for the study of nitrogen fixation process and hydrogen production. Interestingly, when it is grown under metal cofactor limitation, such as Fe, it uses to release chelating pigments called siderophores, having the role of catching even little metals concentrations in the surrounding area (MacRose et al., 2017).

As Figure 1-7 presents, it has a rod shape cell ranging from 2 to 5 µm. However, its dimensions vary with cultivation conditions (Peña et al., 2002) (Post et al, 1982)

Interestingly, *A. vineladii* can take advantages on a wide variety of carbon substrate, such sugars, alcohols, fatty acid and organic compounds that render the application of this bacterium a good candidate for the development of biotechnological processes (Page et al., 1992).

Several studies were conducted for understanding the metabolisms of this specie. Mainly, it is remarkable the cellular regulation among carbon, nitrogen and oxygen concentration. As described in the works of Oezle and Inomura, in *A. vinelandii* the carbon consumption is linked to the amount of oxygen available, which, in turns, is consumed on the base of the C/N ratio. Furthermore, under nitrogen-limiting condition, the cell produces NH_4^+ *per se*, by the nitrogenase complex, and the oxygen consumption assumes a constant profile (Oelze et al., 2000) (Inomura et al., 2017).

Because of the capacity to produce at the same time alginate and PHB, in this study, a natural mutant strain in which only the PHB pathway is activated will be used. It is *A. vinelandii* OP (or UW) that naturally lost the activity of the *algU* gene, responsible for the alginate synthesis and cyst formation. Hence, the excess of carbon units is addressed on PHB accumulation (Martinez-Salazar et al., 1996)

PHB production in *Azotobacter vinelandii*

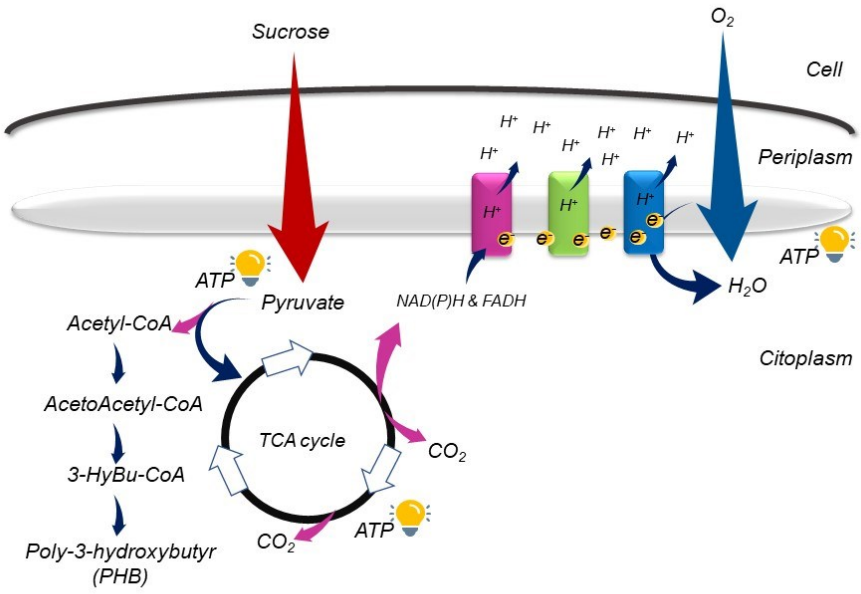

Figure 1-8 Simplified PHB biosynthetic path of *A. vinelandii*.

Essentially, in *A. vinelandii* the PHB accumulation is favourited by unbalanced growth conditions occurring by an excess of carbon sources under an oxygen-limited environment. In these conditions, the increase of the reducing power (NADH/NADPH), favourited by a decrease of cellular respiration, and the growth of acetyl-CoA units block the Kreb's cycle, shifting these compounds into the PHB production route (Figure 1.8) (Page at al., 1992)(Senior et al., 1972)(Haaker and Veeger, 1976). In *Azotobacter* family, *A. vinelandii* OP can store up to 80% w/w of the cellular dried weight as PHB, also when the oxygen-limiting condition is not strictly satisfied (Jackson and Dawes al., 1976) (Diaz-Barrera et al., 2016)(Garcìa et al., 2014)(Pena et al. 2014).

Moreover, it was demonstrated that the PHB production is strictly regulated by the aeration conditions or by feeding strategies. For instance, it was shown that under oxygen-limited condition, the PHB productivity of *A. vinelandii* OP is dependent on oxygen transfer rate (OTR), consequently influenced by airflow and by agitation speed adopted (Diaz-Barrera et al., 2016). Indeed, in a batch fermentation system and 1 vvm of aeration, the productivity peaked the value of 0.18 g L^{-1} h^{-1} under 600 rpm of agitation speed in 2 L reactor, in comparison to a decrease of PHB accumulation caused by lower agitation rates. The application of feeding pulses strategy can positively guarantee an increase in biomass production and therefore, of the final PHB accumulated (Castillo et al., 2017). As claimed for the parental mutant *A. vinelandii* OPNA, in which the combination of feeding pulse of sucrose and yeast extract pushed

a 7-fold increment in PHB productivity. On the other side, repetitive pulsing feeding or high concentration of protein-rich nutrients could also activate growth inhibition events caused by amino acids accumulation (Castillo et al., 2016) (Castillo et al. 2014).

1.4. An overview of bioplastic extraction

The PHB purification process consists in the recovery of the bio-polyester hosted inside the cell, and in its purification from non-polymer cell mass fractions (NPCM). It is one of the most expensive steps in the entire bioplastic production chain, representing around 50% of the final biopolymer price (Jacquel et al., 2018).
Literature has a vast collection of PHA-extraction reviews describing techniques in use, both at bench and pilot-scale (Madkour et al., 2013) (Kourmentza et al., 2017) (Koller et al, 2013). Because of a profound description of the extraction process is far from the primary goals of this thesis, a brief report of the PHA-extraction process is here exposed.
The PHA purification involves five main passages, as represented in Figure 1-9 (Kourmentza et al., 2017):

a) *Biomass harvesting*, it is the first step in which biomass is collected from the fermentation broth. Generally, this step is made by centrifugation or a membrane filtration phase.
b) *Biomass pre-treatment*, it is the step used for disrupting or damaging the membrane cell wall, made in order to improve the extraction yield of the biopolymer. This step is usually designed on the base of the microorganism. For instance, Gram-positive bacteria are characterized by a thicker and more resistant cell membrane than Gram-negative ones. Hence, a heavier protocol is usually adopted in the case of Gram-positive microorganism. There are several ways used for destabilizing the cell membrane and generally, these techniques are classified into physical (e.g., sonication, homogenisation, osmotic stresses), chemical (e.g., surfactant degradation, hypochlorite digestion, acid or basic digestion), or biological disruption methods (e.g., enzymatic degradation). Among them, the most used methods are thermal treatments or lyophilization at lab scale. This step gives ends with two main fractions: the PHAs, which should be successively recovered, and the residual NPCM;
c) *PHA extraction* phase. It is usually represented by a solvent-extraction method, where the biopolymer passes from a solid-state into the liquid-phase of the solvent. On the other side, when the polymer remains in its solid phase, the extraction is characterized by the dissolution of the cell membrane (mediated by an oxidizing agent as NaClO for instance) and the successive recover of the polymer *via* supercritical fluid extraction or by floatation;
d) *PHA concentration*. It is the phase where the dissolved PHA into the solvent is concentrated principally by polymer precipitation, using a poor-PHA solution or by solvent evaporation;

e) *PHA drying*. It is the step in which PHA is dried and collet for the market. Basically, after the polymer concentration, PHAs need a sequence of washing cycles. They serve to remove bacterial residues and to ensure a complete cleaning from NPMC, that usually present pyrogenic activity, and limit a further application of PHAs on the medical sector, for instance.

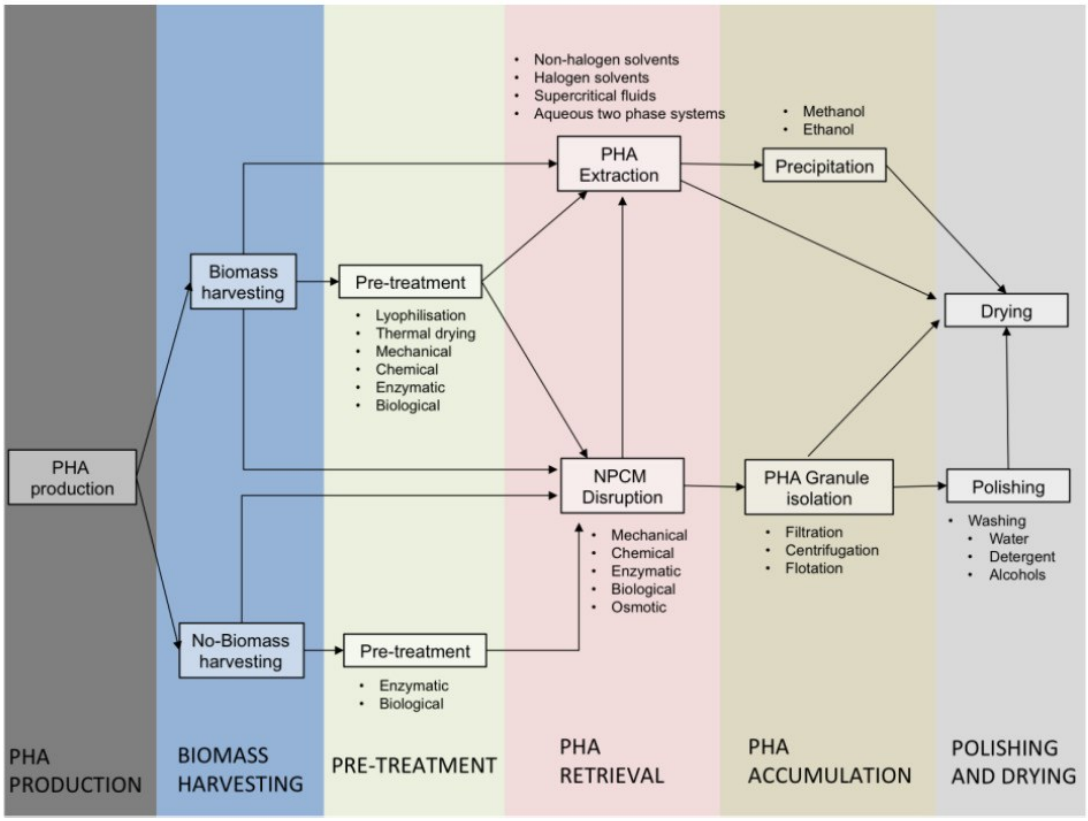

Figure 1-9 Overview of PHB extraction process.
In the Figure, NPCM stands for "non-PHA cell mass" (Kourmentza et al., 2017).

As the scheme presents, there is not a unique extraction method, and new procedures or combinations of different extraction processes are facing the markets. As the application of poor-solvents (solvents able to dissolve less than 1%) that guarantee lower environmental impact; or the use of a mixture of poor and good-PHA solvents under controlled pressure and temperature conditions (Kurdikar et al., 1998). Or, the use of a consequential thermal and enzymatic cell-membrane disruption, which allows the recovery flocculated PHA after by a spray-drying technique (Koning et al., 1997). In addition, there are even methods based on the release of the PHA by the application of a natural bacteria predator, as the small *Bdellovibrio bacteriovorus*, which as a parasite can lysate the cell membrane and releasing the PHA as a consequence (Martinez et al., 2016).

1.4.1. Solvent-based extraction

The solvent extraction is the most spread method for the polyester harvesting step. In this procedure, the PHA is dissolved into an organic phase, from which it is recovered by anti-solvent precipitation or by solvent evaporation (Figure 1-10).

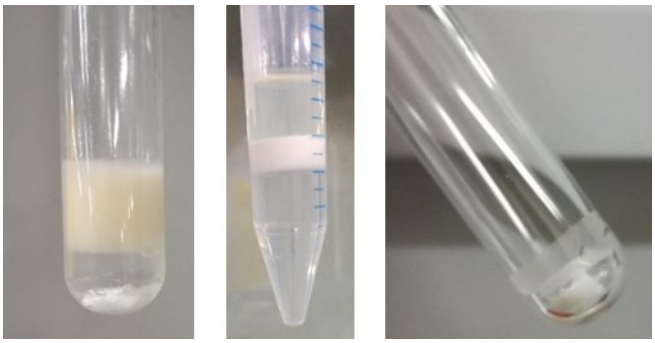

Figure 1-10 PHB recovery by solvent extraction, as performed in our laboratories.
On the left: the glass tube with the biomass (yellow), the chloroform (transparent solution at the bottom) and a magnetic white bar set during the extraction phase. In the middle: the tree phases coming successive centrifugation that separate: the organic phase at the bottom with the dissolved PHB, on the top the aqueous phase and the remaining NPCM in the middle. On the right: the PHB, after the recovering of the organic phase and its evaporation.

Best organic solvents for extracting the PHA are halogenated solvent as chloroform, dichloroethane, polychlorinated ethane, among which chloroform ($CHCl_3$) is the golden standard for small chain PHA, as the poly-3-hydroxybutirate (Koller et al., 2013) (Ramsay et al., 1994). On the contrary, for the PHB recovery, its solubility is quickly minimized by the addition of an anti-solvent (e.g., ethanol, hexane, water, acetone) (Figure 1-10). However, high toxicity, and a high amount of solvents for allowing a fruitful PHA recovery, are the main disadvantages of this technique.

Due to these drawbacks, alternatives solvent extraction methods have been proposed (Divyashree et al., 2008). Usually, the selection of a solvent is based on the standard approach "*like dissolve like*". On a theoretic point of view, the affinity between new solvent and PHA can be selected by solubility parameters as described in the work of Tereda, in which 98 of most used compounds were classified defining a three-dimensional solubility sphere for amorphous poly-hydroxy alkenoates (Tereda et al., 1999). On the other side, other parameters should be considered as the toxicity, the solvent end-of-life and the cost.

Considering these parameters, a promising alternative to chlorinated solvents is represented by the class of cyclic or linear carbonic esters as ethylene carbonate, 1,2-propylene carbonate or the dimethyl carbonate. Interestingly, this class of solvent has low toxicity, low environmental impact and it is associated with high purity and recovery PHA values (Madkour et al., 2013) (Righi et al., 2016).

Pre-treatment	Solvent	Temperature	Antisolvent	Recovery /Purity	Reference
Lyophilisation	Dimethylcarbonate	90 °C x 4h	Evaporation or EtOH precipitation	92% / >95%	(Samorì et al., 2015)
NaOH and heat	11,2 propylen carbonate	130 °C x 30 min	Acetone	95% / 84%	(Fiorese et al, 2009)
Isopropanol/Hexan wash or Sonication	Acetone : EtOH : propylencarbonate	130 °C x 1 h	Hexane	85% / 92%	(Fei et al., 2016)

Table 1-1Comparison of recovery and purity values referred to the application of carbonates-based solvent for PHB extraction, as presented by the literature.

1.5. Aim of the work

This investigation was focused on the study and optimization of the poly-3-hydroxybutyrate microbial production process, facing three main issues related to the biotechnological PHB production and extraction.

Firstly, this study addressed the issues related to the conversion of waste gasses, like carbon monoxide as the principal source of energy and carbon for the production of PHB. Secondly, the work faced the problem of the process scalability on the base of gas-transfer rate issues. And lastly, it took care of the PHB purification step, addressing the PHB extraction efficiency *via* the application of a gree-based solvent.

In particular, the consequences related to the concentration of carbon monoxide were investigated on *R. rubrum* under anaerobic conditions, and the limited-CO growth was studied (Chapter 2). Hence, a pressurized reactor dedicate to gas-fermentation was designed, and the effects of the gas availability on the biomass and PHB accumulation due to a pressure increase were defined (Chapter 3). Due to the low productivity of gas-based fermentation process, the investigation of a PHB productivity optimization was developed in an aerobic strain. Therefore, a method for scale a PHB fermentation up, working on the variation of gas-transfer rate was designed in A. *vinelandii* OP (Chapter 4). This optimization work was reached thanks to a fruitful collaboration with Professor Àlvaro Díaz-Barrera and its group, that hosted me at the *Escuela de Ingeniería Bioquímica* of PUCV, in the city of Valparaiso (Chile).

Finally, the PHB extraction was examined by a dedicated case-study, challenging the purification of PHB with the application of a more cost-effective and environmentally friendly method (Chapter 5).

1.6 References

Amos, W. A. (2004). Biological Water-gas Shift Conversion of Carbon Monoxide to Hydrogen: Milestone Completion Report (No. NREL/MP-560-35592). *National Renewable Energy Lab*., Golden, CO.(US).

Balaji, S., Gopi, K., & Muthuvelan, B. (2013). A review on production of poly β hydroxybutyrates from cyanobacteria for the production of bio plastics. *Algal Research*, 2(3), 278-285.

Bátori, V., Åkesson, D., Zamani, A., Taherzadeh, M. J., & Horváth, I. S. (2018). Anaerobic degradation of bioplastics: A review. *Waste management*, 80, 406-413.

Bonam, D., Murrell, S. A., & Ludden, P. W. (1984). Carbon monoxide dehydrogenase from *Rhodospirillum rubrum*. *Journal of bacteriology*, 159(2), 693-699.

Bresan, S., Sznajder, A., Hauf, W., Forchhammer, K., Pfeiffer, D., & Jendrossek, D. (2016). Polyhydroxyalkanoate (PHA) granules have no phospholipids. *Scientific reports*, 6, 26612.

Brody, A. L., Bugusu, B., Han, J. H., Sand, C. K., & McHugh, T. H. (2008). Innovative food packaging solutions. *Journal of food science*, 73(8), 107-116.

C. Munk, A. Copeland, S. Lucas, A. Lapidus, T. G. Del Rio, K. Barry, J. C. Detter1, N. Hammon, S. Israni, S. Pitluck, T. Brettin, D. Bruce, C. Han, R. Tapia, P. Gilna, J. Schmutz, F. Larimer, M. Land , N. C. Kyrpides, K. Mavromatis, P. Richardson, M. Rohde, M. Göker, H.-P. Klenk, Y. Zhang, G. P. Roberts, S. Reslewic and D. C. Schwartz, "Complete genome sequence of *Rhodospirillum rubrum* type strain (S1T)". *Standards in Genomic Sciences*, vol. 4, pp. 293-302, 2011.

Castillo, T., Flores, C., Segura, D., Espín, G., Sanguino, J., Cabrera, E., ... & Peña, C. (2017). Production of polyhydroxybutyrate (PHB) of high and ultra-high molecular weight by *Azotobacter vinelandii* in batch and fed-batch cultures. *Journal of Chemical Technology & Biotechnology*, 92(7), 1809-1816.

Cordero, P. R., Bayly, K., Leung, P. M., Huang, C., Islam, Z. F., Schittenhelm, R. B., ... & Greening, C. (2019). Atmospheric carbon monoxide oxidation is a widespread mechanism supporting microbial survival. *The ISME journal*, 1-14.

Dadak, A., Aghbashlo, M., Tabatabaei, M., Najafpour, G., & Younesi, H. (2016). Sustainability assessment of photobiological hydrogen production using anaerobic bacteria (Rhodospirillum rubrum) via exergy concept: Effect of substrate concentrations. *Environmental Progress & Sustainable Energy*, 35(4), 1166-1176.

De Koning, G. J. M., & Witholt, B. (1997). A process for the recovery of poly (hydroxyalkanoates) from Pseudomonads Part 1: solubilization. *Bioprocess Engineering*, 17(1), 7-13.

Díaz-Barrera, A., Andler, R., Martínez, I., & Peña, C. (2016). Poly-3-hydroxybutyrate production by *Azotobacter vinelandii* strains in batch cultures at different oxygen transfer rates. *Journal of Chemical Technology & Biotechnology,* 91(4), 1063-1071.

Divyashree, M. S., Shamala, T. R., & Rastogi, N. K. (2009). Isolation of polyhydroxyalkanoate from hydrolyzed cells of *Bacillus flexus* using aqueous two-phase system containing polyethylene glycol and phosphate. *Biotechnology and Bioprocess Engineering*, 14(4), 482-489.

Do, Y. S., Smeenk, J., Broer, K. M., Kisting, C. J., Brown, R., Heindel, T. J., ... & DiSpirito, A. A. (2007). Growth of *Rhodospirillum rubrum* on synthesis gas: Conversion of CO to H2 and poly-β-hydroxyalkanoate. *Biotechnology and Bioengineering*, 97(2), 279-286.

Drennan, C. L., Heo, J., Sintchak, M. D., Schreiter, E., & Ludden, P. W. (2001). Life on carbon monoxide: X-ray structure of *Rhodospirillum rubrum* Ni-Fe-S carbon monoxide dehydrogenase. *Proceedings of the National Academy of Sciences*, 98(21), 11973-11978.

Drzyzga, O., Revelles, O., Durante-Rodríguez, G., Díaz, E., García, J. L., & Prieto, A. (2015). New challenges for syngas fermentation: towards production of biopolymers. *Journal of Chemical Technology & Biotechnology*, 90(10), 1735-1751.

Ensign, S. A., & Ludden, P. W. (1991). Characterization of the CO oxidation/H_2 evolution system of *Rhodospirillum rubrum*. Role of a 22-kDa iron-sulfur protein in mediating electron transfer between carbon monoxide dehydrogenase and hydrogenase. *Journal of*

Biological Chemistry, 266(27), 18395-18403.

European Bioplastics, "Bioplastic Market Data 2017". *Eur. Bioplastics*, pp. 1–7, 2017.

Fox, J. D., Kerby, R. L., Roberts, G. P., & Ludden, P. W. (1996). Characterization of the CO-induced, CO-tolerant hydrogenase from *Rhodospirillum rubrum* and the gene encoding the large subunit of the enzyme. *Journal of Bacteriology*, 178(6), 1515-1524.

García, A., Segura, D., Espín, G., Galindo, E., Castillo, T., & Peña, C. (2014). High production of poly-β-hydroxybutyrate (PHB) by an *Azotobacter vinelandii* mutant altered in PHB regulation using a fed-batch fermentation process. *Biochemical engineering journal*, 82, 117-123.

Garcia-Gonzalez, L., & De Wever, H. (2018). Acetic Acid as an Indirect Sink of CO2 for the Synthesis of Polyhydroxyalkanoates (PHA): Comparison with PHA Production Processes Directly Using CO_2 as Feedstock. *Applied Sciences*, 8(9), 1416.

Georgios, K., Silva, A., & Furtado, S. (2016). Applications of green composite materials. *Biodegrad Green Compos*, 16, 312.

Getachew, A., & Woldesenbet, F. (2016). Production of biodegradable plastic by polyhydroxybutyrate (PHB) accumulating bacteria using low cost agricultural waste material. *BMC research notes*, 9(1), 509.

Godoy, M. S., Mongili, B., Fino, D., & Prieto, M. A. (2017). About how to capture and exploit the CO 2 surplus that nature, per se, is not capable of fixing. *Microbial biotechnology*, 10(5), 1216-1225.

Grammel, H., Gilles, E. D., & Ghosh, R. (2003). Microaerophilic cooperation of reductive and oxidative pathways allows maximal photosynthetic membrane biosynthesis in *Rhodospirillum rubrum*. *Applied and. Environmental Microbiology*, 69(11), 6577-6586.

Haaker, H., & Veeger, C. (1976). Regulation of respiration and nitrogen fixation in different types of *Azotobacter vinelandii*. *European journal of biochemistr*y, 63(2), 499-507.

Haas, T., Krause, R., Weber, R., Demler, M., & Schmid, G. (2018). Technical photosynthesis involving CO_2 electrolysis and fermentation. *Nature Catalysis*, 1(1), 32.

Hädicke, O., Grammel, H., & Klamt, S. (2011). Metabolic network modelling of redox balancing and biohydrogen production in purple nonsulfur bacteria. *BMC systems biology*, 5(1), 150.

Harayama S. and Iino T., Phototaxis and membrane potential in the photosynthetic bacterium *Rhodospirillum rubrum*, *Journal of Bacteriology*, vol. 131, no. 1, pp. 34-41, 1977.

Heinrich, D., Raberg, M., & Steinbüchel, A. (2015). Synthesis of poly (3-hydroxybutyrate-co-3-hydroxyvalerate) from unrelated carbon sources in engineered *Rhodospirillum rubrum*. *FEMS microbiology letters*, 362(8).

https://www.marketsandmarkets.com/Market-Reports/pha-market-395.html

Hustede, E., Steinbüchel, A., & Schlegel, H. G. (1993). Relationship between the photoproduction of hydrogen and the accumulation of PHB in non-sulphur purple bacteria. *Applied Microbiology and Biotechnology*, 39(1), 87-93.

Imhoff J., Truper H. and Pfenning N., Rearrangement of the Species and Genera of the Phototrophic Purple Nonsulfur Bacteria. *Int J Syst Evol Microbiol*, vol. 34, pp. 340-343, 1984.

Inomura, K., Bragg, J., & Follows, M. J. (2017). A quantitative analysis of the direct and indirect costs of nitrogen fixation: a model based on *Azotobacter vinelandii*. *The ISME journal,* 11(1), 166.

Jackson, F. A., & Dawes, E. A. (1976). Regulation of the tricarboxylic acid cycle and poly-β-hydroxybutyrate metabolism in *Azotobacter beijerinckii* grown under nitrogen or oxygen limitation. *Microbiology*, 97(2), 303-312.

Jacquel, N., Lo, C. W., Wei, Y. H., Wu, H. S., & Wang, S. S. (2008). Isolation and purification of bacterial poly (3-hydroxyalkanoates). *Biochemical Engineering Journal,* 39(1), 15-27.

Jambeck, J. R., Geyer, R., Wilcox, C., Siegler, T. R., Perryman, M., Andrady, A., ... & Law, K. L. (2015). Plastic waste inputs from land into the ocean. *Science*, 347(6223), 768-771.

Jin, H., & Nikolau, B. J. (2014). Evaluating PHA productivity of bioengineered *Rhodosprillum rubrum. PloS one*, 9(5), e96621.

Kerby, R. L., Ludden, P. W., & Roberts, G. P. (1995). Carbon monoxide-dependent growth of *Rhodospirillum rubrum*. *Journal of Bacteriology*, 177(8), 2241-2244.

Khanna, S., & Srivastava, A. K. (2005). Recent advances in microbial polyhydroxyalkanoates. *Process biochemistry*, 40(2), 607-619.

Klasson, K. T., Lundbäck, K. M. O., Clausen, E. C., & Gaddy, J. L. (1993). Kinetics of light limited growth and biological hydrogen production from carbon monoxide and water by *Rhodospirillum rubrum*. *Journal of biotechnology*, 29(1-2), 177-188.

Koku, H., Eroğlu, I., Gündüz, U., Yücel, M., & Türker, L. (2002). Aspects of the metabolism of hydrogen production by *Rhodobacter sphaeroides. International Journal of Hydrogen Energy*, 27(11-12), 1315-1329.

Koller, M., Niebelschütz, H., & Braunegg, G. (2013). Strategies for recovery and purification of poly [(R)-3-hydroxyalkanoates](PHA) biopolyesters from surrounding biomass. *Engineering in Life Sciences*, 13(6), 549-562.

Kourmentza, C., Plácido, J., Venetsaneas, N., Burniol-Figols, A., Varrone, C., Gavala, H. N., & Reis, M. A. (2017). Recent advances and challenges towards sustainable polyhydroxyalkanoate (PHA) production. *Bioengineering*, 4(2), 55.

Kurdikar, D.L., Strauser, F.E., Solodar, A.J., Paster, M.D. (1998) High temperature PHA extraction using PHA-poor solvents. US Patent 6,087,471

Kusaka, S., Abe, H., Lee, S., & Doi, Y. (1997). Molecular mass of poly [(R)-3-hydroxybutyric acid] produced in a recombinant *Escherichia coli. Applied microbiology and biotechnology*, 47(2), 140-143.

MacArthur, D. E., Waughray, D., & Stuchtey, M. R. (2016, January). The new plastics economy, rethinking the future of plastics. *In World Economic Forum*.

Madkour, M. H., Heinrich, D., Alghamdi, M. A., Shabbaj, I. I., & Steinbüchel, A. (2013). PHA recovery from biomass. *Biomacromolecules*, 14(9), 2963-2972.

Maness, P. C., Huang, J., Smolinski, S., Tek, V., & Vanzin, G. (2005). Energy generation from the CO oxidation-hydrogen production pathway in *Rubrivivax gelatinosus*. *Applied and Environmental Microbiology*, 71(6), 2870-2874.

Maness, P. C., Smolinski, S., Dillon, A. C., Heben, M. J., & Weaver, P. F. (2002). Characterization of the oxygen tolerance of a hydrogenase linked to a carbon monoxide oxidation pathway in *Rubrivivax gelatinosus*. *Applied and Environmental Microbiology*, 68(6), 2633-2636.

Martínez, V., Herencias, C., Jurkevitch, E., & Prieto, M. A. (2016). Engineering a predatory bacterium as a proficient killer agent for intracellular bio-products recovery: The case of the polyhydroxyalkanoates. *Scientific reports*, 6, 24381.

Martinez-Salazar, J. M., Moreno, S., Najera, R., Boucher, J. C., Espín, G., Soberon-Chavez, G., & Deretic, V. (1996). Characterization of the genes coding for the putative sigma factor AlgU and its regulators MucA, MucB, MucC, and MucD in *Azotobacter vinelandii* and evaluation of their roles in alginate biosynthesis. *Journal of bacteriology*, 178(7), 1800-1808.

McRose, D. L., Baars, O., Morel, F. M., & Kraepiel, A. M. (2017). Siderophore production in *Azotobacter vinelandii* in response to Fe-, Mo-and V-limitation. *Environmental microbiology*, 19(9), 3595-3605.

Najafpour, G., Younesi, H., & Mohamed, A. R. (2003). Continuous hydrogen production via fermentation of synthesis gas. *Petroleum and coal*, 45(3/4), 154-158.

Noar, J. D., & Bruno-Bárcena, J. M. (2018). *Azotobacter vinelandii*: the source of 100 years of discoveries and many more to come. *Microbiology*, 164(4), 421-436.

Oelze, J. (2000). Respiratory protection of nitrogenase in *Azotobacter* species: is a widely held hypothesis unequivocally supported by experimental evidence?. *FEMS microbiology reviews*, 24(4), 321-333.

Oliveira, C. S., Silva, C. E., Carvalho, G., & Reis, M. A. (2017). Strategies for efficiently selecting PHA producing mixed microbial cultures using complex feedstocks: Feast and famine regime and uncoupled carbon and nitrogen availabilities. *New biotechnology,* 37, 69-79.

Page, W. J. (1992). Production of poly-β-hydroxybutyrate by *Azotobacter vinelandii* UWD in media containing sugars and complex nitrogen sources. *Applied microbiology and biotechnology,* 38(1), 117-121.

Page, W. J., & Knosp, O. (1989). Hyperproduction of poly-β-hydroxybutyrate during exponential growth of *Azotobacter vinelandii* UWD. *Applied and Environmental Microbiology*, 55(6), 1334-1339.

Page, W. J., Manchak, J., & Rudy, B.. (1992). Formation of poly (hydroxybutyrate-co-hydroxyvalerate) by *Azotobacter vinelandii* UWD. *Applied and Environmental Microbiology*, 58(9), 2866-2873.

Passanha, P., Esteves, S. R., Kedia, G., Dinsdale, R. M., & Guwy, A. J. (2013). Increasing polyhydroxyalkanoate (PHA) yields from *Cupriavidus necator* by using filtered digestate liquors. *Bioresource technology*, 147, 345-352.

Patel, S. H., & Xanthos, M. (2001). Environmental issues in polymer processing: A review on volatile emissions and material/energy recovery options. *Advances in Polymer Technology: Journal of the Polymer Processing Institute*, 20(1), 22-41.

Peña, C., López, S., García, A., Espín, G., Romo-Uribe, A., & Segura, D. (2014). Biosynthesis of poly-β-hydroxybutyrate (PHB) with a high molecular mass by a mutant strain of *Azotobacter vinelandii* (OPN). *Annals of microbiology*, 64(1), 39-47.

Peña, C., Reyes, C., Larralde-Corona, P., Corkidi, G., & Galindo, E. (2002). Characterization of *Azotobacter vinelandii* aggregation in submerged culture by digital image analysis. *FEMS microbiology letters*, 207(2), 173-177.

Pohlmann, A., Fricke, W. F., Reinecke, F., Kusian, B., Liesegang, H., Cramm, R., ... & Strittmatter, A. (2006). Genome sequence of the bioplastic-producing "Knallgas" bacterium Ralstonia eutropha H16. *Nature biotechnology*, 24(10), 1257-1262.

Post, E., Golecki, J. R., & Oelze, J. (1982). Morphological and ultrastructural variations in *Azotobacter vinelandii* growing in oxygen-controlled continous culture. *Archives of Microbiolog*y, 133(1), 75-82.

Ragsdale, S. W. (2004). Life with carbon monoxide. *Critical reviews in biochemistry and molecular biology*, 39(3), 165-195.

Ramsay, J. A., Berger, E., Voyer, R., Chavarie, C., & Ramsay, B. A. (1994). Extraction of poly-3-hydroxybutyrate using chlorinated solvents. *Biotechnology Techniques*, 8(8), 589-594. b

Revelles, O., Tarazona, N., García, J. L., & Prieto, M. A. (2016). Carbon roadmap from syngas to polyhydroxyalkanoates in *Rhodospirillum rubrum. Environmental microbiology,* 18(2), 708-720.

Righi, S., Baioli, F., Samorì , C., Galletti, P., Stramigioli, C., Tugnoli, A., & Fantke, P. (2016). A life-cycle assessment of poly-hydroxybutyrate extraction from microbial biomass using dimethylcarbonate. *In 10th Italian LCA Conference: 10th Convegno dell'Associazione Rete Italiana LCA 2016*

Rochman, C. M., Browne, M. A., Halpern, B. S., Hentschel, B. T., Hoh, E., Karapanagioti, H. K., ... & Thompson, R. C. (2013). Policy: Classify plastic waste as hazardous. *Nature*, 494(7436), 169.

Senior, P. J., Beech, G. A., Ritchie, G. A. F., & Dawes, E. A. (1972). The role of oxygen limitation in the formation of poly-β-hydroxybutyrate during batch and continuous culture of *Azotobacter beijerinckii. Biochemical Journal*, 128(5), 1193.

Shelver, D., Kerby, R. L., He, Y., & Roberts, G. P. (1997). CooA, a CO-sensing transcription factor from *Rhodospirillum rubrum*, is a CO-binding heme protein. Proceedings of the *National Academy of Sciences*, 94(21), 11216-11220.

Slater, J. H., & Morris, I. (1973). The pathway of carbon dioxide assimilation in *Rhodospirillum rubrum* grown in turbidostat continuous-flow culture. Archiv für Mikrobiologie, 92(3), 235-244.

Tabita, F. R. (1995). The biochemistry and metabolic regulation of carbon metabolism and CO 2 fixation in purple bacteria. *In Anoxygenic photosynthetic bacteria* (pp. 885-914). Springer, Dordrecht.

Terada, M., & Marchessault, R. H. (1999). Determination of solubility parameters for poly (3-hydroxyalkanoates). *International Journal of Biological Macromolecules*, 25(1-3), 207-215.

The future of plastic, *Nature Communications*, vol. 9, no. 1, pp. 1–3, 2018.

Tian, Y., Yue, T., Yuan, Y., Soma, P. K., & Lo, Y. M. (2010). Improvement of cultivation medium for enhanced production of coenzyme Q10 by photosynthetic *Rhodospirillum rubrum. Biochemical Engineering Journal*, 51(3), 160-166.

Troschl, C., Meixner, K., & Drosg, B. (2017). Cyanobacterial PHA production—Review of recent advances and a summary of three years' working experience running a pilot plant. *Bioengineering*, 4(2), 26.

Troschl, C., Meixner, K., Fritz, I., Leitner, K., Romero, A. P., Kovalcik, A., ... & Drosg, B. (2018). Pilot-scale production of poly-β-hydroxybutyrate with the cyanobacterium Synechocytis sp. CCALA192 in a non-sterile tubular photobioreactor. *Algal research*, 34, 116-125.

Verlinden, R. A., Hill, D. J., Kenward, M. A., Williams, C. D., & Radecka, I. (2007). Bacterial synthesis of biodegradable polyhydroxyalkanoates. *Journal of applied microbiology*, 102(6), 1437-1449.

Wawrousek, K., Noble, S., Korlach, J., Chen, J., Eckert, C., Yu, J., & Maness, P. C. (2014). Genome annotation provides insight into carbon monoxide and hydrogen metabolism in *Rubrivivax gelatinosus. PloS one*, 9(12), e114551.

www.newlight.com

Xu, C. R., Wu, P., Lang, L., Liu, R. J., Li, J. Z., & Ji, Y. B. (2015). Magnesium ions

improving the growth and organics reduction of *Rhodospirillum rubrum* cultured in sewage through regulating energy metabolism pathways. *Water Science and Technology*, 72(3), 472-477.

Yeo, J. C. C., Muiruri, J. K., Thitsartarn, W., Li, Z., & He, C. (2018). Recent advances in the development of biodegradable PHB-based toughening materials: Approaches, advantages and applications. *Materials Science and Engineering:* C, 92, 1092-1116.

Zhu, Q. (2019). Developments on CO_2-utilization technologies. *Clean Energy*, 3(2), 85-100.

Chapter 2

Gas-to-liquid fermentation: Characterization studies

2.1. Introduction

Carbon monoxide is a harmful and toxic molecule for the majority of living beings. It is mainly produced by human activities, and in the atmosphere, it reaches a concentration that shifts from 35 to 220 ppb, depending on the region and the period of the year (Novelli at al., 1998) (www.earthobservatory.nasa.gov). In nature exist microorganisms able to grow on carbon monoxide (Yu et al., 1998). One of these is *Rodospirillum rubrum*, a specie that not only consume CO, but that is also able to synthesize bioplastic when it is fed under CO and acetate. Therefore, it is a suitable model organism for addressing the issue of PHB production from waste gasses.

In the past, *R. rubrum* was mainly studied for the hydrogen production starting from syngas or sole CO feeding under light irradiation (Najafpour et al., 2003), or supplying syngas in darkness condition (Revelles et al., 2016). However, little information is available on the bacterium performances under exclusive feeding of carbon monoxide in darkness.

Consequently, this experimental session aimed to identify the behaviour of *R. rubrum* under daily feeding of carbon monoxide in darkness, in order to characterize its behaviour and to standardize its cultivation, for further bioreactor tests.

2.2 Materials and method

2.2.1. Cultivation *Rhodospirillum rubrum*

R. rubrum was cultured in 120 mL bottle closed by a rubber stop-cap in 20 mL on RNNCO[1] medium, pH 7, with 15 mM of acetate as carbon source, changing the amount of carbon monoxide into the headspace on the basis of the experimental need. The preculture was made under the same culture conditions with 20% of CO into the

[1] To find more information on RRNCO medium, go to Appendix

headspace. The preparation of the culture media and gas supplied were based on the work of Revelles (Revelles et al., 2015).

Therefore, before feeding each gas bottles were purged with a vacuum pump and filled washed by N_2 before to be filled with CO. The gas was supplied by syringe, previously filled with the amount of gas requires. To fill completely the headspace of the bottles, the remaining volume was supplied by N_2.

In all the experiments the condition of agitation at 220 rpm, darkness and temperature at 30°C were maintained

2.2.2. Cultivation strategy for investigating the effect of the preculture condition in *Rhodospirillum rubrum*

In the case of the investigation of *R. rubrum* behaviour on different pre-culture condition. The bacterium was cultured as described in the paragraph below following this scheme of CO concentration (Table 2-1), for pre-culture and culture conditions, respectively.

CO adds for the preculture	CO adds for the cultivation
30	20
	30
	40
50	30
	40
	50

Table 2-1 Experimental strategy for CO-feeding tests.
The numbers are referred to carbon monoxide concentrations add in the headspace of the bottles.

2.2.3. Cultivation of *Rhodospirillum rubrum* under mixotrophic conditions.

R. rubrum was pre-cultured in 160 mL bottle closed by a rubber stop-cap in 80 mL on RNNCO medium with 15 mM of fructose as carbon source and the absence of acetate. The preculture was growth for 48 h, during which the culture growth up to ad OD_{660} of 1.5 consuming all the fructose present in the medium. The experiment was set in 160 mL bottle filled with 30 mL of RNNCO medium with a different carbon source at an initial OD_{660} of 0.08 and headspace of 130mL composed by a 10% of CO and remaining part filled with N_2 (pCO 10%). The carbon source tested were fructose at a final concentration of 5 mM or 10 mM of acetate, or pulse feeding of fructose were fed each 24 hours by a syringe. During the cultivation period, the headspace of the bottles was purged for 30 sec with a vacuum pump and filled washed with N_2 for one time and re-purged for other 30 seconds for being filled with the final CO and N_2. This procedure was repeated each 24 h. The experiments were made in triplicate and the bacteria were cultured under 200 rpm at 30 °C.

2.2.4. Analytical determination for the biomass

Optical quantification of biomass was made measuring samples absorbance at 660 nm. So, samples of 1 mL were picked from bottles were read in a spectrophotometer (Thermophischer). Cell dry weight was made gravimetrically. Thus, the sample collected was centrifuged at 10000 rpm for 5 minutes, washed two-times and airdried at 80°C for 12 hours in an oven. To have an estimation of the biomass produced during the growth a calibration curve on the base of the optical density was made. Therefore, *R. rubrum* was cultured by the standard procedures above reported under 50% of carbon monoxide. During the cultivation, the relative biomass was centrifuged and airdried. Hence, the respective weighs were estimated, as shown in the graph below.

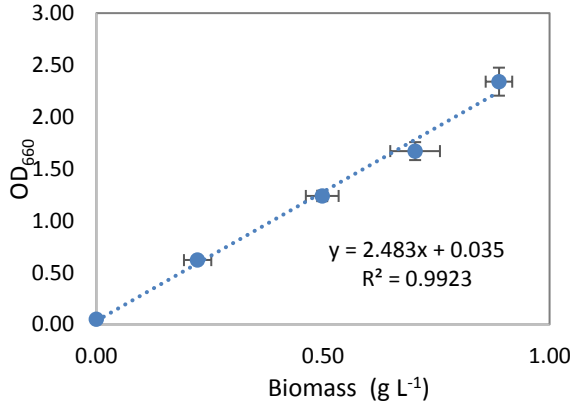

Figure 2-1 Calibration curve of *R. rubrum* biomass on optical density values.

2.2.5. Acetate, Fructose and Formic Acid Determination

Acetic Acid, Fructose and Formic Acid were detected by HPLC analysis (Shimatzu). After the sampling of the culture, the medium filtered by a 0.2 µm cellulose nitrate filter and were analysed with a column ROA-Organic Acid H^+ (8%) (Phenomenex) under an isocratic flux of 0.7 mL min^{-1} of 5 mM of H_2SO_4 and a temperature of 50 °C. Respectively, the acetate, the fructose and the formic acid were detected after 13.59 minutes 9.17 minutes and 12.3 minutes of retention time. In particular, the acetic acid and the fructose were identified by a RID detector, while formic acid was detected by a PDA detector under 206 nm.

2.2.6. PHB quantification

Samples collected were centrifuged at 10000 rpm for 5 minutes, washed two-times and dried at 80°C for 12 hours in an oven. Once estimated the correspondent biomass concentration (g L^{-1}), the dry biomasses were hydrolysed by 1 mL of 96% H_2SO_4 under stirring of 800 rpm, into an agitated oil bath at 90°C for one hour. At the end of the reaction, a dilution of 1:125 was done and the samples were analysed by a HPLC (Shimatzu) with a column ROA-Organic Acid H^+ (8%) (Phenomenex)

under an isocratic flux of 0.7 mL min^{-1} of 5 mM of H_2SO_4 and a temperature of 50 °C. The PHB related signal appeared at 210 nm after 23.09 from the sample injection, which corresponds to the crotonic acid (the monomer coming from the hydrolysed PHB) (Braunegg et al., 1979).

2.2.6. Gas composition analysis

For the analysis of the gas composition present in the headspace of the bottle, a gas bag, previously purge and put under vacuum by a vacuum pump, was connected woth the bottle by a needle and the gas was sampled. This procedure was favourited by the overpressure that after 24 h of cultivation was developed by the culture for the conversion of CO in CO_2 and H_2. The collected gas was analysed by SRA Micro-GC equipped by a Molsive 5A column at a temperature of 100°C under argon as carrier gas (for the quantification of H_2, CO, N_2), and by a PoraPLOT U column at 85°C using helium as carrier gas (for CO_2 analysis).

Gas quantification

Starting from the relative concentration of the carbon monoxide add into the bottle or into the reactor headspace, the correspondent amount of CO was calculated by the following formula, where P is the environmental pressure, V is the volume of the headspace, R is the Boltzman constant (0.082 L atm mol^{-1} K^{-1}) and T is the temperature used expressed in Kelvin:

$$PV = nRT \qquad \text{Eq. 2}$$

Knowing the respective values of P and V, the number of moles, n, was found. Multiplying n for the relative gas concentration, the correspondent number of moles of CO, H_2 and CO_2 were found. Hence, the concentration of the CO in the gas and liquid phase was found on the base of Henry's law:

$$[Gas] = H\,p \qquad \text{Eq. 3}$$

Where H is the Henry constant and p stands for the value of partial pressure.
In particular, for the studied gas, the values of H listed in Table 2-2.

Gas	**H** (mol bar^{-1} kg^{-1})	**H** (mol atm^{-1} L^{-1})
CO	0.001	0.0010
CO_2	0.034	0.0345
H_2	0.001	0.0008
N_2	0.001	0.0007

Table 2-2 Henry's gas constant.

2.2.7. Calculations

For investigating the biomass *specific growth rate* (μ) data were linearized by the Eq. 4:

$$y = lnX/X_0 \qquad \text{Eq. 4}$$

Starting from the assumption that the growth of the bacterium followed an exponential trend. Therefore, the μ was found in correspondence with the slope in which the biomass assumed a linear trend.
The molar growth yield (Y_{mol}) was calculated after the complete depletion of the consumed substrate, and it was calculated by the following formula, based on the work of Schultz and implemented by the normalization of the total carbon atom present in the substrate (Schults at al., 1982)

$$Y_{mol} = \frac{mg\ of\ collected\ biomass}{mmol\ of\ consumed\ substrated\ x\ atoms\ of\ C\ presented\ into\ the\ substrate} \qquad \text{Eq. 5}$$

2.3. Results and discussion

2.3.1. Correlation of growth performances and CO concentrations

Dependence of *Rhodospirillum rubrum* growth on CO supply

First experimental trials consisted in culturing *R. rubrum* under darkness, in batch configuration, applying different carbon monoxide concentrations in the headspace of the serum bottles used for culturing the bacterium. Figure 2.1 shows the growth curves under 0, 20, 30 or 40% of CO added in the headspace.

By single CO feeding, *R. rubrum* took more time to reach the stationary phase as a consequence of carbon monoxide amount fed into the culture. Under 20% of CO, the stationary phase was reached on the second day of cultivation, while under 30% of CO, it was reached on the third day. The same trend was followed by the experiment carried out with 40% of CO. Hence, an increase of fed carbon monoxide generated a more extended lag phase. These variations demonstrated that carbon monoxide acts both as a *substrate* and an *inhibitor* for *R. rubrum* because, under a higher concentration of this gas, the biomass required more time for growing.

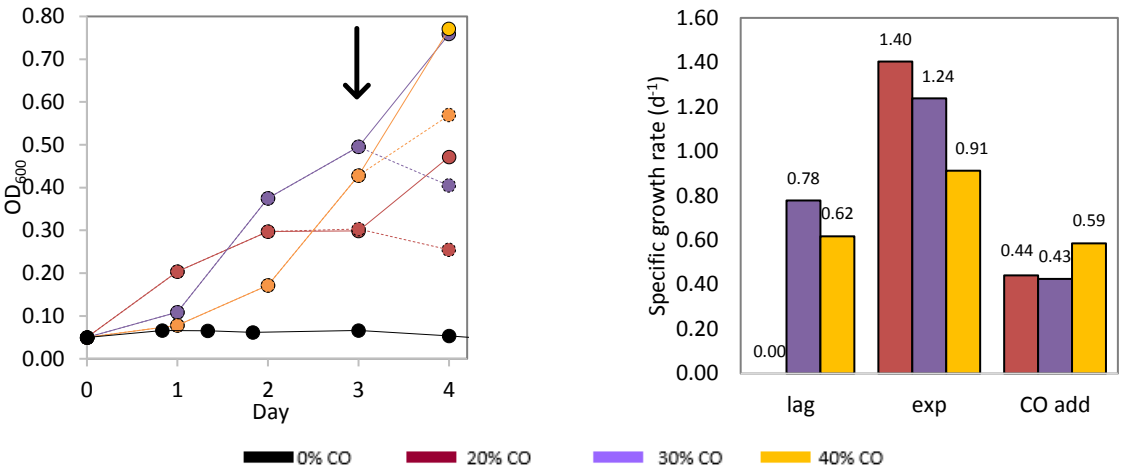

Figure 2.2-2 *R. rubrum* average growth in 120 mL bottle, under different CO concentrations added in the bottle headspace.
On the left: the growth of *R. rubrum* represented with correspondent optical density values taken at 660 nm (OD660) under: 0% (black), 20% (red), 30% (purple) and 40% (yellow) of CO. In this experiment, after three days of cultivation, new CO was supplied to the culture (black arrow) guaranteeing growth for the biomass. On the other side, samples which did not receive new CO, represented with dotted lines, show a decrease in the optical density. On the right: the growth rates found before and after the CO addition, where "lag" stands for lag phase, "exp" for the exponential phase and "CO add" for the growth rate found after the addition of CO. The experiment was made in triplicate, but for a graphical reason, only the average is reported.

When CO was supplied into the headspace during the third day of cultivation, biomass growth restarted. This trend was also observed in those cultures already entered into the stationary phase (cultures fed with 20% and 30% of CO). After this gas feeding, the specific growth rate was almost the same, around 0.4 d^{-1} for samples fed by 20% and 30% of CO. While it appreciably peaked 0.6 d^{-1} under addition of 40% of CO. Cultures exposed to the addition of the highest CO concentrations, received the gas supply in correspondence with or close to their exponential growth phase, in comparison with samples fed with 20% of CO. Thus, these cultures could better face new feedstocks of CO, accordingly to a more active metabolic state.

On the contrary, under the first CO supply, the highest growth rate was found under the lowest CO concentration (12 hours at 20% of CO). An increase of the carbon monoxide generated a decrease of the duplication rate, with a 1.5-fold decrement between 40% and 20% of CO.

Even if carbon monoxide showed a slowing down activity on *R. rubrum* duplication rate, it is the primary carbon and energy source for the cells in darkness, as demonstrated by the control experiment made under 100% of N_2. In this condition, any growth activity was observed. As supported by the work of Do and colleagues, CO is the limiting nutrient under darkness (Do et al., 2007). Then, for basing a CO-limited continuous growth, the dependency between growth trend and carbon monoxide supplies was investigated.

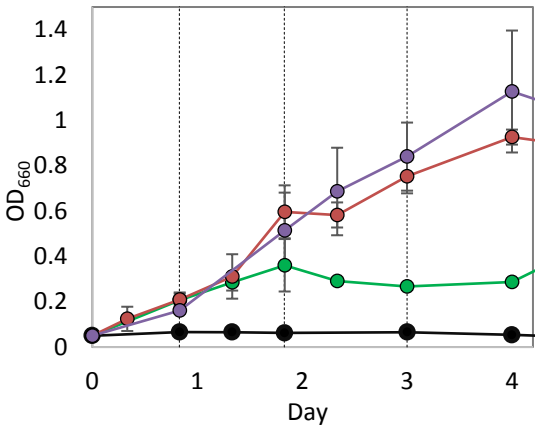

Figure 2.2-3 *R. rubrum* growth under 20% CO fed each 24 hours in bottle headspace.
Single feeding (green line), repetitive feeding every 24 hours (red line), and at 8 and every 24 hours (purple line) are represented. The dotted lines mark the repetitive feeding. Growth trends show that daily feeding can sustain strain growth.

	OD_{660} (/)	**Final biomass** (g L^{-1})	**Specific growth rate** (d^{-1})
Single CO feeding	0.36 ± 0.12	0.13 ± 0.04	1.4
Dayly feeding	0.93 ± 0.30	0.36 ± 0.12	1.5
No CO addition	0.05	0.01	0

Table 2-3 Growth curves parameters under daily feedings of carbon monoxide.

Figure 2.2-3 and Table 2-3 show the bacterial growth dependency on CO feeding. Differently from a single CO feeding, a daily feeding resulted in a constant growth for the period tested. A three-fold increase in the final biomass was achieved in comparison of single gas supply, with a biomass titre going from 0.13 ± 0.04 to 0.36 ± 0.12 g L^{-1} in the 4th day of cultivation. During the experimental campaign, also a CO supply during the early exponential phase (8 hours from the inoculation) was tested, but it did not result in a significant change on *R. rubrum* growth trend.

Summing up, these first trials confirmed a dependency of *R. rubrum* grown on carbon monoxide in darkness conditions. The use of carbon monoxide in high concentrations made aware of a growth-inhibiting activity caused by this gas on the duplication rate, even if higher biomass titres resulted in correspondence with higher gas concentrations. Moreover, under not inhibiting CO concentration, a daily CO feeding succeeded in CO-limited growth.

As literature reports, carbon monoxide is usually a toxic substrate for microbial biomass, by its tendency to interact with metal cofactors inside enzymes catalytic pockets, or by blocking putative substrate accesses and reactions too. On the other side, there are species close to *R. rubrum* that can take advantage of it, even if some growth limiting events can occur. This is also the case of *Rubrivivax gelatinosus*, a specie that grows on CO, but that slowed its duplication rate at increasing gas concentrations. In particular, a modified Monod's kinetic model was designed on this bacterium for

correlating the duplication rate to carbon monoxide concentration going from 0 to 0.8 mM (Amos, 2004) (Yasin et al., 2015). Further, a decrease of growth performance was also demonstrated in *R. rubrum* too, when it was cultured under serial dilutions of syngas (25% CO, 25% H_2, 5% CO_2, and 45% N_2 v/v), in which the inhibition activity was verified at the highest syngas concentrations (Karmann et al., 2019).

Influence of pre-adaptation conditions on *Rhodospirillum rubrum*

In previous experiments, *R. rubrum* showed a high dependence on CO in darkness culture conditions. Nevertheless, high CO concentrations affected the growth, decreasing the duplication rate and extending the lag phase. Therefore, the effect of carbon monoxide used during the pre-culture cultivation phase was investigated.

The bacterium was pre-adapted under specific CO concentration (30 and 50% of CO) (*pre-adaptation phase*). Successively, aliquots coming from these cultivation conditions were used as seeding cultures for testing *R. rubrum* growth (*cultivation phase*) under three distinct CO concentrations, ranging from -10% to +10% of CO in respect to the CO concentrations supplied during the pre-adaptation phase.

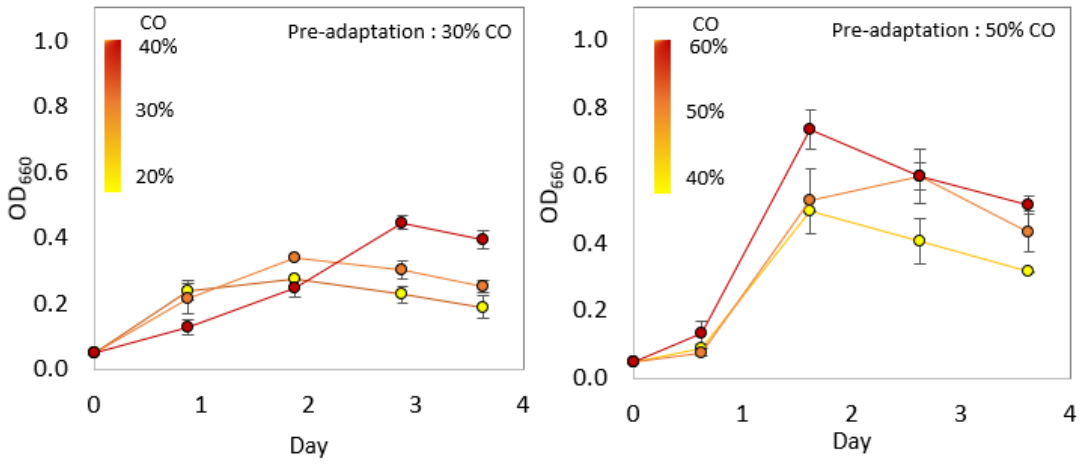

Figure 2-4 *R. rubrum* growth under different CO concentrations.
In the figure, seeding culture pre-adapted at 30 or 50 % CO v/v in the headspace and tested supplying from -10% to 10% CO of the CO concentration used in the phase of adaptation. Left: growth curve of cultures adapted under 30% of carbon monoxide and tested under a single feeding of CO at 20, 30 and 40% of CO. Right: growth curve of cultures previously adapted under 50% of carbon monoxide and tested under a single feeding of CO at 40, 50 and 60% of CO.

(Table 2-4 and Figure 2-4) Increasing CO concentration from the pre-adaptation to cultivation phases resulted in a rise of the amount of biomass reached at the end of the growth, under the same time range. The highest biomass was reached in the culture pre-adapted under 50% of CO and exposed to 60% of CO, with 0.19 ± 0.03 g L^{-1} of final biomass. While, the lowest biomass accumulation, 0.08 g L^{-1}, was measured in correspondence with the lowest CO concentration supplied (20% of CO). Overall, *R.*

rubrum had a specific duplication rate, ranging between 9 to 19 hours. Increasing the concentration of the carbon monoxide in the culture caused a parallel decrease in the duplication rate under 30% of CO fed in pre-adaptation. While cultures pre-adapted under 50% of carbon monoxide evolved an almost stable duplication rate, in parallel of the different CO concentrations tested.

Pre-adaptation	**Fermentation**				
CO (%)	CO (%)	CO (mM)	μ (d^{-1})	Duplication time (hour)	Biomass (g L^{-1})
30	20	0.2	1.78	9.3	0.08 ± 0.01
	30	0.3	1.67	10	0.12 ± 0.01
	40	0.4	0.85	19.6	0.17 ± 0.01
50	40	0.4	1.41	11.9	0.19 ± 0.01
	50	0.5	1.44	11.9	0.20 ± 0.04
	60	0.6	1.65	10.4	0.28 ± 0.02

Table 2-4 The variation of biomass accumulation and specific growth rate caused by pre-adaptation conditions. In the table, the CO concentration dissolved in the liquid phase, the specific growth rate (μ), the correspondent duplication time and the final biomass reached are reported. The experiment was made in triplicate.

From the results, it can be concluded that *R. rubrum* assumed a peculiar behaviour concerning carbon monoxide concentrations used both during the pre-adaptation phase and culture steps. Growth trends suggested that, when the concentration of carbon monoxide fed during the pre-adaptation was low (around 0.3 mM of CO in the liquid phase), cells were not ready to metabolize higher CO concentrations. On the contrary, the pre-adaptation made at higher CO concentrations (0.5 mM of CO into the liquid phase) ensured no inhibition events on successive cultivations.

In all the conditions, the analysed headspace gas composition confirmed that at the end of the fermentation the entire amount of carbon monoxide was consumed, in return to biomass and an equal molar ratio of CO_2 and H_2. Besides, the concentration of gas affected lag phase: under little amounts of CO, the lag phase was barely absent, while under higher CO concentration the growth required a longer adaptation time.

In *R. rubrum*, the chance to take advantage from CO depends at least on three different genes (CooS, CooF and CooH), activated by CO, which respectively bringing genetic information for CODH, an electron transfer protein as ferredoxin and a CO-dependent hydrogenase. It is reported that the activation of transcription factors for protein expression is governed by a rapid kinetic, which takes around 10 minutes for reaching the maximum transcriptional rate. Even if this mechanism has a strong dependence on substrate concentration (Shelver et al., 1995) (Bonam et al., 1989).

On the other side, in our laboratory, it was noted that after a pre-adaptation phase, the bacterium faster carbon monoxide metabolism, taking less time in the lag phase. Therefore, as well as it was demonstrated for other carboxydotrophs species, on the base of our findings, the activation of the transcriptional factors in *R. rubrum* should be subjected to the pre-culture conditions. For instance, in *Carboxydothermus hydrogenoformans* Z-2901 a modular expression of the CODH isoform depending on CO concentration was found too (Wu et al., 2005) (Tirado-Acevedo et al., 2011).

The CO concentration in the liquid phase was close to the published Michaelis-Menten constant value referred to *R. rubrum* CODH, which was estimated equal to 0.11 mM *in vitro* measurement. And, such value is in the same order of magnitude of the supplied CO in this work (Table 2-4)(Bonam et al., 1984).
As data shows, when CO used during the pre-adaptation was low (30%), the growth was slowed down in the cultivation phase that hosted higher CO concentrations. As a consequence, a negative influence on *R. rubrum* metabolism could be gathered before a suitable protein transcription level for CO consumption could be available.
Moreover, literature offers different examples in which the growth rate varies with the CO concentration and pre-culture conditions. For instance, *R. rubrum* fed with 80% of CO showed a duplication time of 5 hours in the work of Kerby and colleagues, while under a syngas feeding (40:10:10:40 of $CO:N_2:CO_2:H_2$), a duplication rate of 33 hours was reported. In particular, both studies were made under comparable fermentation conditions, like temperature, the absence of light and the medium, suggesting how the pre-culture condition could result in a strong influence on the strain behaviour (Revelles et al., 2016) (Kerby et al., 1992). As demonstrated for *Clostridium ljungdahlii*, the pre-adaptation significantly influences successive growth steps, because of the biomass can become more metabolically active, determining a skip of the lag phase (Mohammadi et al., 2014) (Tirado-Acevedo et al., 2011).
Summing up, the pre-adaptation phase has an appreciable influence on *R. rubrum* metabolism. However, over a particular value of carbon monoxide used, which in this study was fixed at 0.5 mM, a more active population overcame the effect of CO inhibition, and any CO-dependent inhibition effects appeared.

1.3.3. Fermentation of *R. rubrum* under daily CO feeding

Characterization of substrates and products trends

Once defined the cultivation conditions under carbon monoxide, the PHB production in *R. rubrum* was tested. The bacterium was cultured in a closed bottle, with daily feeding of 50% of CO and 3 mM of sodium acetate as the carbon substrate for PHB biosynthesis, in addition to the stander medium. As for the experimental setting already tested, the bacterium was cultured in darkness, maintaining a stable temperature of 30°C, and gentle agitation of 200 rpm. During the cultivation, the biomass, the PHB, the headspace gas composition and the substrate consumption were analysed.

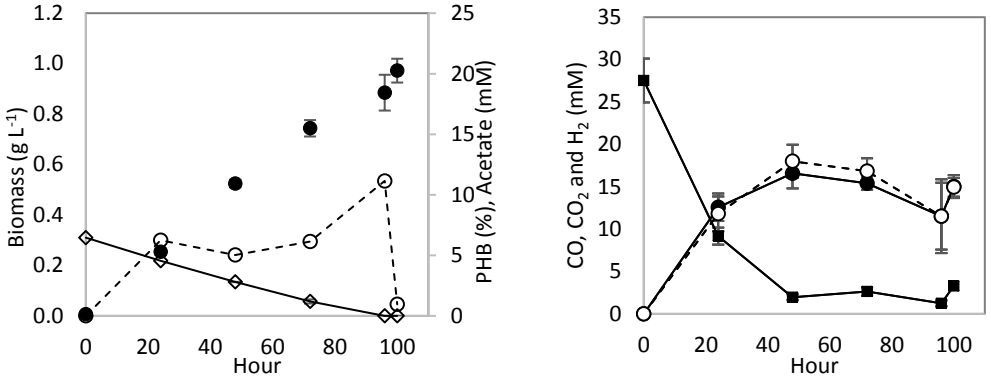

Figure 2-5 *R. rubrum* growth under 50% of daily feeding of carbon monoxide, gas evolution and PHB production.
On the left, the biomass (●), the PHB (○) and sodium acetate concentration (◊). On the right, the CO (■), H_2 (○) and CO_2 (●) measured every 24 hours during the entire cultivation time. In the graph, the washing phase and the new feeding of carbon monoxide were not reported, but only the final concentration of the two gasses was presented.

Consumption		**Production**	
Acetate (mM d^{-1})	CO (mM d^{-1})	H_2 (mM d^{-1})	CO_2 (mM d^{-1})
1.52 ± 0.53	25.25 ± 0.88	14.63 ± 2.18	15.82 ± 2.83

Table 2-5 Fermentation parameters of *R. rubrum* under daily feeding of carbon monoxide.

Figure 2-5 presents biomass growth, PHB biosynthesis, acetate consumption and relative CO, CO_2 and H_2 found each 24 hours, during the entire fermentation. Under this condition, *R. rubrum* had a specific growth rate of 0.023 h^{-1}, developing a final biomass concentration of 1 g L^{-1}.

During the biomass growth, the acetate was linearly consumed, up to be entirely metabolised at the end of the 4th day of cultivation, in which its consumption was around 1.52 ± 0.53 mM d^{-1}. Carbon monoxide was consumed from 67%, registered after the first day of cultivation, up to 95% correspondent to the successive days of growth (Figure 2-6). Consequently, the consumption of the carbon monoxide realized an equal molar amount of CO_2 and H_2.

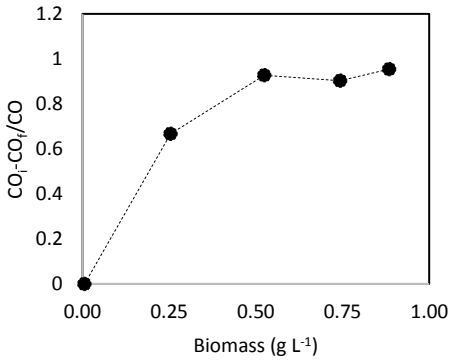

Figure 2-6 Gas conversion during CO-based fermentation tested in a closed bottle on biomass concentration.

As far as the PHB production was concerned, a little amount of the polymer started to appear after 24 hours of cultivation. Its concentration remained stable, around 5%

for improving up to 11%. However, after complete depletion of acetate, PHB concentration fell to 1%, maybe for maintaining the cell metabolism.

Phenotypic evolution of *R. rubrum* under repetitive CO cultivation

In order to ensure shorter adaptation time, a seeding culture was kept alive under a fixed CO concentration. It is a typical working strategy applied for slow-growth microorganisms, generally used to maintain a strain under an active metabolic state and for reducing the experimental time as well.
However, applying this procedure, it was noted an evolution of the strain with the carbon monoxide exposition, and in three months of independent trials, the biomass accumulation changed, as showed in Figure 2.8 and Table 2-6.

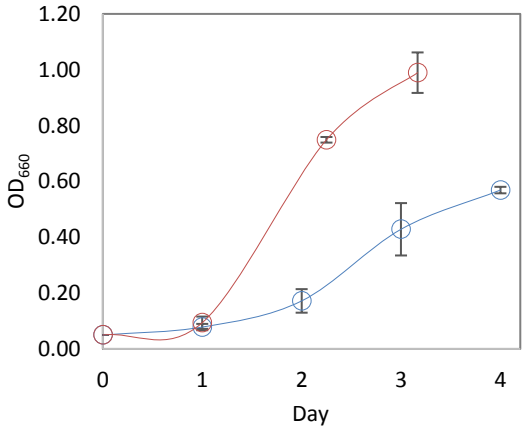

Figure 2-7 Phenotypic evolution in *R. rubrum*.
The graph shows a variation growth trend, applying the same experimental procedure three months apart. In blue a cultivation made during December 2017, in red a cultivation made in March 2018. In both cases, the strain was cultured under a daily feeding of 40% of carbon monoxide. The strain expressed by a red line came from repetitive culture seeding in new media taken under the same amount of CO.

R. rubrum developed an adaptive evolution, growing more efficiently in CO after three months of adaptation than firsts adaptation cycles. Therefore, it was more prone to metabolise carbon monoxide, minimizing CO inhibition effects and improving the specific growth rate, which passed from 0.006 to 0.17 h^{-1}(Lee at al., 2016).

A DNA sequencing for investigating a possible accumulation of genetic mutation over the time considered was far from our goal. Therefore, it was decided to address the investigation to a cultivation method which could guarantee a stable behaviour for further scale-up development.

40% daily feeding of CO under darkness	**Specific growth rate** (h^{-1})	**Final biomass reached** ($g\ L^{-1}$)
December 2017	0.006	0.19 ± 0.003
March 2018	0.017	0.34 ± 0.02

Table 2-6 Growth parameters of the cultivation run made under the same conditions three months apart.

2.3.3. Effect of mixotrophic feeding

Discovering that *R. rubrum* developed an adaptive evolution on repetitive CO exposition, pushed the decision to address a new propagation strategy. The behaviour of this strain under CO and fructose, which is a strong reducing sugar associated with high biomass yield, was studied (Zeiger et al., 2010). Therefore, the so-called *mixotrophic* condition (which is a combination of *heterotrophic* and *autotrophic* growth), was investigated in order to avoid those issues related to an adaptive evolution behaviour.

Comparison of *Rhodospirillum rubrum* biomass growth under mixotrophic and autotrophic pre-culture conditions

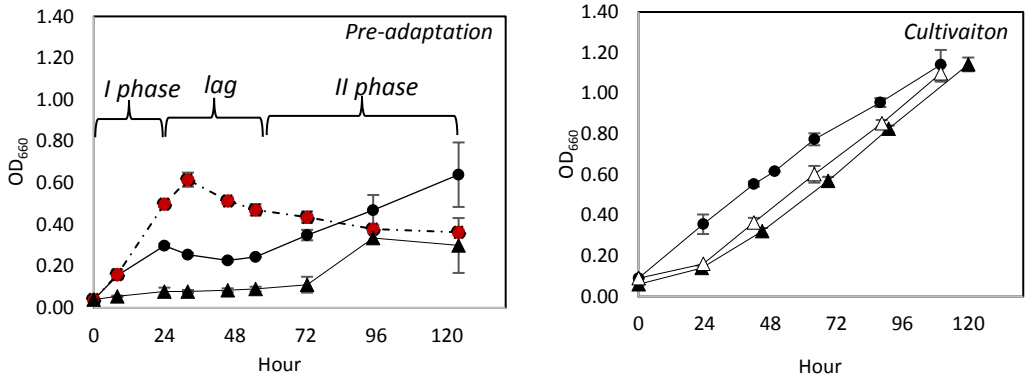

Figure 2-8 Comparison of *mixotrophic* and *autotrophic* pre-adaptation and fermentation steps.
On the left: the pre-adaptation. *R. rubrum* was grown under anaerobiosis with 5 mM of fructose and 20% of CO (●), under 15 mM of fructose and 20% of CO (●) and 3 mM of sodium acetate and 20% of CO (▲). On the right, *R. rubrum* fermentation from pre-adapted cultures: cultured under 3 mM of sodium acetate and 20% CO coming from autotrophic pre-adapted cultures (▲), or mixotrophic pre-adapted cultures (Δ), and *R. rubrum* cultured under 5 mM of fructose and 20% of CO, coming from mixotrophic pre-adapted cultures (●).

Aliquots of *R. rubrum* stored in glycerol at -20°C were cultured under two successive growth runs, which represents the pre-adaptation and the cultivation phase, respectively. *R. rubrum* was cultured under two different carbon-based feedings consisting in: i) acetate and CO, and ii) fructose and CO. The fermentations were made in a fed-batch configuration: the headspace was restored every 24 hours with 20% of pure CO and 80% of N_2. This low amount of carbon monoxide was selected for avoiding long adaptation phase, as previous experimental session suggested.

Figure 2-8 compares growth trends of *R. rubrum* during the pre-adaptation, and fermentation phase. In the pre-culture phase, the presence of fructose gave a rapid growth characterized by a specific growth rate, μ, of 0.8 h^{-1}, even in the presence of

CO (Table 2-7). Although, the autotrophic cultures started to rise the biomass after a while, supported by sole CO and acetate.

Under a mixotrophic pre-adaptation and in correspondence of a sugar depletion, *R. rubrum* entered in a new lag phase with a second growth rate of 0.01 h^{-1}. This event did not appear under the highest sugar supplied (15 mM), which in turn was characterized by higher optical density (OD_{660} = 0.6), followed by a cellular death phase (Maness et al., 2001). This second growth trend is recognised as a metabolic switch for the bacterium. The strain preferentially consumed fructose, reaching the maximum biomass concentration (as a control experiment confirmed in Figure 2.10). However, it was ready to begin a new growth under CO. Hence, only cultures fed by a single feeding of 5 mM of fructose and CO assumed this *diauxic* growth trend.

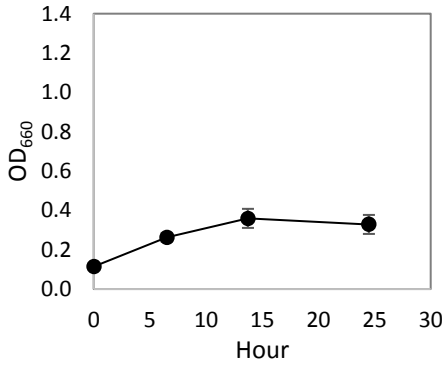

Figure 2-9 *R. rubrum* growth under anaerobic environment (N_2) in CO-free condition, fed by 5 mM of fructose

In the cultivation phase, mixotrophic and autotrophic pre-adapted cultures presented similar trends, showing a μ of 0.06 and 0.03 h^{-1}, respectively. This condition was not tested on cultures pre-adapted under 15 mM of fructose and CO, because the pre-cultivation condition gave the slowest adaptation. However, in the cultivation phase, the diauxic trend almost disappeared, and *R. rubrum* grown up to an OD_{660} of 1.2, in all conditions tested.

During the sampling of seeding aliquots, the bacterium was already under an autotrophic condition, and mixotrophic and autotrophic pre-culture seeds did not differ in their culture trends. However, the supply of at least 5 mM of fructose during the preculture gave the advantage to reach higher biomass concentration, which is useful for the setting of further fermentations.

Analysis of the headspace gas composition under mixotrophic feeding

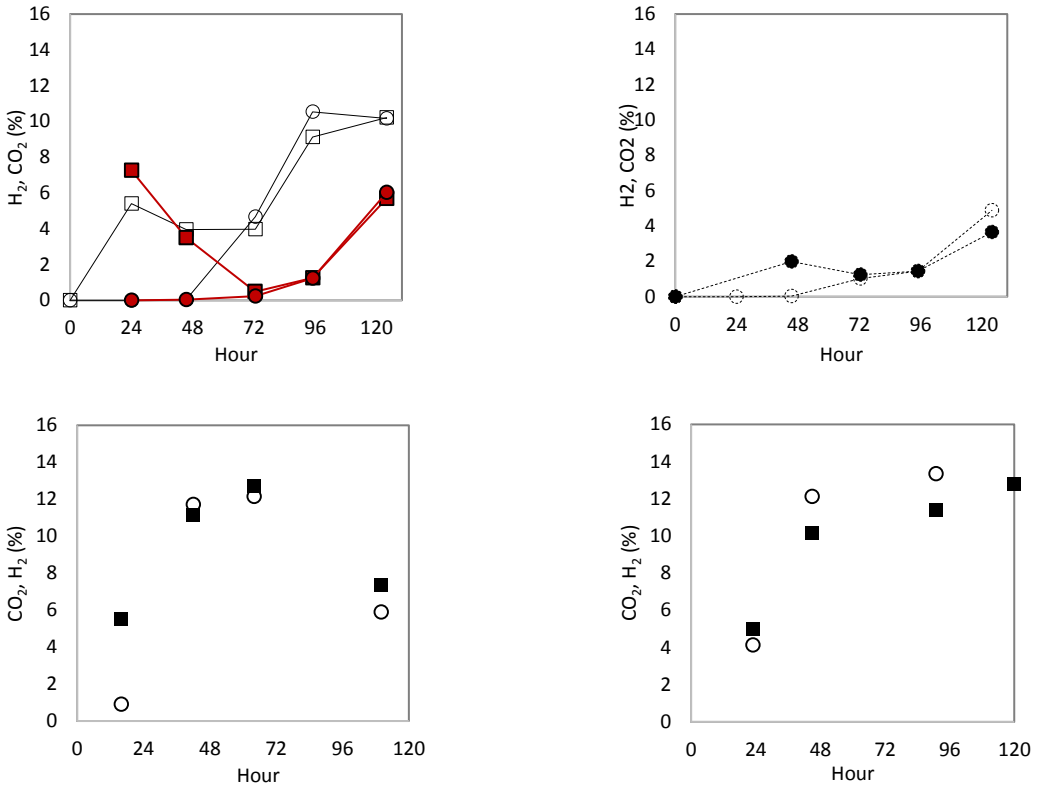

Figure 2-10 Headspace composition during pre-adaptation and successive fermentation phase.
On the top: gas composition found during the pre-adaptation. On the left: under 15 (red) and 5 mM (white) of fructose and 20% of CO. On the right: under 3 mM of acetate and 20% of CO. On the bottom: gas composition found during the fermentation. On the left: under 5 mM of fructose and 20% of CO. On the right: under 3 mM of acetate and CO. In all the figures, CO_2 is reported by squares, while H_2 by circles.

The analysis of the headspace composition confirmed what observed in growth curves. Figure 2-10 presents the headspace composition taken each 24 hours before new CO feeding in the pre-adaptation and cultivation cultures. During these experimental trials, any CO-limitation occurred, and at least 1% of CO was recovered after 24 hours. However, a parallel increase of H_2 and CO_2, directly coming from the water-gas shift reaction ($CO \rightarrow H_2 + CO_2$), was registered.

Data confirmed that CO consumption started after the depletion of fructose, as well as the diauxic curve suggested. In the pre-adaptation cultures, under 5 mM of fructose and 20% of CO, the H_2: CO2 had a ratio of 1:1 after 72 hours. While before, only high amounts CO_2, coming from fructose metabolism were found. Parallelly, samples fed by 15 mM of fructose, released higher CO_2 amounts and any H_2 was found up to 72 hours. Such a little variation that was not appreciable in optical density data, in which the OD_{660} did not rise after fructose depletion.

In the samples coming from the culture phase, the gas released confirmed that acclimation to CO was reached both under mixotrophic and autotrophic conditions. *R.*

rubrum started an earlier release of the carbon dioxide/hydrogen gas couple, and a shift on the evolution of these two gasses was appreciable one day before in respect to pre-culture samples.

Characterization of fermentation products

Figure 2-11 presents the HPLC data of autotrophic and mixotrophic cultivations referred to the cultivation phase. For the mixotrophic condition, data confirmed that fructose was rapidly consumed, and as a consequence, the biomass converted it into acetate, with a ratio of 0.6 mol mol^{-1} (moles of acetate over moles of consumed fructose). However, any acetate consumption was appreciable differently from the autotrophic fermentations, in which the consumption was linear.

Samples cultivated under autotrophic regime presented a little increase in acetate concentration during the first hours of cultivation. Such an increment that could be addressed to some metabolized products coming from the yeast extract presented in the medium composition.

As far as the PHB production was concerned, in both conditions the production of PHB was very similar, around 7 and 8% of the cell dried weigh for the mixotrophic and the autotrophic cultures, respectively. While pH values remained constant in both trials.

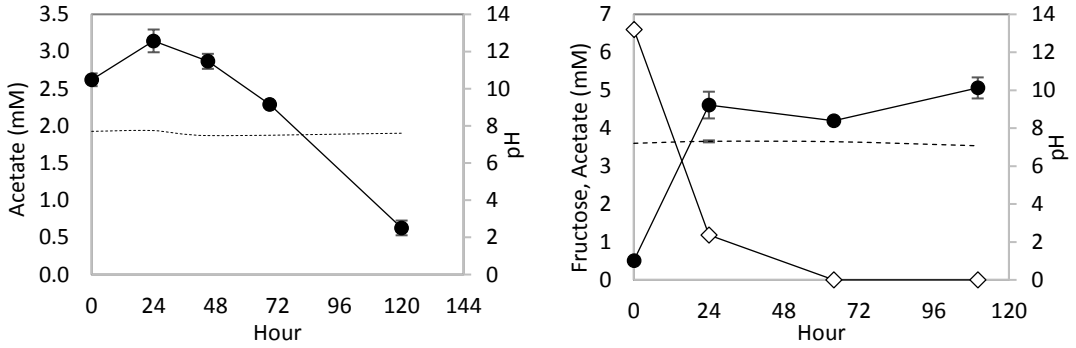

Figure 2-11 Trend of fructose and acetate under 20% CO supply into the headspace.
On the left: fermentation made under CO and acetate (●). On the right: fermentation made under CO and fructose (◊), in which it is shown the acetate formation (●). In both graphs, the value of the pH measurement is represented by a dotted line.

Influence of fructose pulses and CO supply

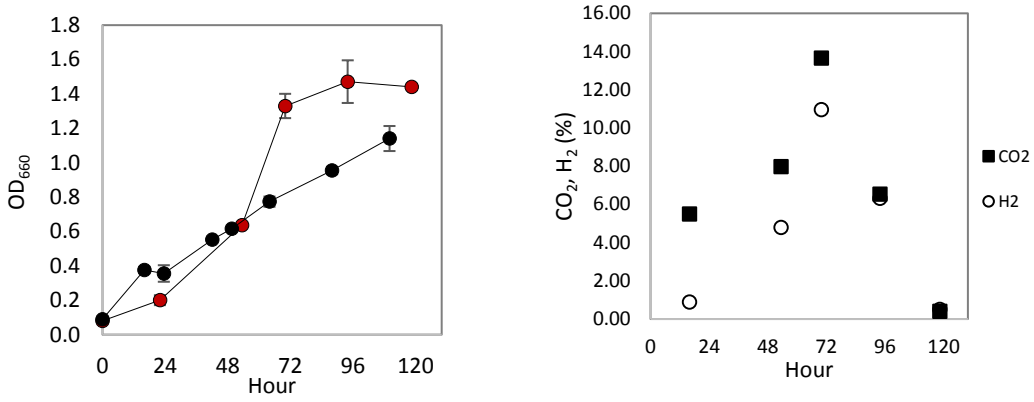

Figure 2-12 Single fructose feeding *vs* repetitive fructose supply.
On the left: growth trend of *R. rubrum* under 20% CO and 5 mM of fructose in the media (black circle) and under repetitive fructose feeding (red circle). On the right: hydrogen and carbon dioxide released under pulse feeding.

In addition to the mixotrophic condition proposed, a repetitive feeding of fructose was tested. Hence, samples daily fed with 5 mM of fructose and with CO were analysed after a pre-adaptation phase.

Figure 2-12 presents a comparison between single and daily pulse feeding of fructose under 20% of CO. A daily feeding of sugar improved *R. rubrum* biomass accumulation. The bacterium showed an exponential growth characterized by a μ of 0.04 h^{-1}, reaching a maximum OD_{660} of 1.5 in 96 hours. However, differently from single fructose feeding, the cultures ended to grow in 72 hours for entering the stationary phase. During the growth, presence of H_2 and a decreased concentration of CO confirmed that *R. rubrum* was able to use both substrates at the same time, with a higher evolution of carbon dioxide coming from the sugar oxidation.

(Figure 2-13.) The production of acetate was not parallel to the fructose consumption, and its concentration decreased after the first 24 hours of cultivation. In this case, the HPLC spectrum was generally more complex with respect to acetate fermentation, because of the high number of organic acids produced. Among them, it was recognised formic acid, which peaked 11 ± 2 mM in repetitive fructose feeding, while it reached 8.4 ± 0.4 mM under single fructose pulse.

On the other side, the analysis of PHB concentration inside the cell demonstrated that the accumulated PHB inside the cell was the lowest found, equal to 3%. From this information, it can be assumed that the carbon units coming from fructose (like acetate) were addressed more to biomass and other parallels metabolic routes, as the production of formic acid, or for the accumulation of the biomass than for the PHB accumulation. Acetate can participate to the pyruvate synthesis under CO feeding, from which a pyruvate-formate lyase synthesizes the formic acid (Revelles et al., 2016) (Jungermann and Schon, 1974; Schön and Voelskow, 1976). Because of the reactivity of this enzyme depends on the relative concentration of both compounds, once a threshold concentration of acetate coming from fructose (5 mM) was reached, it may have contributed to the pyruvate and formic acid production. In this way, the cell could

realise carbon and energy units in excess, and the production of PHB, depending also on NADH concentrations, was reduced.

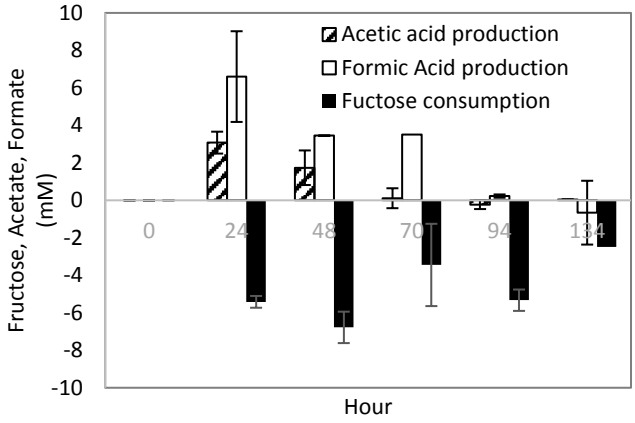

Figure 2-13 Fructose consumption and acetate and formic acid production over time, under daily fructose feeding pulse.

Analysis of carbon source investment in mixotrophic and autotrophic feeding

All the performed trials confirmed that during the cultivation phase, in *R. rubrum* the feeding of sugar serves to the accumulation of residual biomass, and the PHB biosynthesis was not favourited. However, a mixotrophic pre-adaptation gave the advantage to gain a higher titre of active biomass.
(Table 2-7) During the cultivation phase, repetitive fructose pulses improved biomass accumulation, which passed from 0.37 ± 0.05 to 0.5 ± 0.1 of g L^{-1} in respect to 0.29 ± 0.03 g L^{-1} of the autotrophic condition. The growth *R. rubrum* did not take advantage of the energy equivalents supplied by the sugar for a further PHB accumulation differently from what was found for *Clostridium ljundali*. Indeed, in this specie, the pre-adaptation made under syngas and fructose had a positive effects on the production of its cellular product, the ethanol, which jumped to a 20%, because more energy equivalents (e.g., ATP and GTP) and reducing power (e.g., NADH) were provided by a previous syngas-fructose adaptation (Tirado-Acevedo et al., 2011).
Calculation of carbon molar growth yield confirmed that autotrophic cultivations resulted in a better investment of carbon resources. The highest value was found in correspondence with autotrophic cultivation, with 48.33 mg $mmol^{-1}$ C mol^{-1}, in respect to mixotrophic conditions, in which it was 12 and 4 mg $mmol^{-1}$ C mol^{-1} for single and repetitive fructose feeding. Therefore, even if fructose guaranteed more carbon and energy power supply, a more fruitful investment of resources in terms of final biomass and PHB collected was guaranteed by a feeding strategy based on acetate and CO.

	CO	Condition	μ_1	μ_2	Biomass	Molar growth yield	PHB
			(h^{-1})	(h^{-1})	(gL^{-1})	(mg mol^{-1})[2]	(%)
Anaerobic, pure N_2	-	5 mM Fructose	0.08		0.13	4.3	
Pre-culture	-	5 mM Fructose	0.08	0.01			
Test trial	+	5 mM Fructose	0.06	0.01	0.37 ± 0.05	12	7%
	+	5 mM Fructose			0.5 ± 0.1	4	3%
Test trial		(pulse feeding every 24 h)	0.04				
Pre-culture	+	3 mM Acetate	0	0.03			
Culture	+	3 mM Acetate	0.03		0.29 ± 0.03	48.3	8%
Pre-culture		15 mM Fructose	0.08		0.23 ±0.01	7.6[3]	n.d.

Table 2-7 Growth rate, biomass and PHB production parameters found in different nutrient condition tested.

Phenotypic variation under mixotrophic cultivation conditions

During the experimental campaign, it was noted a change in the pigmentation of the biomass (Figure 2-14). In anaerobiosis, *R. rubrum* synthesized a purple-coloured chromophore, a bacteriochlorophyll, for catching natural sunlight in the photosynthetic membrane. However, in our samples, the colour of the biomass was pale pink, which is very different from what observed under syngas feeding, where it is usually purple (Karmann et al., 2019). Moreover, only in the samples fed by fructose, two different phenotypes appeared after culture centrifugation: (Figure 2-14): i) pale pink sedimentation, similar to those obtained in autotrophy condition, and ii) white pellet.

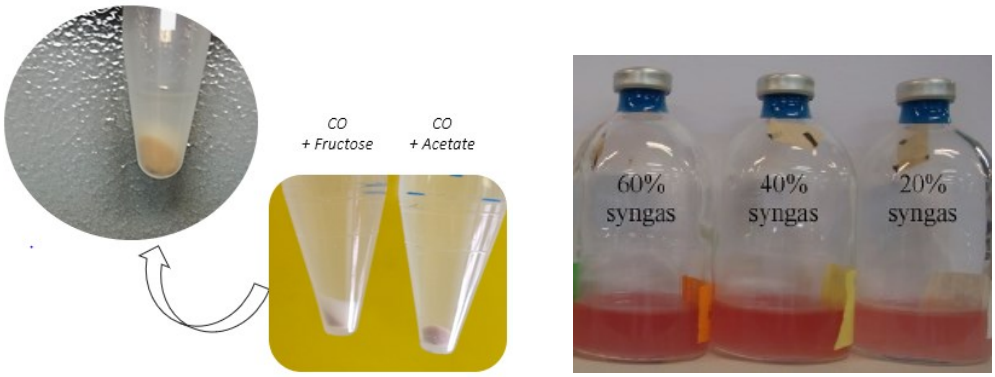

Figure 2-14 Variations in *R. rubrum* phenotype under different culture sugar feeding.
In yellow square, on the left the biomass cultured under fructose in presence of CO, on the right ones cultured under acetate and CO. On the right, an image taken from the work of Karmann, in which the bacterium was cultured under the same media composition, with 10 mM of acetate, changing syngas concentration into the headspace (Karmann et al., 2019).

[2] The molar growth yield was calculated as reported in the work of Schultz et al. 1982.
[3] This value was calculated taking into account the highest biomass concentration registered.

The loss of the bacteriochlorophyll under darkness was also reported in the work of Gorrel and Uffen, in which this strain was cultured in darkness with sodium pyruvate under anaerobiosis (Gorrel and Uffen, 1977). Moreover, it was reported that the production of the photosynthetic membrane depends on the redox potential of the cell. Indeed, under fructose and succinate, a decreased production of the photosynthetic membrane was related to a decrement of the central metabolic carbon cycle (Carius et al., 2013). Therefore, the phenotypic variation observed in the condition tested could be attributed to the metabolic conditions caused by the continues fructose feeding, which could block in part the synthesis of the photosynthetic membrane and pigments, as consequence.

2.4 Conclusions

This study faced the behaviour of *R. rubrum* exposes to different fermentation strategies applied under darkness in the presence of CO as the primary carbon source. The variation of carbon monoxide fed into the headspace evidenced a substantial limitation operated by CO on the biomass accumulation because carbon monoxide acts as a substrate and an inhibitor at the same time. It is the only source of energy for the cells, but it slows down the growth phase on the base of CO concentration fed. Therefore, the setting of a pre-adaptation phase resulted in a winning strategy for shortening the lag phase.

The concentration of carbon monoxide fed in pre-adaptation culture played an essential role in the trends observed in the cultivation phase. During pre-adaptation condition, 50% of carbon monoxide was identified as a threshold value for setting a homogeneous cultivation phase even at higher CO concentration. Therefore, samples pre-adapted under 50% of carbon monoxide showed similar growth trends. Such a behaviour that could depend on an acquired capacity to activate an efficient protein expression for the carbon monoxide conversion.

Besides, under a mixotrophic pre-adaptation, the CO exposition gave similar effect to *R. rubrum*, with a second cultivation cycle characterized by a faster growth rate and a shortening of the lag-phase.

As far as the production of PHB is concerned, the best feeding strategy was represented by autotrophic feeding, in which a more fruitful carbon units utilization could ensure higher PHB production. Hence, in autotrophic conditions, under 50% of daily CO feeding, the trend of PHB accumulation inside was linear and dependent on the acetate concentration.

Summing up, results indicated that for addressing a PHB production under sole CO as an energy source, the best liquid carbon source is acetate, which guarantees the highest biomass yield. However, a pre-adaptation phase based on 5 mM of fructose under continuous feeding of CO is suggested in order to obtain enough seeding culture ready to test.

2.5. References

Amos, W. A. (2004). Biological Water-gas Shift Conversion of Carbon Monoxide to Hydrogen: Milestone Completion Report (No. NREL/MP-560-35592). *National Renewable Energy Lab*., Golden, CO.(US).

Bonam, D., Lehman, L., Roberts, G. P., & Ludden, P. W. (1989). Regulation of carbon monoxide dehydrogenase and hydrogenase in *Rhodospirillum rubrum*: effects of CO and oxygen on synthesis and activity. *Journal of bacteriology*, 171(6), 3102-3107.

Bonam, D., Murrell, S. A., & Ludden, P. W. (1984). Carbon monoxide dehydrogenase from *Rhodospirillum rubrum*. *Journal of bacteriology*, 159(2), 693-699.

Braunegg, G., Sonnleitner, B. Y., & Lafferty, R. M. (1978). A rapid gas chromatographic method for the determination of poly-β-hydroxybutyric acid in microbial biomass. *European journal of applied microbiology and biotechnology*, 6(1), 29-37.

Carius, L., Hädicke, O., & Grammel, H. (2013). Stepwise reduction of the culture redox potential allows the analysis of microaerobic metabolism and photosynthetic membrane synthesis in *Rhodospirillum rubrum. Biotechnology and bioengineering*, 110(2), 573-585.

Do, Y. S., Smeenk, J., Broer, K. M., Kisting, C. J., Brown, R., Heindel, T. J., ... & DiSpirito, A. A. (2007). Growth of *Rhodospirillum rubrum* on synthesis gas: Conversion of CO to H2 and poly-β-hydroxyalkanoate. *Biotechnology and Bioengineerin*g, 97(2), 279-286.

Gorrell, T. E., & Uffen, R. L. (1977). Fermentative metabolism of pyruvate by *Rhodospirillum rubrum* after anaerobic growth in darkness. *Journal of bacteriology*, 131(2), 533-543.

https://earthobservatory.nasa.gov/global-maps/MOP_CO_M

Jungermann, K., & Schön, G. (1974). Pyruvate formate lyase in *Rhodospirillum rubrum* Ha adapted to anaerobic dark conditions. *Archives of microbiology*, 99(1), 109-116.

Karmann, S., Panke, S., & Zinn, M. (2019). Fed-Batch Cultivations of *Rhodospirillum rubrum* under multiple nutrient-limited growth conditions on syngas as a novel option topProduce poly (3-Hydroxybutyrate)(PHB). *Frontiers in bioengineering and biotechnology*, 7.

Kerby, R. L., Ludden, P. W., & Roberts, G. P. (1995). Carbon monoxide-dependent growth of *Rhodospirillum rubrum. Journal of Bacteriology*, 177(8), 2241-2244.

Lee, S. H., Kim, M. S., Lee, J. H., Kim, T. W., Bae, S. S., Lee, S. M., ... & Lee, J. H. (2016). Adaptive engineering of a hyperthermophilic archaeon on CO and discovering the underlying mechanism by multi-omics analysis. *Scientific reports*, 6, 22896.

Maness, P. C., & Weaver, P. (2001). Evidence for three distinct hydrogenase activities in Rhodospirillum rubrum. *Applied microbiology and biotechnology*, 57(5-6), 751-756.

Mohammadi, M., Mohamed, A. R., Najafpour, G. D., Younesi, H., & Uzir, M. H. (2014). Kinetic studies on fermentative production of biofuel from synthesis gas using *Clostridium ljungdahlii*. *The Scientific World Journal*, 2014.

Murray, P. A., & Uffen, R. L. (1988). Influence of cyclic AMP on the growth response and anaerobic metabolism of carbon monoxide in *Rhodocyclus gelatinosus. Archives of microbiology*, 149(4), 312-316.

Najafpour, G., Younesi, H., & Mohamed, A. R. (2003). Continuous hydrogen production via fermentation of synthesis gas. *Petroleum and coal*, 45(3/4), 154-158.

Novelli, P. C., Masarie, K. A., & Lang, P. M. (1998). Distributions and recent changes of

carbon monoxide in the lower troposphere. *Journal of Geophysical Research: Atmospheres*, 103(D15), 19015-19033.

Revelles, O., Calvillo, I., Prieto, A., & Prieto, M. A. (2015). Syngas Fermentation for Polyhydroxyalkanoate Production in *Rhodospirillum rubrum*. *In Hydrocarbon and Lipid Microbiology Protocols* (pp. 105-119). Springer, Berlin, Heidelberg.

Revelles, O., Tarazona, N., García, J. L., & Prieto, M. A. (2016). Carbon roadmap from syngas to polyhydroxyalkanoates in *Rhodospirillum rubrum*. *Environmental microbiology*, 18(2), 708-720.

Schön G, Voelskow H (1976) Pyruvate fermentation in *Rhodospirillum rubrum* and after transfer from aerobic to anaerobic conditions in the dark. *Arch Microbiol* 107:87–92

Schultz, J. E., & Weaver, P. F. (1982). Fermentation and anaerobic respiration by *Rhodospirillum rubrum* and *Rhodopseudomonas capsulata*. *Journal of bacteriology*, 149(1), 181-190.

Shelver, D., Kerby, R. L., He, Y., & Roberts, G. P. (1995). Carbon monoxide-induced activation of gene expression in *Rhodospirillum rubrum* requires the product of cooA, a member of the cyclic AMP receptor protein family of transcriptional regulators. *Journal of Bacteriology*, 177(8), 2157-2163.

Tirado-Acevedo, O., Cotter, J. L., Chinn, M. S., & Grunden, A. M. (2011). Influence of carbon source preadaptation on *Clostridium ljungdahlii* growth and product formation. J *Bioprocess Biotechniq* S, 2, 001.

Wu, M., Ren, Q., Durkin, A. S., Daugherty, S. C., Brinkac, L. M., Dodson, R. J., ... & Tallon, L. J. (2005). Life in hot carbon monoxide: the complete genome sequence of Carboxydothermus hydrogenoformans Z-2901. *PLoS genetics*, 1(5), e65.

Yasin, M., Jeong, Y., Park, S., Jeong, J., Lee, E. Y., Lovitt, R. W., ... & Chang, I. S. (2015). Microbial synthesis gas utilization and ways to resolve kinetic and mass-transfer limitations. *Bioresource technology*, 177, 361-374.

Yu, J., Flagan, R. C., & Seinfeld, J. H. (1998). Identification of products containing− COOH,− OH, and− CO in atmospheric oxidation of hydrocarbons. *Environmental Science & Technology*, 32(16), 2357-2370.

Zeiger, L., & Grammel, H. (2010). Model-based high cell density cultivation of *Rhodospirillum rubrum* under respiratory dark conditions. *Biotechnology and bioengineering*, 105(4), 729-739.

Chapter 3

Rhodospirillum rubrum growth and PHB production under medium-high pressure

3.1 Introduction

A significant limitation for gas-to-liquid fermentation is represented by the gas-liquid mass transfer, especially for carbon monoxide, which solubility in water is characterized by a low Henry's constant (because it is around 1 mmol amt^{-1} L^{-1} at 30°C). For *R. rubrum*, it was already demonstrated that a continuous suppliant of carbon monoxide at ambient pressure causes a decrease of specific CO consumption (Karmann et al., 2019). In our previous studies, the behaviour of *R. rubrum* was characterized on carbon monoxide feeding, concluding that an increase of CO concentration corresponded with an increase of biomass accumulation and a decrease of the specific growth rate. Moreover, in little scale (30 mL of medium in a closed bottle), *R. rubrum* converted around 100% of CO at ambient pressure producing at least 11% of PHB (Chapter 2).
In a liquid phase, the gas solubility is defined by Henry's law (Eq. 6):

$$c = Hp \qquad \text{Eq. 6}$$

which relates the concentration of a gas dissolved, c, with its partial pressure, p, and with a proportionality factor H. In particular, c is referred to the thermodynamic equilibrium conditions in the liquid phase, while H, called Henry's law constant, is specific for the gas analysed, that depends on the gas nature, on temperature and liquid phase composition. In turn, the partial pressure, p, depends on ambient pressure, P, and gas molar fraction, χ, as described by the following equation:

$$p = P\chi \qquad \text{Eq. 7}$$

In Eq. 7 the increase of environmental pressure affects gas partial pressure and, therefore, the gas concentration in the liquid phase. Consequently, a variation of this thermodynamic equilibrium also influences the kinetic trend of the gas transfer, due to a variation on the relative gas concentration. Indeed, the increase in the amount of gas

present into the liquid phase at the thermodynamic equilibrium, *C**, determines a relative improvement of the gas transfer motive force *(C*-Cl),* taking away the gas concentration at the gas-liquid interface, C_l, (Eq. 8):

$$\text{Gas Transfer Rate} = k_L a\ (C^* - C_l) \quad \text{Eq. 8}$$

In recent years, several works have focused on the gas transfer mechanism caused by the application of overpressure into microbial communities. Principally because this strategy reduces oxygen limitation in high-density aerobic cultures, giving the advantages to reach higher and higher products concentrations. For example, in 1992, Yang and colleagues tested a rise of pressure up to 2.7 atm, discovering that a significant availability of oxygen corresponded to a higher biomass yield (Yang and Wang, 1992). Such results were confirmed by the studies of Belo and colleagues, in which an increase of pressure up to 5 atm in *E. coli* fermentations, resulted into biomass and relative bioproduct increment (Belo et al., 1998). In addition, from a morphological point of view, in *S. caerevisiae,* it was proved that a gradual pressure rise, from 1 to 10 atm, prevents cellular damage.
On the other side, the application of pressure also carries some limitations. For instance, into aerobic fermentation, the increase of O_2 solubility is often associated with a production of reactive oxygen species, which are responsible for cellular oxidative stress (Belo et al., 2003). While, when the oxygen is not necessary to the cultivation, as in the case of deep-sea cultures of microorganisms, these problems are easily overcome (Zhang et al., 2011).
In the frame of PHB production under a gas-fermentation approach, any information is available on the effect of pressure on biomass growth and PHB accumulation into bioreactor scale. Therefore, for investigating it, a tailor-made reactor was designed to guarantee a maximum operating condition up to 8 atm, and the influence of the pressure on *R. rubrum* under CO feeding was tested concerning PHB production.

3.2. Material and methods

3.2.1. Fermentation strategy

The experimental design consisted of testing *R. rubrum* fermentation at 1 atm, and under a step-by-step pressure increase from 1 to 8 atm. The experimentation was made in 2L stainless steel bioreactor, designed for reaching up to 10 atm of working pressure. To limit CO inhibition events, a gradual pressure increase was applied, and the value of pressure was risen by 1 atm per 2 days (Figure 3-1).

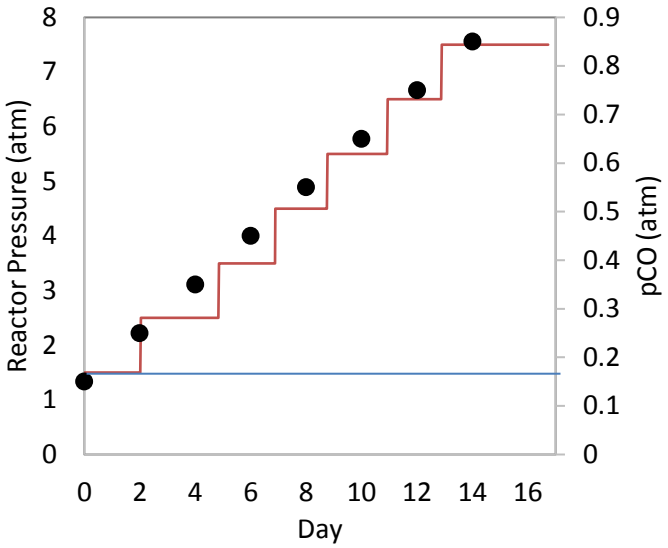

Figure 3-1 Scheme of fermentation strategy with increasing pressure.
The scheme represents both pressure conditions investigated: at ambient pressure (blue line), under a pressure increase (red line), and the respective CO partial pressure values (pCO) (black dots).

3.2.2. Bacterial strain cultivation

R. rubrum S1 (ATCC 11170), stored in 1.5 mL 15% glycerol stocks at -20°C was cultured in the experiment. As described by Karmann and colleagues (Karmann et al., 2017) precultures were grown in 160 mL screw-capped bottles, filled with 80 mL of RNNCO[4] medium at pH 7 supplied by 15 mM of fructose as primary carbon liquid source. The glycerol stocks were directly inoculated in the closed bottles and put under a gentle agitation of 200 rpm, at 30°C for 32 - 36 hours, up to reach an OD_{660} close to 1. During this first phase of growth, the cultures passed from aerobiosis to anaerobiosis consuming all the oxygen available.

Before reaching the stationary phase, an aliquot of grown cultures was seed into an anaerobic 130 mL screw-capped bottle to reach an OD_{660} of 0.1 (30 mL of RNNCO[5] medium at pH 7 supplied by 5 mM of fructose). Bottle headspace was filled with 20% CO and 80% N_2, which was restored every day. The pre-adaptation bottles were grown under a gentle agitation of 200 rpm, at 30°C for 5 days up to reach an OD_{660} over 1. On average for the seeding of 1 L of culture broth in the bioreactor, at least 4 bottles were prepared.

3.2.3. Bioreactor settings under pressure fermentation

A 2L stainless steel bioreactor was used for culturing the strain under different pressure conditions (Figure 3-2)[6]. A gas fed-batch fermentation was set to reproduce the same culture condition verified in screw-capped bottles. Hence, 1 L of sterile O_2-free RRNCO medium was added into the bioreactor vessel under anaerobic conditions.

[4,5] To find more information on RRNCO medium, go to Appendix

[6] For the reactor scheme look at Appendix

Pre-adapted seeding culture was inoculated at a final OD_{660} of 0.1. The fermentation was made under 30 °C at 200 rpm. During the fermentation, the bioreactor was sparged with 0.1 mL min^{-1} flux of 10% CO, 90% N_2. The pH was maintained constant by 4 M KOH and 3M H_2SO_4.

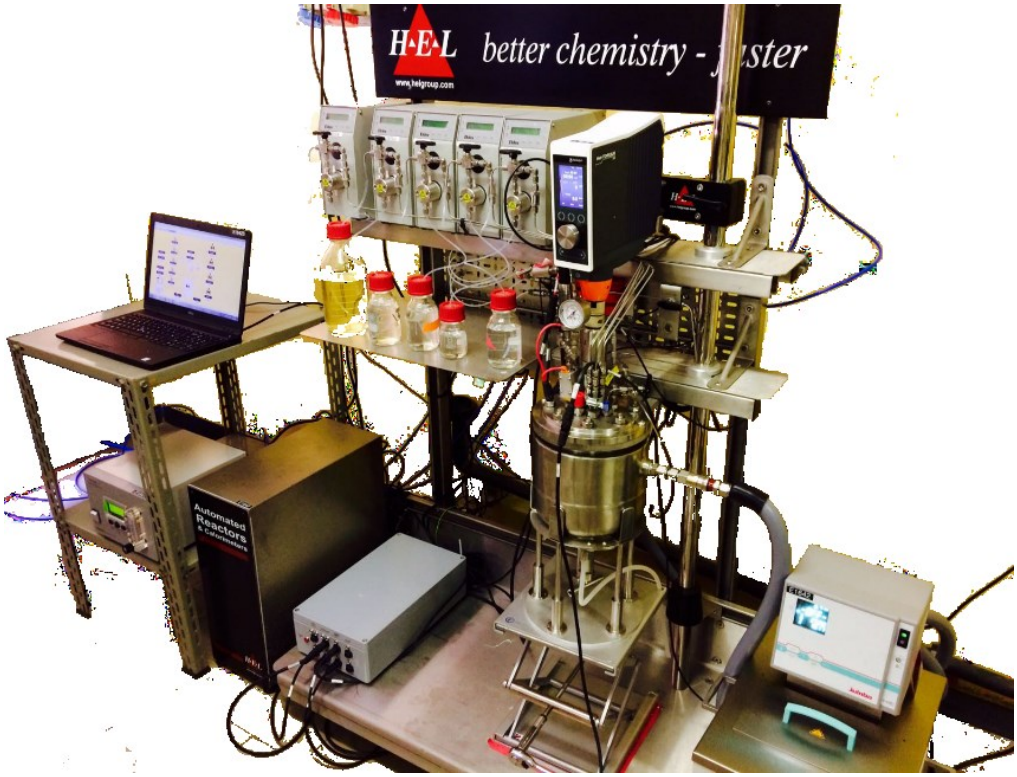

Figure 3-2 2L pressurized bioreactor designed for overpressure reactions and used during the experimentation.

3.2.4. Biomass quantification

Optical quantification of biomass was made measuring samples absorbance at 660 nm (Thermophischer). Cell dry weight was made gravimetrically. Hence, the samples collected were centrifuged at 10000 rpm for 5 minutes, washed two-times and air-dried at 80°C for 12 hours.

3.2.5. Acetate consumption determination

Acetic acid was detected by HPLC analysis (Shimatzu). After the sampling of the culture, the medium was filtered by a 0.2 µm cellulose nitrate filter and analysed with a column ROA-Organic Acid H^+ (8%) (Phenomenex) under an isocratic flux of 0.7 mL min^{-1} of 5 mM of H_2SO_4 and a temperature of 50 °C. Acetate was detected after 13.59 minutes of retention time, by RID detector.

3.2.6. PHB quantification

Biomass samples collected from the culture broth were centrifuged at 10000 rpm for 5 minutes, washed two-times and air-dried at 80°C for 12 hours. Once estimated

the correspondent biomass concentration (g L^{-1}), the dry biomasses were hydrolysed by 1 mL of 96% H_2SO_4 under stirring of 800 rpm, in an agitated oil bath at 90°C for one hour. At the end of the reaction, a dilution of 1:125 was done and the samples were analysed by a HPLC (Shimatzu) with a column ROA-Organic Acid H^+ (8%) (Phenomenex) with an isocratic flux of 0.7 mL min^{-1} of 5 mM of H_2SO_4 and a temperature of 50 °C. The PHB related signal appeared at 210 nm after 23.09 from the sample injection, which corresponds to the crotonic acid (the monomer coming from the PHB hydrolysate) (Braunegg et al., 1979).

3.2.6. Gas composition analysis

Gas was collected in 500 mL gas-bag, previously purged and put under vacuum. The collected gas was analysed by SRA Micro-GC equipped by a Molsive 5A column at a temperature of 100°C under argon as carrier gas (for the quantification of H_2, CO, N_2), and by a PoraPLOT U column at 85°C using helium as carrier gas (for CO_2 analysis).

Gas quantification

Starting from the relative concentration of the carbon monoxide added into the bottles or inside the reactor headspace, the correspondent amount of CO was calculated by the Eq. 9, where *P* is the pressure, *V* is the volume of the headspace, *R* is the Boltzman constant (0.082 L atm mol^{-1} K^{-1}), and *T* is the temperature:

$$PV = nRT \qquad \text{Eq. 9}$$

Hence, the number of moles, *n,* was determined and multiplying it for the relative gas concentration, the correspondent number of moles of CO, H_2 and CO_2 were found. Consequently, the concentration of gas on the base of Henry's law (Eq. 6)[7] was determined.

3.2.7. Calculations

The specific growth rate (μ), was calculated during the exponential growth phase. Data were fitted with exponential and linear growth trend as reported in Table 3-1.

Kinetic growth models		
Linear growth	$X = \mu X + at$	Eq. 10
Exponential growth	$X = X_0\, e^{\mu t}$	Eq. 11

[7] Henry's law: $c = Hp$

Logistic growth (Volterra's model)	$X = \frac{X_0 e^{\mu t}}{1-\left(\frac{X_0}{X_{max}}\right)(1-e^{\mu t})}$	Eq. 12

Table 3-1 Growth model used for fitting biomass accumulation data.

The fitting was corrected by the least square method, so the model presenting the highest R^2 was chosen and correspondent μ was calculated.
The yield of PHB on the substrate and the volumetric productivity were calculated with Eq. 13 and Eq. 14 :

$$Y_{\frac{PHB}{S}} = \frac{(PHB_{fin} - PHB_{in})}{(S_i - S_f)} \quad \text{Eq. 13}$$

$$Q_{PHB} = \mu \, x \, PHB \quad \text{Eq. 14}$$

3.3. Results and discussions

3.3.1 Biomass growth

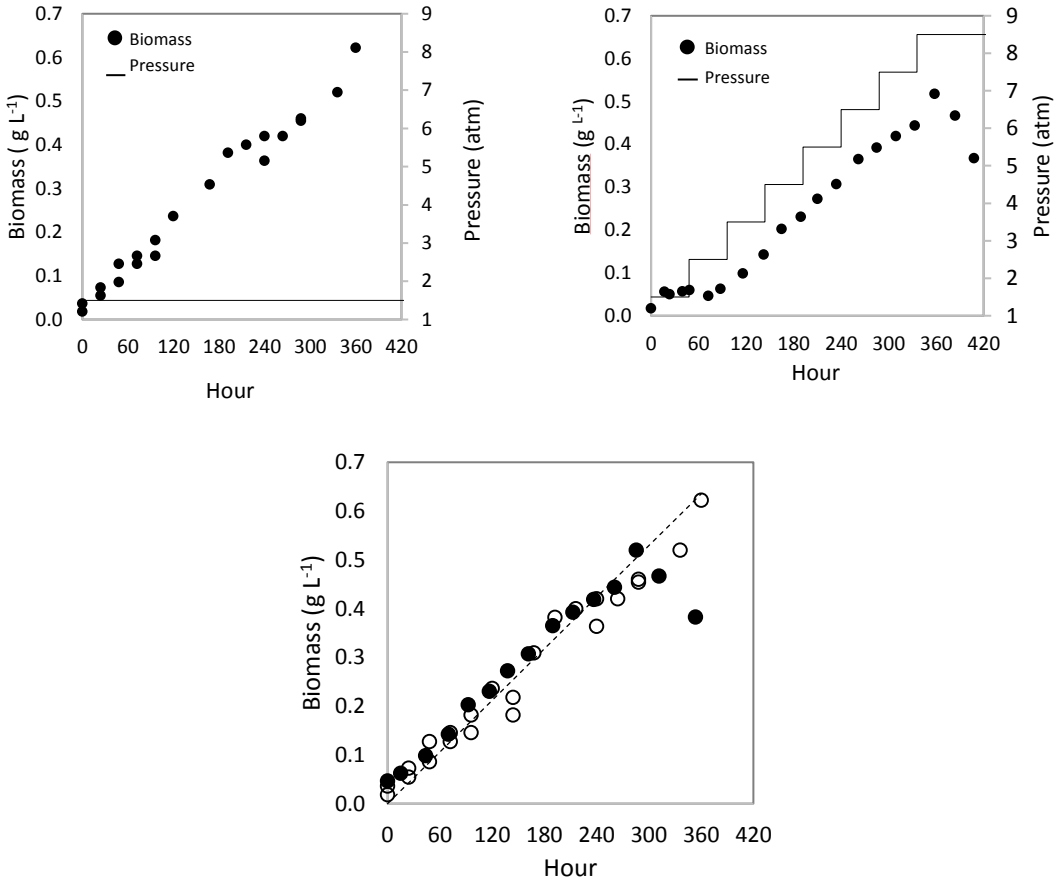

Figure 3-3 The *R. rubrum* growth under different pressure conditions.
On the left: biomass accumulation at constant pressure. On the right: biomass accumulation under pressure increasing strategy. On the bottom, a comparison of both fermentation strategies where: (○) (●) represent the fermentation with constant and increasing pressure, respectively. In dotted line the liner fitting which presented an R^2 of 0.97.

Figure 3-3 presents a comparison between *R. rubrum* biomass accumulation at 1 atm and under an increase of pressure from 1 to 8 atm made with a step-by-step pressure increasing. Due to technical reason, the trial made under pressure was not pre-adapted; therefore, a more prolonged lag phase of around 60 hours was present. As demonstrated in Chapter 2, pre-adaptation influences the lag phase, while the biomass yield is not negatively affected by carbon dioxide feeding. In this case, after the 4^{th} day of cultivation, the growth proceeded linearly, allowing to compare both experimental settings during the growth phase.

Even with pressure increase, *R. rubrum* maintained the same linear growth trend characterized by a biomass accumulation of 1.47 ± 0.03 mg L^{-1} h^{-1}. This accumulated biomass was well fitted with a linear growth model, having an R^2 of 0.97, and the specific growth rate, μ, was calculated. The results showed a μ of 0.06 h^{-1} for both fermentation systems, confirming that any influence from pressure increase on the biomass accumulation occurred.

The step-by-step pressure increase resulted in a suitable fermentation condition for avoiding slowing down events caused by CO inhibition. During the last days of cultivation, the *R. rubrum* biomass decreased, probably because the culture entered a stationary phase, while under constant pressure it continued linearly.

The linear trend is typical of gas-fermentation. It was verified when *R. rubrum* was cultured under syngas, in darkness and under ambient pressure. For instance, this trend was verified when the strain was cultured with a mixture of $CO:H_2:CO_2:N_2$ at a ratio of 40:40:10:10 (Karmann et al., 2019). However, even in the presence of carbon monoxide, its growth can assume an exponential fitting when the energy source for the cell is coming from the light (Klasson et al., 1993)(Najafpour et al., 2007). Consequently, the bacterial growth is strongly affected by the energy supplied represented by light, or by the sole presence CO under darkness. Therefore, it could be concluded that in the range of pressure tested, the improved solubility of CO does not satisfy the cellular energy requirement. As a consequence, a linear-growth model is suggested to forecast the biomass accumulation due to an energy-limited trend.

3.3.2. PHB production and acetate consumption

The acetate consumption was higher at ambient pressure in comparison to the fermentation exposed at increasing pressure. During the fermentation performed at 1 atm, the acetate consumption was almost double, corresponding to 0.023 mM h^{-1} at constant pressure, in comparison with 0.01 mM h^{-1}, obtained under the pressurized system. However, the accumulation of the PHB followed an opposite trend, passing from 11% of accumulated PHB at ambient pressure, to 37% found in the pressurized fermentation, as shown in Figure 3-4.

The most critical difference was in correspondence to the PHB accumulation trend. At constant pressure, PHB accumulation was almost stable, floating between 11 and 13%. While at increasing pressure, it sharply improved in correspondence with the highest pressure tested (7 atm), where an improvement of PHB accumulation rate was

noted in comparison to the residual biomass growth trend. Hence, this increased accumulation of PHB under pressure resulted in a higher volumetric productivity and products yield (with a respective Q_{PHB} 3.7 mg L^{-1} h^{-1}, and $Y_{PHB/S}$ of 0.34 g g^{-1}).
Usually, under syngas *R. rubrum* presented a stable PHB accumulation trend as claimed by the studies published by the group of Prof. Zinn or by the work of Do and colleagues (Karman et al., 2017) (Karmann et al., 2019) (Do et al., 2007). However, to the best literature review made for this study, there aren't other comparable results under overpressure conditions.

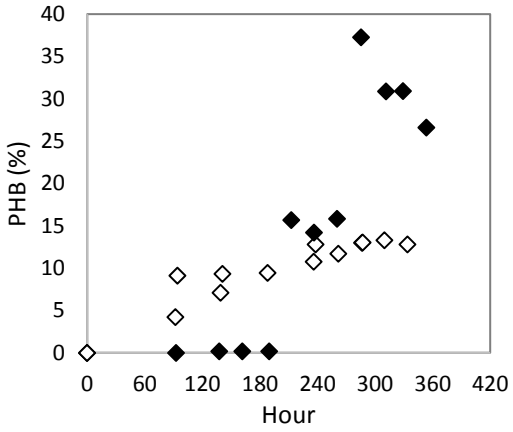

Figure 3-4 PHB production at constant and increasing pressure fermentation.
In the graph, the PHB production correspondent to the growth phase is represented for fermentation made at constant pressure (◊) and for fermentation made with increasing pressure (♦).

pCO/Ptot	X_{max}	μ	Acetate consumption rate	$Y_{PHB/S}$	PHB_{max}	PHB	PHB productivity
(/)	(g L^{-1})	(h^{-1})	(mM h^{-1})	(g g^{-1})	(%)	(g L^{-1})	(mg L^{-1} h^{-1})
0.1	0.49 ± 0.05	0.06	0.023	0.29	13.16 ± 0.18	0.06 ± 0.01	1.3
0.1 – 0.8	0.47	0.06	0.01	0.34	37	0.17	3.7

Table 3-2 Final biomass, growth specific rate "μ", acetate consumption rate and PHB yield and productivity of *R. rubrum* cultured at ambient and at increasing pressure in 2L reactor.

3.3.3. Gas evolution

In darkness condition, the growth of *R. rubrum* is energetically sustained by the presence of CO, which gives birth to the release of CO_2 and H_2 at a ratio 1:1, as demonstrated in Chapter 2.
Due to technical reasons, it was not possible to log gas data belonging to constant pressure fermentations. However, both information coming from literature and our previous studies agree with the fact that under a constant pressure, the consumption of CO and the relative release of CO_2 and H_2 follows a stable trend when the gas feeding is kept constant (Karman et al., 2016).
In Figure 3-5 the amount of carbon dioxide and hydrogen released in the pressurized system is reported. After the lag phase, in which carbon dioxide and hydrogen were not developed, the strain started to grow releasing both H_2 and CO_2 with a linear trend. As well as for the case of environmental pressure condition. Under increasing pressure,

the amount of produced gas remained almost stable with the accumulated biomass, varying between 1 to 2 mmol g^{-1} biomass h^{-1}. Even if a little deviation was appreciable during the last part of the fermentation.

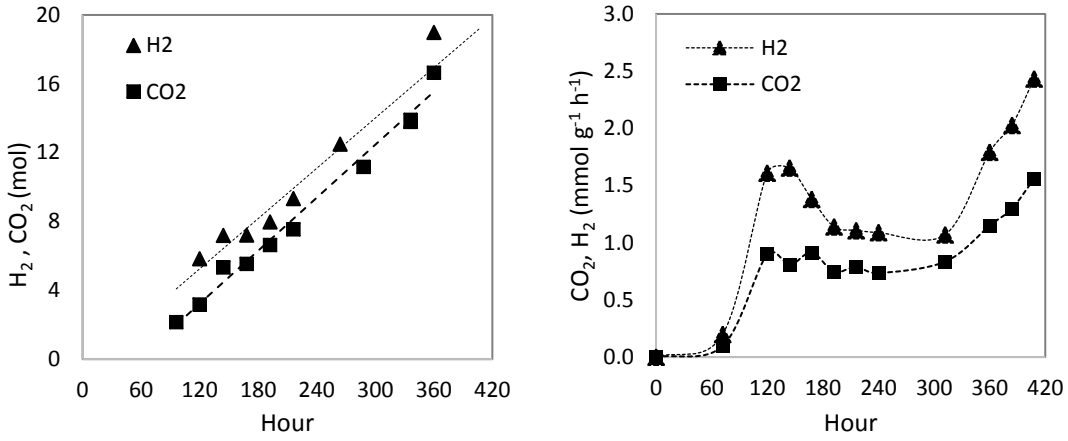

Figure 3-5 Gas evolution profile under increasing pressure.
On the left: the relative concentration of H_2 (triangle) and CO_2 (square) over time. On the right, the gas amount released in relation with biomass concentration.

These data suggest that an increase in pressure did not improve the efficiency of carbon monoxide conversion process since the amount of consumed CO was equal to the amount of hydrogen released.

About the CO consumption efficiency per produced biomass, similar values were also found when the bacterium was cultured at ambient pressure with a stable concentration of carbon monoxide, under a CSTR configuration. In particular, *R. rubrum* performed a CO uptake of 11 mmol g^{-1} biomass h^{-1} under CO and light irradiation, while under continuous feeding of syngas in darkness it showed a consumption of 7 mmol g^{-1} biomass h^{-1}, which are both values very close to what found in this study (Klasson et al., 1993) (Karmann et al., 2019).

It is important to remark that the only difference discovered under the pressurized was referred to CO_2 production that was lower with respect to the theoretical values, with CO_2 sequestration of about 34 ± 5 % than H_2 evolved.

3.3.4. Fermentation strategy comparison

Contrary to what expected, the increase of pressure did not show a different growth trend under the pressure range analysed, and the amount of consumed gas per biomass was in the same order of magnitude of similar researches made at ambient pressure. However, differences in PHB accumulation, acetate consumption and gas releasing were evidenced in the pressurized fermentation.

As demonstrated in the Revelles' work and the study made by Uffen, this family of bacteria can sequestrate carbon dioxide and reduce it using different metabolic routes (Revelles et al., 2016) (Uffen et al., 1983). Among them, the most famous and efficient route is represented by the Calvin-Benson-Bassham (CBB) cycle in which the CO_2 is inserted in a ribulose 1,5-bifosphate. Nevertheless, under darkness, CBB cycle is partially active, taking part only in the balancing of cellular redox potential.

Hence, its contribution to CO_2 assimilation must be excluded from the fermentation conditions tested.

Carboxylation reactions	k_m (mM)	Reference
Pyruvate synthase Acetyl-CoA + NADPH + CO_2 ⇆ Pyruvate + CoA + $NADP^+$	2	(Furdui et al., 2000)
α-ketoglutarate synthase Succinil-CoA + CO_2 + 2-ferredoxin$_{RED}$2 ⇄ 2-oxoglutarate + CoA + 2-ferredoxin$_{OX}$	n.d.	
crotonyl-CoA reductase Crotonyl-CoA + CO_2 + NADH ⇆ ethylmalonyl-CoA + NAD^+	14	(Erb et al., 2007)
propionyl-CoA carboxylase Propionyl-CoA + ATP + CO_2 ⇆ methylmalonyl-CoA + ADP + Pi + H^+	0.3	(Hügler et al., 2003)

Table 3-3 Carboxylation reactions in *R. rubrum*.
The table lists the carboxylation reactions present in *R. rubrum* alternative to the Calvin-Benson-Bassham.

As anticipated in Chapter 1, CO_2 can also be assimilated by other metabolic branches, in which a *pyruvate synthase,* a *α-ketoglutarate synthase*, a *crotonyl-CoA reductase,* and a *propionyl-CoA carboxylase* catalyse carboxylation reactions. The first two enzymes belong to the tricarboxylic acid cycle (TCA), that are exclusively expressed in *R. rubrum* in the class of purple-non-sulphur bacteria. These two enzymes add carbon dioxide on acetyl-CoA and succinyl-CoA, respectively, thanks to electrons coming from reduced ferredoxin. While, crotonyl-CoA reductase and propionyl-CoA carboxylase, which belong to the ethylmalonyl-coenzyme A cycle (EM-CoA), assembled CO_2 on crotonyl and propionyl-Co-A with the energetic contribution of NADH, as reported in the Table 3-3(Revelles et al., 2016)(Hädicke et al., 2011)(Buchanan et al., 1967). It is interesting to note that all the listed enzymes are characterized by a k_m for the solubilized CO_2 (HCO_3^-), ranging from between 0.3 mM to 14 mM, which is lower in respect to the CO_2 concentrations calculated in our experiments, that ranges from 0.01 mM to 0.400 mM, at 3 and 8 atm, respectively. Consequently, it can be concluded that these carboxylases were working below their theoretical optimum conversion rate. However, to an increase of pressure, an increase of solubilized carbon dioxide into the liquid phase could favour carboxylation events, determining significant gas sequestration.

Moreover, as described in Table 3-3, carboxylation reactions need the contribution coming from ATP and NADH units, which depend on the power input coming from carbon monoxide. More in detail, while NADH principally comes from TCA, the main contribution for ATP production depends on the CO conversion. Indeed, in the proximity of the cell membrane, there is the formation of a proton gradient, which supply ATP units by the generation of H_2 coupled with ADP phosphorylation reactions (Maness et al., 2005) (Figure 3.6). Therefore, after a pressure improvement, carboxylation reactions could be advantaged by an increase in carbon dioxide concentration.

Successively, the depending molecular products could be used by the cell to sustain TCA and biomass, favouring the conversion of acetate into PHB. In this way, a lower

acetate cost for cell metabolism under pressurized system could be explained. As demonstrated for *Rhodopseudomonas palustris*, where an increase of CO partial pressure involved an improvement of net ATP production, and of the net bioproduct accumulation, which in this case was the ethanol (Hurts et la., 2010).

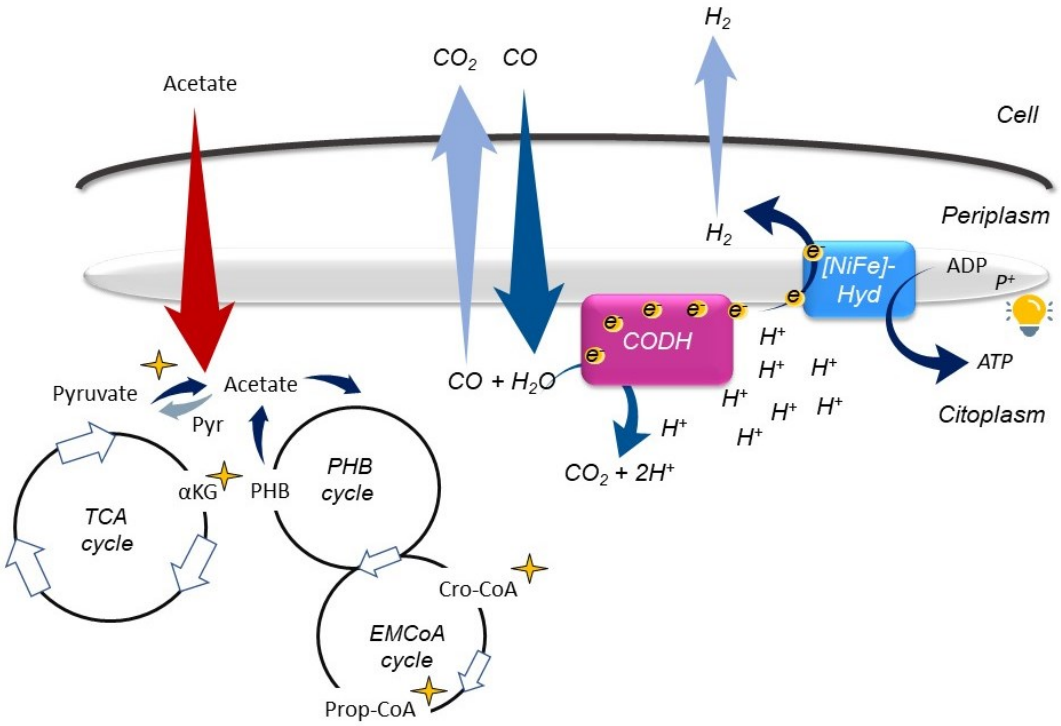

Figure 3-6 Basic *R. rubrum* metabolic map representing carboxylation reactions.
In the image, carbon monoxide (CO) enters in the cell, and a carbon-monoxide dehydrogenase converts it into CO_2 and H^+ and electrons (e^-). Therefore, a flux of protons can be used by the cell for producing H_2 molecules in parallel to the phosphorylation of an ADP in ATP. Then CO_2 can be assimilated by the cell in different carboxylation reactions (stars): in ethylmalonyl-coenzyme A cycle (EM-CoA) by *crotonyl-CoA reductase* (Cro-CoA) and by *propionyl-CoA carboxylase* (Prop-CoA), tricarboxylic acid cycle (TCA) by *α-ketoglutarate synthase* (αKG) and by *pyruvate synthase* (Pyr).

3.5 Conclusions

By this study, it was confirmed that *R. rubrum* shows a linear trend under gas feeding at different pressure conditions. The application of a dynamic increase of pressure did not favour the biomass accumulation, and a linear growth trend was verified even in the presence of an overpressure. As well as an increase in pressure did not support the amount of consumed gas. Hence, up to a pressure of 8 atm, an energy-limited mechanism could influence the growth of *R. rubrum*. However, a parallel rise of carbon dioxide sequestration and of the cellular metabolic activity was evidenced.
In this condition, the PHB synthesised was 3-times higher in respect to the fermentation made at ambient pressure. Thus, the application of mild pressure values could be a winning strategy for improving the production of those reactions depending on more soluble gasses like carbon dioxide. And, as results indicated, higher productivity of PHB could be reached.

3.6. References

Belo, I., & Mota, M. (1998). Batch and fed-batch cultures of *E. coli* TB1 at different oxygen transfer rates. *Bioprocess Engineering*, 18(6), 451-455.

Belo, I., Pinheiro, R., & Mota, M. (2003). Fed-batch cultivation of Saccharomyces cerevisiae in a hyperbaric bioreactor. *Biotechnology progress*, 19(2), 665-671.

Do, Y. S., Smeenk, J., Broer, K. M., Kisting, C. J., Brown, R., Heindel, T. J., ... & DiSpirito, A. A. (2007). Growth of *Rhodospirillum rubrum* on synthesis gas: Conversion of CO to H2 and poly-β-hydroxyalkanoate. *Biotechnology and Bioengineerin*g, 97(2), 279-286.

Erb, T. J., Berg, I. A., Brecht, V., Müller, M., Fuchs, G., & Alber, B. E. (2007). Synthesis of C5-dicarboxylic acids from C2-units involving crotonyl-CoA carboxylase/reductase: the ethylmalonyl-CoA pathway. *Proceedings of the National Academy of Sciences*, 104(25), 10631-10636.

Furdui, C., & Ragsdale, S. W. (2000). The role of pyruvate ferredoxin oxidoreductase in pyruvate synthesis during autotrophic growth by the Wood-Ljungdahl pathway. *Journal of Biological Chemistry*, 275(37), 28494-28499.

Hügler, M., Krieger, R. S., Jahn, M., & Fuchs, G. (2003). Characterization of acetyl-CoA/propionyl-CoA carboxylase in Metallosphaera sedula: Carboxylating enzyme in the 3-hydroxypropionate cycle for autotrophic carbon fixation. *European journal of biochemistry*, 270(4), 736-744.

Hurst, K. M., & Lewis, R. S. (2010). Carbon monoxide partial pressure effects on the metabolic process of syngas fermentation. *Biochemical Engineering Journal*, 48(2), 159-165.

Karmann, S., Follonier, S., Egger, D., Hebel, D., Panke, S., & Zinn, M. (2017). Tailor-made PAT platform for safe syngas fermentations in batch, fed-batch and chemostat mode with *Rhodospirillum rubrum*. *Microbial biotechnology*, 10(6), 1365-1375.

Karmann, S., Panke, S., & Zinn, M. (2019). Fed-Batch Cultivations of *Rhodospirillum rubrum* Under Multiple Nutrient-Limited Growth Conditions on Syngas as a Novel Option to Produce Poly (3-Hydroxybutyrate)(PHB). *Frontiers in bioengineering and biotechnology*, 7.

Klasson, K. T., Lundbäck, K. M. O., Clausen, E. C., & Gaddy, J. L. (1993). Kinetics of light limited growth and biological hydrogen production from carbon monoxide and water by *Rhodospirillum rubrum. Journal of biotechnology*, 29(1-2), 177-188.

Maness, P. C., Huang, J., Smolinski, S., Tek, V., & Vanzin, G. (2005). Energy generation from the CO oxidation-hydrogen production pathway in *Rubrivivax gelatinosus*. *Applied and Environmental Microbiology*, 71(6), 2870-2874.

Najafpour, G. D., & Younesi, H. (2007). Bioconversion of synthesis gas to hydrogen using a light-dependent photosynthetic bacterium, *Rhodospirillum rubrum*. *World journal of microbiology and biotechnology*, 23(2), 275-284.

Najafpour, G., Younesi, H., & Mohamed, A. R. (2003). Continuous hydrogen production via fermentation of synthesis gas. *Petroleum and coal*, 45(3/4), 154-158.

Revelles, O., Tarazona, N., García, J. L., & Prieto, M. A. (2016). Carbon roadmap from syngas to polyhydroxyalkanoates in *Rhodospirillum rubrum. Environmental microbiology,* 18(2), 708-720.

Uffen, R. L. (1983). Metabolism of carbon monoxide by *Rhodopseudomonas gelatinosa*:

cell growth and properties of the oxidation system. *Journal of bacteriology,* 155(3), 956-96

Yang, J. D., & Wang, N. S. (1992). Oxygen mass transfer enhancement via fermentor headspace pressurization. *Biotechnology progress*, 8(3), 244-251.

Zhang, Y., Arends, J. B., Van de Wiele, T., & Boon, N. (2011). Bioreactor technology in marine microbiology: from design to future application. *Biotechnology advances*, 29(3), 312-321.

Chapter 4

Optimization study of volumetric PHB production by *Azotobacter vinelandii* OP

1.4. Introduction

The former and the highly productive way to produce PHB is based on aerobic fermentation and sugars conversions. Even if gas-based fermentations offer the potentiality to reduce economic and environmental costs of production, this cutting-edge investigation area has not reached a sufficient grade of technology readiness level for a rapid diffusion yet.

Among the goals of this investigation, there are also concerns around those fermentations characterized by high growth rates and PHB accumulation, as those offered by aerobic strains. *Azotobacter vinelandii* is a strict aerobic gram-negative soil bacterium, which is able to accumulate up to 80% of PHB of its cellular dry weight. Besides this high PHB accumulation capacity, this specie is known for maintaining constant the polymer molecular mass over standard fermentation conditions, which is a good quality for a further application of plastic material (Peña et al., 2014).

In *A. vinelandii*, oxygen-limited conditions negatively affect the production of the biopolymer inside the cell, but also oxygen favours the biomass accumulation. Indeed, it was demonstrated that the PHB production is regulated by oxygen transfer rate (OTR), and that the PHB productivity peaked 0.18 g L^{-1} h^{-1} in batch fermentation (Díaz-Barrera et al., 2016). However, improvements in its production were verified by the application of pulse feeding strategies, that allowed a 50% increase of biomass yield (Castillo et al., 2017).

Because of this dual effect of oxygen both on biomass and PHB accumulation, this experimental session is dedicated to the optimization of PHB production based on the influence of gas availability on the PHB volumetric productivity (Q_{PHB}). More in detail, in this session of the work the productivity of PHB was put in relation with oxygen mass transfer, considering the variation of the mass transfer constant, k_La, on the final PHB yield., The k_La is a scalable parameter that not only allowed to correlate the fermentation parameters with PHB production trends but also to forecast the fermentation setting for higher volumetric scale-up.

4.2 Material and Methods

4.2.1. Inoculum preparation

A. vinelandii OP (or UW) was cultured into Burk's nitrogen-free medium prepared at pH 7 and hosted 30 g L^{-1} of sucrose. The medium was prepared as described in the Appendix session and sterilized by autoclave at 121 °C for 20 min.

The inoculum was prepared from a glycerol stock, following the scheme here proposed (Figure 4-1).

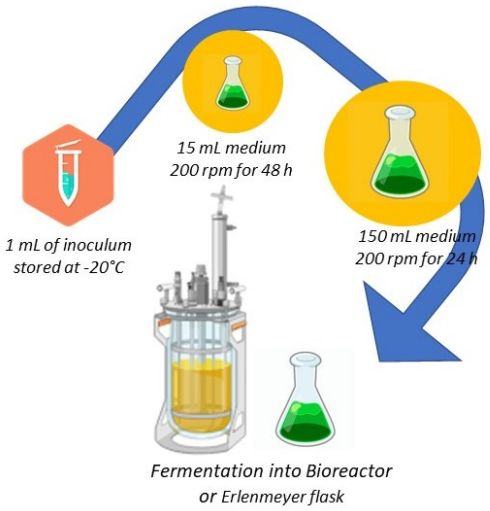

Figure 4-1 Propagation procedure for *A. vinelandii* fermentation.
In the image, the standard procedure of *A. vinelandii* cultivation is reported from the inoculum of a glycerol stock stored at -20°C to the final cultivation set in a bioreactor or flask.

A glycerol stock of the strain was initially cultured into 150 mL of culture medium at 200 rpm and 30 °C in an orbital incubator shaker (New Brunswick, model C24, USA). After 48h of cultivation, this seeding culture was transferred entirely into 500 mL Erlenmeyer flasks, containing 150 mL of the Burk's medium. The biomass was cultured at the same conditions for other 24 hours, after which it will be ready for the experimental run.

4.2.2. Bioreactor setting

A 3L stirred tank bioreactor (Applikon, Schiedam, Netherlands) was used for the upper scale test (Figure 4-2). The tank was filled with 1.5 L of Burk's medium and sterilized. Then, before to inoculate the seeding culture, sterile salt solution and $CaCl_2$ were added under sterile condition.

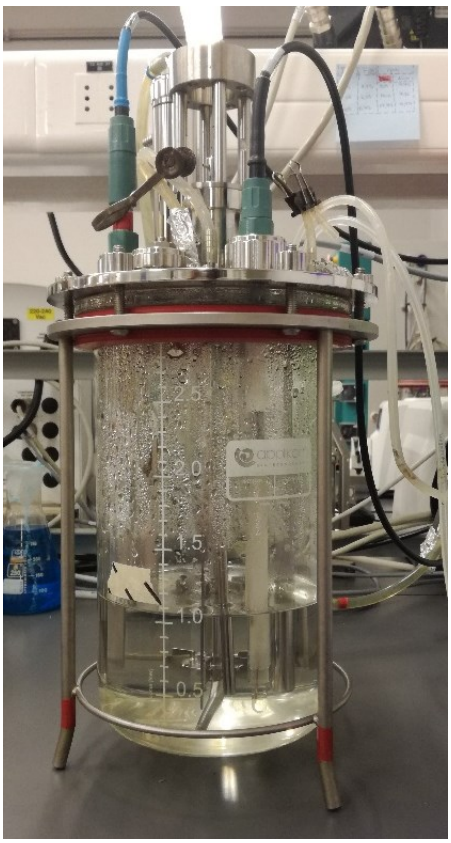

Figure 4-2 The 3L Applikon bioreactor used in this work.
For keeping the temperature constant, the tank was covered by a controlled jacked (here not shown).

For the fed-batch experiment, 0.150 L of seeding culture was inoculated into the reactor, and the batch phase was started under stirring of 600 rpm, which last 30h in order to allow the consumption of the sucrose up to 10 g L^{-1}. Successively, the feeding-stage started. The culture was fed with 10% of concentred Burk's medium for restoring the carbon source, and the micronutrient and the agitation rate was varied from 400 to 1000 rpm.
Fermentations were conducted at 30 ° C, with a controlled airflow fixed at 1.5 L min^{-1}, (1 vvm). A constant pH of 7.0 was maintained by 2 M NaOH and 2 M HCl solutions.

4.2.3. Analytic determinations

The cell dry weight was calculated gravimetrically. 5 mL of culture broth was centrifuged, washed two-times with deionized water and dry over-night at 80.5 °C. Only after these steps, the dried biomass was weighted.
The sugar content is ensured by dinitrosalicylic acid method. Therefore, a sample of the medium taken after centrifugation of the biomass culture was hydrolysed with concentrated HCl at 100°C, and the reducing sugar concentration was estimated by a spectrophotometric detection of reducing sugar at 540 nm.

4.2.4. PHB determination

The quantification of the biopolymer was made by hydrolysing the biomass into pure H_2SO_4 for 1 hour at 90°C. In this way, the conversion of PHB into croton acid unit was ensured. The hydrolysed solution was diluted and quantified by HPLC–UV with an Aminex HPX-87H ion-exclusion organic acid column, with a 0.005 M H_2SO_4 as mobile phase, fluxed at 0.6 mL min^{-1} under a temperature of 35 °C.

4.2.4. k_La determination

The k_La was determined by the dynamic gassing-out method applied to a complete medium without the presence of the cell (Garcia-Ochoa et al., 2000). The culture medium under a temperature of 30°C was first sparged with N_2 up to the reach the medium saturation, and successively, a flux of air was sparged and kept until a saturation signal was reached.
The test was made 1 vvm and applying from 200 to 1000 rpm. During the test, the dissolved oxygen tension (DOT) was measured describing oxygen desorption and absorption trends.

The values of k_La were obtained solving the following equation, respectively for absorption ad desorption curves:

$$\frac{dC}{dt} = k_L a(C^* - C_l) \quad \text{Eq. 15}$$

where, C^* is the gas dissolved at the thermodynamic equilibrium, and C_l is the gas concentration in the bulk and measured by a probe. The results of Eq. 15 are:

Absorption equation: $ln\left(1 - \frac{C_l}{C^*}\right) = k_L a\ t$ Eq. 16

Desorption equation: $ln\left(\frac{C^*}{C_l}\right) = k_L a\ t$ Eq. 17

The k_La value was obtained graphing the obtained data, previously linearized following the equation solutions (Eq. 16,Eq. 17).
(Eq. 15)The gas transfer coefficient, k_La, is a physics parameter necessary for the identification of the gas transfer rate from the gas phase of the sparged gas, to the liquid phase in which the bacteria growth.
This constant is strongly dependent on the experimental conditions used and on the geometrical feature of the vessel, it is also a scalable fermentation parameter. Therefore, to understand if the influence of the agitation rate on PHB productivity, the respective k_La was characterized for each stirring rate tested.

4.2.5. Parameters calculation

The specific growth rate (μ), was calculated during the exponential growth phase. Data referring to the exponential phase were linearized, and the correspondent growth rate was calculated. This value was also corrected, fitting the data by the exponential growth model and adjusting it with the least square method. Here, the exponential growth is reported in Eq. 18:

$$X = X_0\, e^{\mu t} \qquad \text{Eq. 18}$$

Other fermentation parameters were calculated as follows.

Sucrose yield on biomass $Y_{X/S} = \frac{X_{max} - X_0}{S_0 - S};$ Eq. 19

Where X represents the biomass (g L^{-1}), while S (g L^{-1}) stands for the sucrose concentration, respectively at the beginning of the fermentation X_0 and S_0, and X_{max} and S at a time when the cellular concentration it is maximum.

PHB yield on sucrose consumption $Y_{PHB/S} = \frac{PHB_{max} - PHB_0}{S_0 - S};$ Eq. 20

Calculated as well as for the $Y_{X/S}$.

PHB volumetric productivity $Q_{PHB} = \mu \cdot PHB_{max};$ Eq. 21

To evaluate the influence of eddies and evaluate possible shear stress, the dimension of the littlest eddies generated at each tested agitation rate was analysed by the following equation:

Kolmogorov's scale $\eta = (\frac{\nu^3}{\varepsilon})^{\frac{1}{4}};$ Eq. 22

where ν was the cinematic viscosity, ε was the energy dissipation rate per unit mass, which were calculated as by:

$$\nu = \frac{\mu}{\rho}; \qquad \text{Eq. 23}$$

in which the μ is the molecular viscosity and ρ the density of the medium. Assuming that the cultivation medium behaves like water, μ is equal to 0.7978 mPas and ρ is 1000 kg m^{-3}; which gave a ν of 0.801 x 10^{-6} m^2 s^{-1}.

$$\varepsilon = N_p \Omega^3 D^5 V^{-1}; \qquad \text{Eq. 24}$$

where, N_p is the reactor power number, set as 1.5; Ω is the impeller velocity expressed in rps, D is the impeller diameter (0.06 m) and V the working volume (expressed in m^3). Therefore, ε was defined for each agitation rate tested.

4.3 Results and discussions

4.3.1. Biomass accumulation, sucrose consumption and DOT trends

A. vinelandii OP was cultured under several agitation rates for testing the effect of oxygen transfer rate on the biomass and PHB accumulation. The strain was cultured under batch for 30 hours at 600 rpm. Successively, the culture, fed by a feeding pulse of the complete medium, was put under different agitation regimes.

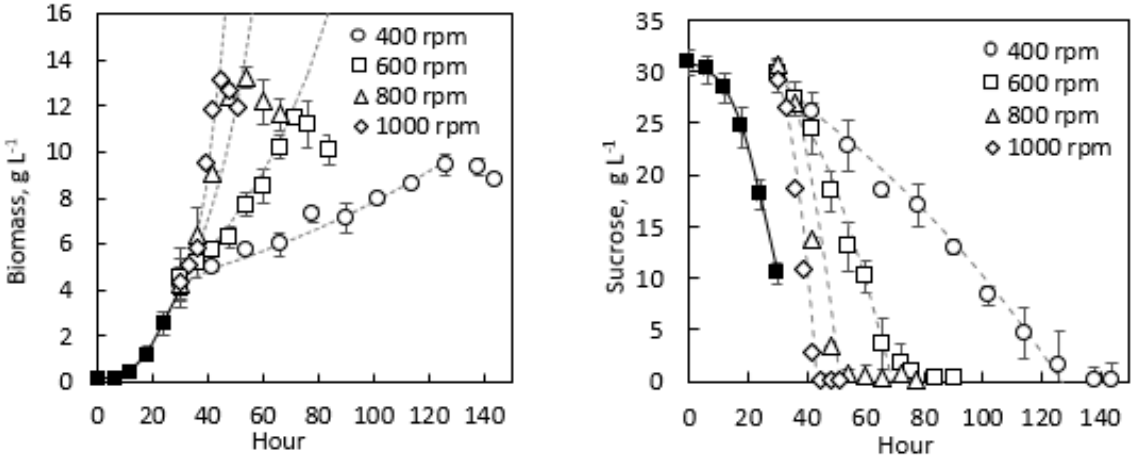

Figure 4-3 Biomass growth and sucrose consumption under different agitation conditions.
On the left: *A. vinelandii* OP growth under different agitation rates. On the right: respective sucrose consumption. In the graphs batch and fed-batch phases are divided by colour, with the first cultivation period illustrated by black symbols followed by white dots representing the fed-batch window. Besides, the exponential growth trend was modelled on the experimental data, here represented as a dotted line.

Figure 4-3 shows the trend of biomass evolution at the different agitation rates. During the first batch phase, the biomass consumed two-third of the total substrate, reaching a biomass accumulation of 3.54 ± 0.56 g L^{-1}. After the feeding pulse, the biomass increased with the rise of the agitation rate (800 and 1000 rpm), while it followed a downturn trend with an agitation rate decrease. However, under 1000 rpm the accumulated biomass was lower in comparison of 800 rpm, 11.77 ± 0.05 g L^{-1}, against 13.6 ± 0.49 g L^{-1}, respectively. (Figure 4-3).

Biomass accumulation was a result of a variation of the specific growth rates (μ). In all the tested conditions, *A. vinelandii* OP assumed an exponential growth trend, here modelled on the experimental data as presented in the graph above.

During the batch phase, it grew under a μ of 0.03 h^{-1}, while in fed-batch phase a decrease of the stirring at 400 rpm diminished the duplication of one-third, and an increase of the agitation pushed the growth rate up to 0.088 ± 0.001 h^{-1}, as it can be seen in Table 4-1 located in the following pages.

The carbon source was depleted entirely during the fermentations, becoming the limiting growth factor. After its complete depletion, biomass went into stationary phase and started to decrease its concentration. As well as for the μ, the substrate consumption rises with stirring rates, passing from 0.31 g L^{-1} h^{-1} at 400 rpm to 2.6 g L^{-1} h^{-1} found at 1000 rpm (Table 4-1).

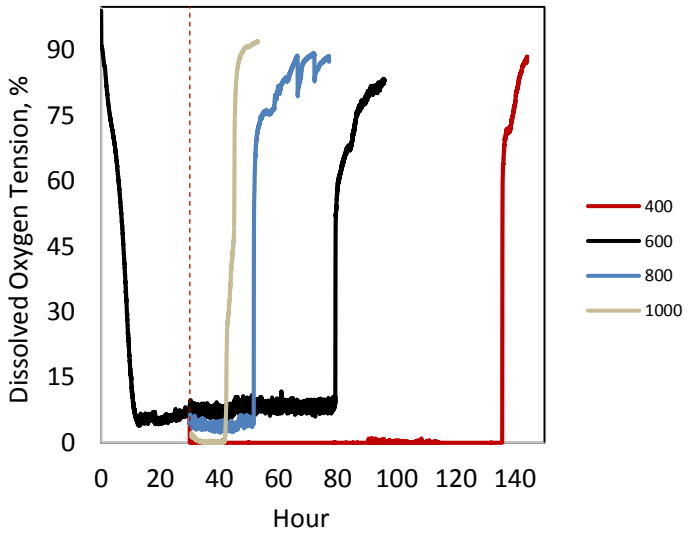

Figure 4-4 Dissolved oxygen transfer tension registered under different agitation rates.

The dissolved oxygen tension (DOT) was monitored, as shown in Figure 4-4. The trends of DOT graph indicate that a strict oxygen-limited condition was verified under 400 and 1000 rpm, while under the other agitation stirring rates DOT oscillated from 4% (at 800 rpm) up to 10% (at 600 rpm after the feeding pulse). In particular, during the batch phase, DOT stayed around 6%. Similar results were found in the study of Castillo, in which *A. vinelandii* OPNA strain was cultured by a similar agitation regime (Castillo et al., 2017).

Due to its high respiration rate, *A. vinelandii* uses to have an oxygen consumption rate (OCR) equals or more elevated than OTR, showing a characteristic DOT of 0% (Diaz-Barrera et al., 2016) (Diaz-Barrera et al., 2019). Nonetheless, when the agitation rate increased, the amount of diffused gas into the liquid phase overcame the biomass oxygen requirement, showing a DOT different from zero. Therefore, the biomass oxygen requirement was satisfied and μ had the potentiality to reach its highest value (Garcia-Ochoa et al., 2010).

4.3.2. PHB accumulation

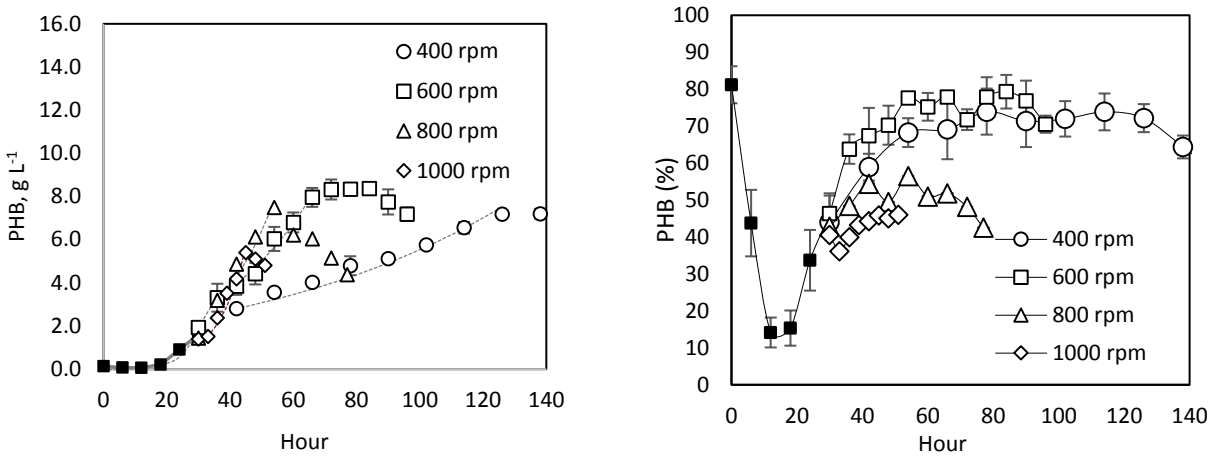

Figure 4-5 PHB production under different agitation rates.
On the left: PHB titre reached during the fermentation under different agitation speeds. On the right: relative PHB accumulation inside the cell found in the same conditions. In the graph, the batch phase is represented with black symbols, while fed-batch stage is shown with white symbols.

Figure 4-5 presents the PHB accumulation as titre and relative PHB cell concentration from 400 to 1000 rpm tested. Generally, PHB accumulation followed the same trend of the biomass accumulation, reaching the highest concentration by an agitation rate increase. During the batch phase, after a steep decrease of PHB inside the cell, the biomass accumulated up to 45%. After the feeding pulse, the highest PHB accumulation was registered under 600 rpm, peaking 76% of concentration into the biomass. The lowest one appeared under 1000 rpm (45%). Hence, low agitations favoured the biopolymer accumulation, while high stirring rates showed an opposite trend. Therefore, PHB titre varies from 5.4 to 8.5 g L^{-1}, under 1000 and 600 rpm, respectively.

The PHB concentration inside the cell remained constant because linked to the oxygen transfer conditions. Interestingly, even if aeration conditions remained stable, at 600 rpm the restoring of the carbon source had a positive effect on the PHB production. Similar behaviour was also observed in *Alcaligens latus*, when it was cultured under nitrogen-limited conditions (Kim et al., 1994) (Wang et al., 1997). On the contrary, under the highest agitation rate, this phenomenon did not appear, because increased agitation and OTR slowed down the production, as a consequence.

Also, during the first ten hours of the batch phase, a steep decrease of the PHB accumulation came out, as presented in Figure 4-5. This phenomenon could be related to the environmental conditions faced by the bacterium once inoculated into the bioreactor. Indeed, the protocol used for starting the fermentation began by a preparation of a seeding culture made into a 500 mL Erlenmeyer flask, in which it got used to a particular oxygen-limited condition. Here, the gas exchange was favoured only by gentle shaking. Successively, the seeding culture was moved into the bioreactor, and the aeration conditions were drastically changed. As described by Page, the high oxygen availability promoted by Rushton impellers and constant airflow

could start a phenomenon called "areoadaptation". Under it, the high oxygen presence should cause a shift of carbon source utilization, from an accumulation of PHB into the expression of scavengers of reactive oxygen species (Page et al., 1988).
On the other hand, during the stationary phase in the range 400-800 rpm, another PHB decreasing trend showed up. In this case, the responsible of PHB consumption should be addressed to the PhbZ depolymerase, a putative PHB depolymerase, which participates to biopolymer hydrolysis during the stationary phase (Adaya et al., 2018).
Summing up, the PHB productivity is strongly linked to the agitation and on the oxygen transfer rate. In accordance with the behaviour observed, Millan and colleagues showed that the production of *A. vinelandii* OP changes in correspondence with a variation on the DOT. In this work, this species was cultured applying a controlled DOT, fixed at 4% or 15%, and as a result, the production of PHB shifted from 80% to 50%, respectively (Muriel-Millán et al., 2016).

4.3.4 Influence of the stirring rate on *A. vinelandii* OP performances

Stirring rate (rpm)	**k_La** (h^{-1})	**μ** (h^{-1})	**SCR** (g h^{-1})	**Yx/s** (g g^{-1})	**PHB_{max}** (g L^{-1})	**PHB_{max}** (%)	**$Y_{PHB/S}$** (g g^{-1})	**η** (μm)
400	28	0.009 ± 0	0.31 ± 0.01	0.19 ± 0	7.28 ± 0.10	71.51 ± 2.18	0.18 ± 0	0.39
600	56	0.030 ± 0	0.7 ± 0	33 ± 0	8.51 ± 0.19	76.64 ±2.48	0.22 ± 0.01	0.29
800	103	0.068 ± 0.01	1.61 ± 0.13	0.31 ± 0.02	7.48	51.38 ± 3.13	0.18	0.24
1000	158	0.088 ± 0.01	2.6	0.29	5.40	44.85	0.14	0.19

Table 4-1 Influence of stirring rate on fermentation parameters.
In the table is shown the influence of the gas transfer coefficient (kLa) on the biomass duplication rate (μ), on the substrate consumption rate (SCR), on the biomass yield (YX/S), PHB maximum produced and accumulated, yield of PHB on the substrate (YPHB/S) and the Kolmogorov scale (η).

Table 4-1 presents μ, the substrate consumption rate (SCR) and biomass yield ($Y_{X/S}$) referred to the agitation rate and the correspondent k_La, calculated for each agitation condition. k_La represents the physical parameter that, changing with the agitation rate, directly influences the OTR, and the oxygen supply for the biomass, as a consequence (Eq. 15). Moreover, in comparison to the stirring rate, the application of k_La is more appropriate for making a general assumption on *A. vinelandii* behaviour and successive scale-up design. As described in the previous paragraphs, an increase k_La had a positive influence on μ and SCR, while the PHB titre diminished with the rise of agitation speed.
$Y_{X/S}$ rose from 0.19 to 0.33 g g^{-1} by improving the stirring rate from 400 to 600 rpm. At higher stirring rates, the biomass yield on the substrate remained constant, even if SCR increased linearly with the agitation. Hence, it can be hypnotised that variations of OTR strongly affected metabolic fluxes inside the cell.

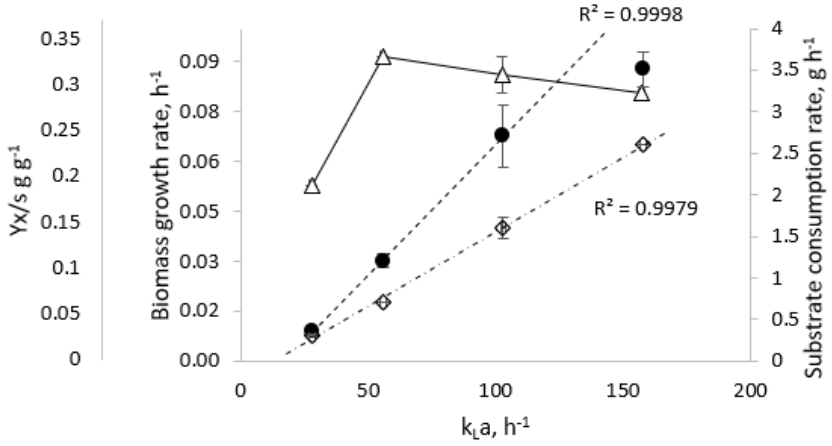

Figure 4-6 Effect of mass transfer constant on biomass growth, substrate consumption and biomass yield.
The graph represents the trends of biomass yield on the consumed substrate (Δ), specific growth rate (●) and substrate consumption rate (◊) over the gas transfer constant (k_La). Trends show that Yx/s did not depend on the agitation rate, while SCR and μ did.

For a deeper understanding of this mechanism on *A. vinelandii* OP, μ, $Y_{X/S}$ and SCR were put in relationship with k_La in Figure 4-6. Therefore, even if the SCR and μ had a linear trend over the agitation rate ($R^2 = 0.99$), the $Y_{X/S}$ remained almost constant after k_La of 50 h^{-1}(corresponding to 600 rpm for the bioreactor used). The increase of SCR on the stirring rate correspondent to a stable $Y_{X/S}$, demonstrating that the consumed carbon favoured the cellular respiration and the accumulation of residual biomass more than PHB accumulation. Similarly, this positive influence of the aeration of biomass growth was also attested for other strain as *A. vinelandii* ATCC, *A. vinelandii* AT6 and *A. chrococcum* (Pena et al., 2000)(Kim et al., 2000)(Moral et al., 2012)(Mejia et al. 2010)(Quagliano et al., 1997).

High agitation speeds did not damage *A. vinelandii* OP cells. The direct microscope observation revealed any shear stress on cells morphology. For supporting this evidence, eddies dimension caused by impellers agitation were also evaluated. The calculated Kolmogorov's scale (η) evidenced that the diameter *A. vinelandii* OP cell, ranging from 2 to 4 μm, was higher in comparison of the smallest eddies generated under 1000 rpm (having a diameter of 0.19 μm) (Post et al., 1982).

The agitation condition in which the substrate was more efficiently directed on PHB accumulation corresponded to a k_La of 56 h^{-1} (or 600 rpm), at which the $Y_{PHB/S}$ assumed the highest value of 0.22 ± 0.01 g g^{-1}.

From the data set available by these different trials, the volumetric PHB productivity (Q_{PHB}) was calculated. This value is influenced both by μ and by PHB titre (Eq. 21). The highest amount of stored PHB was in correspondence with of k_La of 56 h^{-1} (600 rpm), while the faster μ was verified at 158 h^{-1} (1000 rpm). However, as reported in Figure 4-7, the best Q_{PHB} is located in the region around 100 h^{-1} of k_La, with a value of 0.51 g L^{-1} h^{-1}.

Under this agitation condition, the compromise between the cell duplication rate and the accumulated PHB ensured the highest biopolymer productivity.

This confirms that Q_{PHB} positively depends on OTR because of the sustaining of cellular duplication if the stored PHB overcomes 50% of cell dry weight.

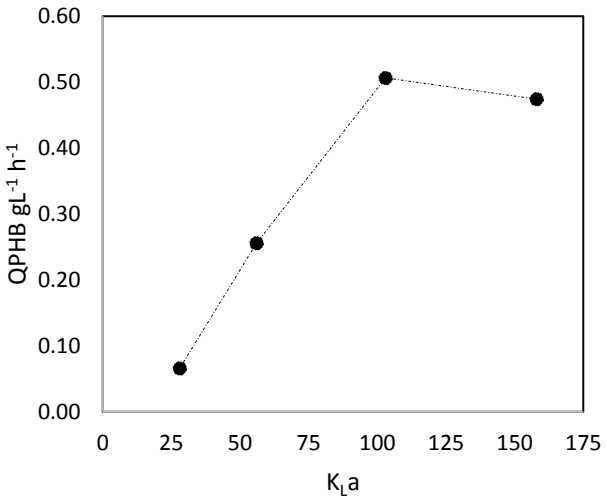

Figure 4-7 PHB volumetric productivity over k_La.

Fed-batch feeding had a positive effect on the final PHB amount. It allowed reaching higher biomass concentration by the addition of fresh carbon source, which ensured a higher PHB titre, as a consequence. In respect to a batch fermentation, the feeding pulse has the advantage to supply biomass by new carbon source for supporting an exponential growth and PHB production, as shown in Table 4-2(Muriel-Milláand et al., 2016). Comparing productivity values with literature, it is evident that higher Q_{PHB} were obtained in *A. vinelandii* by the feeding of liquid nitrogen source, as demonstrated in the work of Castillo (Castillo et al., 2017) (Table 4-2). However, the supply of this kind of nitrogen source is often affected by contamination events, which is a real failure for the process scalability. Therefore, by this work, it was possible to design a reliable fermentation strategy under which *A. vinelandii OP* reaches the highest PHB productivity in a poor medium.

	This work	Muriel-Millan et al., 2016	Castillo et al. 2017
PHB_{max} (g L^{-1})	7.5	2.4	22.9
PHB (%)	51	80	74
Cell dry weight (g L^{-1})	13.6	3	28.1
μ (h^{-1})	0.068	0.08	0.06
Q_{PHB} (g L^{-1} h^{-1})	0.51	0.19	0.57
Operative condition	Fed-batch, nitrogen limitation under 800 rpm, 1 vvm	Batch-fermentation No nitrogen limitation, 500 rpm	Fed-batch fermentation under nitrogen supply, 500 rpm, 0.5 vvm

Table 4-2 PHB productivity comparison among this work and literature data.

4.4 Conclusions

During this experimental activity, the PHB productivity of *A. vinelandii* OP was tested under different agitation rate with the main goal to investigate the variation of PHB production in those systems that shows a scalable production. The study reveals that as for other *Azotobacter* species, agitation and the related oxygen transfer rate caused

marked effects on the overall cell metabolism, influencing the growth, the production of PHB and the biomass yield on the substrate, as consequence.
An increase of OTR got off the specific growth trend and substrate consumption rates. On the contrary, the accumulation of PHB follows an opposite trend, decreasing by an increase in the oxygen transfer made by increasing the agitation rate. In particular, the biopolymer production was favourited under low agitations, and the highest PHB accumulation of 76% emerged in the correspondence of a k_La of 56 h^{-1}.
It was found that varying the agitations the metabolic flux of carbon utilization inside the cell could be influenced. Therefore, high k_La values were associated with low PHB accumulation in comparison of the amount of carbon consumed, that increased linearly with k_La, as well as for the specific growth rate. However, even if μ and the accumulated PHB assumed opposite trends, it was identified a region in which the volumetric productivity reached its maximum. It showed up a correspondence with of a k_La of 100 h^{-1}, where Q_{PHB} peaked 0.51 g L^{-1} h^{-1} in N-poor medium
Summing up, by the application the aerobic *A. vinelandii* OP strain, it was possible to verify the relationship that linked gas availability and the PHB production into an aerobic system, proposing a strategy for scale-upping this process for further PHB production processes.

4.5 References

Adaya, L., Millán, M., Peña, C., Jendrossek, D., Espín, G., Tinoco-Valencia, R., ... & Segura, D. (2018). Inactivation of an intracellular poly-3-hydroxybutyrate depolymerase of *Azotobacter vinelandii* allows to obtain a polymer of uniform high molecular mass. *Applied microbiology and biotechnology*, 102(6), 2693-2707.

Castillo, T., Flores, C., Segura, D., Espín, G., Sanguino, J., Cabrera, E., ... & Peña, C. (2017). Production of polyhydroxybutyrate (PHB) of high and ultra-high molecular weight by *Azotobacter vinelandii* in batch and fed-batch cultures. *Journal of Chemical Technology & Biotechnology*, 92(7), 1809-1816.

Díaz-Barrera, A., Andler, R., Martínez, I., & Peña, C. (2016). Poly-3-hydroxybutyrate production by *Azotobacter vinelandii* strains in batch cultures at different oxygen transfer rates. *Journal of Chemical Technology & Biotechnology*, 91(4), 1063-1071.

Díaz-Barrera, A., Urtuvia, V., Padilla-Córdova, C., & Peña, C. (2019). Poly (3-hydroxybutyrate) accumulation by *Azotobacter vinelandii* under different oxygen transfer strategies. *Journal of industrial microbiology & biotechnology*, 46(1), 13-19.

Garcia-Ochoa, F., Gomez, E., Santos, V. E., & Merchuk, J. C. (2010). Oxygen uptake rate in microbial processes: an overview. *Biochemical Engineering Journa*l, 49(3), 289-307.

Kim, B. S. (2000). Production of poly (3-hydroxybutyrate) from inexpensive substrates. *Enzyme and Microbial Technology*, 27(10), 774-777.

Kim, B. S., Lee, S. C., Lee, S. Y., Chang, H. N., Chang, Y. K., & Woo, S. I. (1994). Production of poly (3-hydroxybutyric acid) by fed-batch culture of *Alcaligenes eutrophus* with glucose concentration control. *Biotechnology and Bioengineering*, 43(9), 892-898.

Mejía, M. A., Segura, D., Espín, G., Galindo, E., & Peña, C. (2010). Two-stage fermentation process for alginate production by *Azotobacter vinelandii* mutant altered in

poly-β-hydroxybutyrate (PHB) synthesis. *Journal of applied microbiology*, 108(1), 55-61.

Moral, C. K., & Sanin, F. D. (2012). An investigation of agitation speed as a factor affecting the quantity and monomer distribution of alginate from *Azotobacter vinelandii* ATCC® 9046. *Journal of industrial microbiology & biotechnology*, 39(3), 513-519.

Muriel-Millán, L. F., Castellanos, M., Hernandez-Eligio, J. A., Moreno, S., & Espín, G. (2014). Posttranscriptional regulation of PhbR, the transcriptional activator of polyhydroxybutyrate synthesis, by iron and the sRNA ArrF in *Azotobacter vinelandii*. *Applied microbiology and biotechnology*, 98(5), 2173-2182.

Page, W. J., Jackson, L., & Shivprasad, S. (1988). Sodium-dependent *Azotobacter chroococcum* strains are aeroadaptive, microaerophilic, nitrogen-fixing bacteria. *Applied and Environmontal. Microbiology.*, 54(8), 2123-2128.

Peña, C., López, S., García, A., Espín, G., Romo-Uribe, A., & Segura, D. (2014). Biosynthesis of poly-β-hydroxybutyrate (PHB) with a high molecular mass by a mutant strain of *Azotobacter vinelandii* (OPN). *Annals of microbiology*, 64(1), 39-47.

Peña, C., Trujillo-Roldán, M. A., & Galindo, E. (2000). Influence of dissolved oxygen tension and agitation speed on alginate production and its molecular weight in cultures of *Azotobacter vinelandii*. *Enzyme and microbial technology*, 27(6), 390-398.

Post, E., Golecki, J. R., & Oelze, J. (1982). Morphological and ultrastructural variations in *Azotobacter vinelandii* growing in oxygen-controlled continous culture. *Archives of Microbiology,* 133(1), 75-82.

Quagliano, J. C., & Miyazaki, S. S. (1997). Effect of aeration and carbon/nitrogen ratio on the molecular mass of the biodegradable polymer poly-β-hydroxybutyrate obtained from *Azotobacter chroococcum* 6B. *Applied microbiology and biotechnology*, 48(5), 662-664.

Wang, F., & Lee, S. Y. (1997). Poly (3-Hydroxybutyrate) Production with High Productivity and High Polymer Content by a Fed-Batch Culture of Alcaligenes latus under Nitrogen Limitation. *Applied and Environemntal. Microbiology*, 63(9), 3703-3706.

Chapter 5

PHB extraction and purification: a case-study dedicated to a green-based solvent application

5.1. Introduction

Standard PHB extraction is based on the use of chlorinated solvents, like chloroform. This class of solvents is the most frequently adopted because it assures high purification yields of the PHB enclosed into bacterial cells. However, it is also associated with high toxicity for the environment and operators. For facing these issues, new and more environmentally friendly solvents have been proposed. Among them, a promising class is represented by carbonates (e.g., ethylene carbonate, 1,2-propylene carbonate or the dimethyl carbonate).

Up to now, several published works showed the potentiality of this class of molecules, that can ensure high extraction yields, over 90%, and high PHB purity values, which are close to 100%.

To render the produced biopolymer appetible for useful market application, the extracted PHB should be characterized by a constant and high molecular weight. These features rely upon the strains, the fermentation conditions, and lastly, on the extraction procedures adopted. Through carbonates-based extraction conducted at temperatures higher than 100°C, a decrease of the molecular weight of the extracted PHB was reported, as a consequence of thermal degradation (Fiorese et al., 2009). Another factor to consider in preserving the biopolymer molecular mass is the application of pre-treatment steps, which are commonly used for modifying the integrity of the cellular membrane, as the effects due to heating, sonication or alkaline solutions, for instance.

Among the PHB producing species one alternative to natural producing strains are genetically modified species, in which PHB-dedicated genes have been engineered for adding or improving the PHB biosynthetic pathway. *Escherichia coli* is a suitable microorganism for hosting the PHB biosynthetic pathway because several advantages characterize it. There are a vast genetic background knowledge, a well-known culturing technology and it shows a high biomass accumulation, even with high PHB concentration (close to 90% of cellular dry weight) (Li et al., 2007)(Lee et al., 1995)(Choi et al., 1998)(Liu et al., 1998). Besides, *E. coli* is a gram-negative species as well as of *R. rubrum* and *A. vinelandii*, with which it shares the same structure of

the cellular membrane and a similar yield in respect with *A. vinelandii* OP (6 g L^{-1} of PHB obtained in a flask). And, unlike natural PHB producing strains, it does not show a depolymerase activity, which renders it an optimal model system for PHA purification trials. Since, once the PHB is synthesized, it is stored maintaining a constant molecular mass (Kahar et al., 2005). In this way, those limitations characterizing *R. rubrum* and *A. vinelandii*, as too little PHB accumulation or the presence of natural depolymerase, can be easily overcome.
Starting from these assumptions, the scope of this experimental part was to define the purification yield and the purity of extracted PHB with a carbonate-based solvent having a low boiling point, such as the dimethyl carbonate (DMC), in dry and wet biomass. Thus, a genetically modified *E. coli* containing PHB biosynthetic genes (*phbABC*) was cultured and exposed to DMC at different exposition time.

5.2. Material and Method

5.2.1. Biomass cultivation

The bacterial strain used in this study was gently provided by the group of Auxiliadora M. Prieto (CSIC, Spain). It is a genetically modified *Escherichia coli* BL21 (DE3), hosting a plasmid with the three genes devoted to the PHB biosynthetic (*phb ABC*) coming from *R. eutropha* H16 and a chloramphenicol resistance, which are activated under glucose feeding (Martínez et al., 2016). The strain, stocked at -20°C in 15% v/v glycerol, was cultured in LB medium with chloramphenicol (20 µg/mL) and glucose (10% v/v). Each culture was prepared in Erlenmeyer Flask filled with around 40% of culture broth. In order to maximize the biomass growth, pre-cultures of 70 mL and culture of 250 mL flask were prepared. 1.5 mL of *E. coli* glycerol stock was transferred to the preculture flask for 12 h, at 30°C and 200 rpm. After it, a pre-culture volume was transferred to a fresh LB medium in order to have an initial OD_{600} of 0.3 into a culture volume of 250 mL. After 16 h at 30°C and 200 rpm, the culture broth was transferred to 50 mL falcon tubes and centrifuged two-times at 5000 rpm for 15 min, to collect the cell pellet. The obtained pellet was washed with deionized H_2O and centrifuged at 5000 rpm for 15 min. Depending on the selected extraction process, the wet cell pellet was directly treated or dried in the oven at 90°C for 12 h and ground by a ceramic mortar and pestle.

5.2.2. Experimental set-up

The image below shows the main protocol process used for the extraction of PHB, using standard solvent/antisolvent reagent or the greener ones selected in this work.

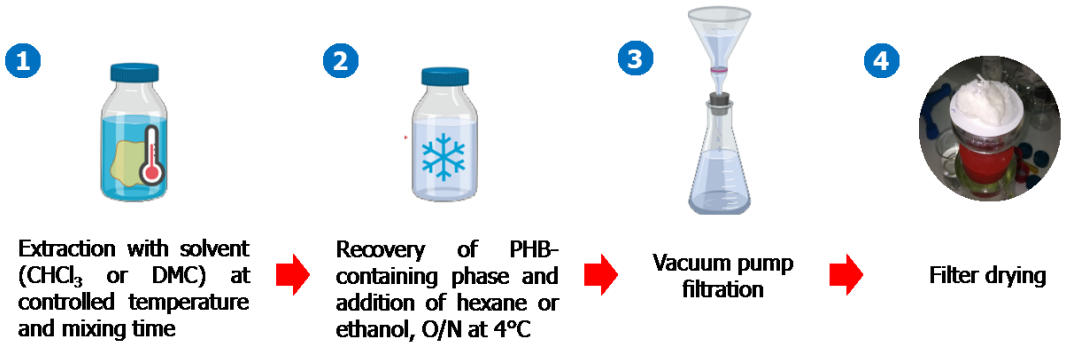

Figure 5-1 Principal steps of PHB solvent extraction as described in the description of the procedure.

5.2.3. Standard PHB extraction: Chloroform/Hexane-based extraction

The PHB was extracted by treating the biomass with chloroform and hexane, as a solvent and antisolvent respectively, according to the work of Fei and colleague (Fei et al., 2013). However, some differences have been introduced to the procedure. In case of extraction from wet biomass, the recovered and washed pellet coming from the culture was transferred into 20 ml glass bottles and mixed with chloroform in order to reach a cell dry weight-chloroform ratio of 1:15 (Fei et al., 2013). So, it was kept stirred in an oil bath at 60°C for 120 minutes. At the end of the reaction, the biomass and solvent mixture was transferred to 50 mL falcon tubes and centrifuged for 10 minutes at 5000 rpm. In case of dry pellet extraction, the biomass was first ground by a ceramic mortar and pestle, before being inserted into a paper filter arrange as a tea-bag container (Whatman n°1) and soaked in the solvent. The filter was then removed, and the solvent phase was directly transferred to a glass bottle for PHB precipitation. There, an amount of antisolvent equal to 3 volumes of solvent was add where hexane was added. The mixture was left at 4°C for 24 hours, after which the precipitated PHB was separated from hexane by vacuum filtration and finally dried.

5.2.4. Dimethyl carbonate/Ethanol PHB extraction

The PHB extracted with DMC and ethanol is based on a modified protocol by Samorì and colleagues (Samorì et al.,2015), with little variation in respect to reaction mixing time, pellet texture and filter use. In case of direct solvent-biomass extraction, wet or dry pellets have been put directly put in 20 mL glass bottles, where DMC was added respecting the ratio 2.5% (w/v %). Then, the reaction was set under continuous stirring at 90°C, for a mixing time corresponding to 60, 90, 120 minutes, which depended on

the experimental run tested. At the end of each extraction reaction, the solution was transferred into 50 mL falcon and centrifuged at 5000 rpm for 10 minutes, in order to separate the organic phase hosting the PHB with the not-PHA cellular mass. After that, the organic phase was recovered and pure ethanol at a DMC:ethanol ratio of 1:3 was added for allowing the PHB precipitation made for 12 hours at 4°C. Hence, the PHB containing solutions was filtered *via* vacuum pump and finally dried. On the other side, in the case of filter-mediated extraction, wet or dry biomass was previously put inside a paper filter arrange as a tea-bag container (Whatman n°1), before the extraction procedure under the same conditions used for a direct extraction. However, in this case, due to the presence of the filter, at the end of the extraction, the reacted DMC solution was directly used for the precipitation step.

5.2.5. PHB quantification

In order to verify the specific amount of PHB produced by genetically modified *E. coli* cells during each test, every time a new culture was stablished a sample corresponding to 5 mL of final culture broth was kept and store at -20°C for successive analysis of the cell dry weight and of the correspondent PHB amount. Cell dry weight was made gravimetrically. The sample collected in this way was centrifuged at 10000 rpm for 5 minutes, washed two-times and dried at 80°C for 12 hours in an oven. Once estimated the correspondent biomass concentration (g L^{-1}), 5 mg of biomass were hydrolysed by 1 mL of 96% H_2SO_4 under stirring of 800 rpm, into an agitated oil bath at 90°C for one hour. At the end of the reaction, a dilution of 1:1000 was done and the samples were analysed by an HPLC with a column ROA-Organic Acid H^+ (8%) (Phenomenex) under an isocratic flux of 0.7 mL min^{-1} of 5 mM of H_2SO_4 and a temperature of 50 °C. The PHB related signal appeared at 210 nm after 23.09 from the sample injection, which corresponds to the crotonic acid (the monomer coming from the PHB hydrolysate) (Braunegg et al., 1979).

5.2.5. PHB purity estimation

The purity of the recovered PHB was investigated by the HPLC above described. So, representative samples of the extracted biomass were ground by a ceramic pestle and mortar, hydrolyzed by H_2SO_4 treatments and analyzed by the respective crotonic acid found.

5.2.6. Analytical calculations

For the calculation of the PHB extraction yield and purity, the following equations were used:

$$\text{PHB extraction yield (\%)} = \frac{purified\ PHB\ (g)}{PHB\ present\ in\ the\ treated\ biomass\ (g)} \quad \text{Eq. 25}$$

$$\text{PHB purity (\%)} = \frac{HPLC\ quantified\ of\ extracted\ PHB\ (g)}{extracted\ PHB\ \ (g)} \qquad \text{Eq. 26}$$

5.3. Results and discussion

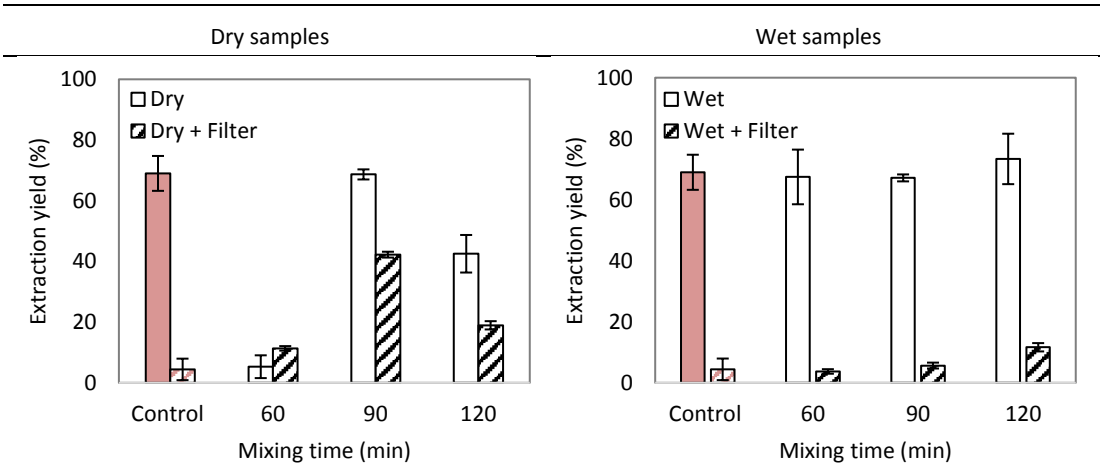

Figure 5-2 Comparison of PHB extraction based on dimethyl carbonate starting from wet and dry biomass. Dry (left) and wet (right) biomass were compared with a standard PHB extraction (chloroform and dry biomass). The application of a filter (coloured bars) *vs* a direct extraction (white bars) is also shown. In both cases, the control was based in a chloroform extraction made on dry biomass.

After 16 hours of cultivation, *E. coli* consumed all the carbon source (10 g L^{-1} of glucose) accumulating around 60% of its dry biomass as PHB. Hence, the biomass was collected and exposed to the extraction protocol. In presence of dry biomass, the optimum reaction time for PHB extraction *via* DMC corresponded at 90 minutes of treatment, which gave an extraction yield of 68.7 ± 1.7 %. Lowering or increasing the exposition time resulted in a lower PHB yield, which was 5.3 ± 3.7 % and 42.5 ± 6.2, in correspondence with 60 minutes and 120 minutes of solvent exposition. On the contrary, when the biomass was wet, DMC recovered a higher amount of polymer independently from the time applied during the purification. And, the extracted PHB titre was as high as the purification yield reached with the standard solvent (consisting in chloroform used on dry biomass). On average, it peaked 73% at 120 minutes. However, no significant differences were observed in wet biomass, and the standard deviation ranged from 2 to 10%.

To investigate if the biopolymer purity could be enhanced, during the extraction procedure, the biomass was closed inside a paper filter, mimicking a *tea-bag-like* extraction, both in the case of wet and dry cells. This purification strategy sharply decreased the efficiency of the protocol, which resulted in the lowest extraction yields observed for wet biomass, with an 85% overall decrease under all the mixing times tested. Similarly, dry biomass lost 42% in the extraction efficiency at 90 minutes and 120 minutes of exposition.

During PHB extraction mediated by the presence of the paper filter, the purification was based on a simple diffusion process. The presence of the paper filter, which

occupied the base of the purification bottles, prevented the application of any stirring bar. As a consequence, the increase of temperature was the primary factor influencing the diffusive movements of solubilized PHB from the biomass through the solution. On the other side, the direct biomass extractions were characterized by a continuous stirring, which could have contributed to a higher purification yield.
However, the most significant variation was evidenced by the differences encountered between dry and wet biomass state. Secondary, the exposition time influenced the extraction yield when the starting biomass was previously dried. For dried samples, the extraction trend reached its maximum at 90 minutes, decreasing after a more extended solvent exposition, even in presence or without the application of a paper filter. In wet samples, this variation was absent. In the presence of a paper filter, an increase of the purification yield was observed linearly to the extraction time, and three-times more PHB was recovered at 120 minutes than 60 minutes using wet biomass. Accordingly, to the diffusion limits explained above.
The variations encountered with the state of the biomass suggest that a change into the biopolymer properties could have occurred during the drying phase.
Generally, a drying treatment is the most common pre-treatment applied to PHB-rich cells because it increases the extraction efficiency (Comeau et al., 1988). It is also known that *in vivo* PHB chains are stabilized by waters molecules, proteins and lipids, arranging the homopolymer in β-conformation-like structures (Lauzier et al., 1992). However, lyophilization or heating treatments involve in a rearrangement of the chains, with a consequent variation of the polymer crystallinity (Porter et al., 2011). As a consequence, this change on the chemical structure determines a modification of the extraction efficiency (McChalicher et al., 2010). Therefore, a correlation between the high and constant extraction yield obtained in wet biomass might be explained by a better interaction between the solvent and the PHB branches.

Figure 5-3 Extracted PHB with chloroform.
On the left, a filter PHB coming from a direct extraction. On the right, a filtered PHB coming from a tea-bag-like extraction made by a paper filter.

For analysing the purity of the extracted PHB, once purified, samples of polymer were ground and hydrolysed for a successive HPLC analysis. In this way, the overall representation of the purity value was realised. In Table 5-1 purity values of the extracted polymer are reported. The application of a filter on control protocol guaranteed higher purification yield, passing from 88% to 100% of purity, as shown in Table 5-1 and Figure 5-3. On the other case, for extraction performed with DMC, the purity values were generally high, even without the paper filter. Hence, DMC had

a more positive influence on the features of the purified polymer to the standard procedure.

	Time	Dry pellet	Wet pellet	Paper filter	PHB yield (/)	Purity (%)
Control	120	+		-	69 ± 5.75	88 ± 7
	120	+		+	4.4	100 ± 13
	60	+		-	5.31 ± 3.75	100 ± 13
	90	+		-	68.67 ± 1.66	103 ± 1
	120	+		-	42.53 ± 6.19	108 ± 1
	60		+	-	67.48 ± 8.96	88 ± 21
	90		+	-	67.16 ± 1.14	109 ± 6
	120		+	-	73.38 ± 8.26	107 ± 1
	60	+		+	11.35 ± 1.68	100 ± 12
	90	+		+	42.23 ± 6.98	105 ± 7
	120	+		+	18.95 ± 3.93	100 ± 10
	60		+	+	3.73 ± 0.74	79 ± 15
	90		+	+	5.66 ± 0.96	100 ± 6
	120		+	+	11.66 ± 1.36	100 ± 1

Table 5-1 Extraction yield and purity of wet and dry biomass traded under different mixing time with DMC.

The presented results showed a higher PHB extraction yield in comparison of what published by Samorì and colleagues, in which the maximum extraction yield obtained from a mixed culture was equal to 20% (Samorì et al., 2015). Higher extraction yields were obtained by the application of butyl acetate at a temperature of 103 °C for 30 minutes from *Cupriavidus necator* (Aramvash et al., 2015). While, similar results were found with propylene carbonates and dimethyl formamide, which presents 75% from cultures of *Alcaligens latus* and 68% from *C. necator* of extraction yield, respectively (Manangan et al, 2010) (Mcchlier et al., 2010) (Table 5-2).

Biomass	Extraction process	Extraction yield (%)	Reference
Dry	Chloroform	39 ± 2	Manangan et al., 2010
Dry*	Dimethyl formamide, solid-liquid extraction	68 ± 4	Manangan et al., 2010
Lyophilised	1,2-propylencarbonate, 120 °C for 15 min	75	Mcchlier at al., 2010
Wet	Butyl acetate, 103 °C, for 30 minutes	96 ± 1	Aramvash et al., 2015
Lyophilised	Dimethyl carbonate, 90°C for 60 min	20 ± 1	Samorì et al., 2015
Dry	Dimethyl carbonate, 90°C for 90 min	69 ± 2	This study
Wet	Dimethyl carbonate, 90°C for 120 min	73 ± 8	This study

Table 5-2 Comparison of extraction yields obtained by different solvents.
*The biomass was pre-treated with ethanol.

As underlined above, 20% of the standard deviation was a characteristic deviation for this kind of approach. Indeed, at a bench scale, the significant limitations encountered are due to PHB losses between one step and another of the followed extraction procedure. In particular, three critical points were noted in: *i)* the little fractions of purified PHB that remained attached to the glass used during the purification; *ii)* a not complete recovery of the organic phase; *iii)* in the PHB remained inside the tea-bag

structure. These losses of material, added to operators' errors, gave the overall reported standard deviation. Hence, by an improvement of the extraction protocol, a higher extraction yield could be reached.

5.4. Conclusions

In this study, it was demonstrated as the PHB extraction can achieve high purification yield applying a more environmentally friendly solvent, as the dimethyl carbonate. A direct extraction using wet biomass resulted in a purification yield of 74%. It represents a significant advantage in the frame of extraction costs and time reduction. DMC also gave positive results as far as the PHB purity values were concerned. Differently to the application of chloroform, the use of DMC resulted in very high purity values.
The maximum extraction yield was reached after a treatment of 90 minutes in case of dried biomass. While when fresh biomass was used, the mixing time does not represent a limiting variable affecting the extraction efficiency. In this case, it is reasonable to claim that the presence of at water into the natural PHB positively influenced the extraction kinetic mechanism.
The results obtained gave a good chance for substituting chloroform-based extraction with DMC. However, a more in-depth investigation for underlying benefits and drawbacks of this green-based solvent, as an LCA analysis, and physical characterization of the collected PHB should be included in future works.

5.4. References

Aramvash, A., Gholami-Banadkuki, N., Moazzeni-Zavareh, F., & Hajizadeh-Turchi, S. (2015). An environmentally friendly and efficient method for extraction of PHB biopolymer with non-halogenated solvents. *J Microbiol Biotechnol*, 25(11), 1936-1943.

Braunegg, G., Sonnleitner, B. Y., & Lafferty, R. M. (1978). A rapid gas chromatographic method for the determination of poly-β-hydroxybutyric acid in microbial biomass. *European journal of applied microbiology and biotechnology*, 6(1), 29-37.

Choi, J. I., Lee, S. Y., & Han, K. (1998). Cloning of the Alcaligenes latus polyhydroxyalkanoate biosynthesis genes and use of these genes for enhanced production of poly (3-hydroxybutyrate) in *Escherichia coli*. *Applied and Environmental Microbiology*, 64(12), 4897-4903.

Comeau, Y., Hall, K. J., & Oldham, W. K. (1988). Determination of poly-β-hydroxybutyrate and poly-β-hydroxyvalerate in activated sludge by gas-liquid chromatography. *Applied and Environmental Microbiology*, 54(9), 2325-2327.

De Koning, G. J. M., Kellerhals, M., Van Meurs, C., & Witholt, B. (1997). A process for the recovery of poly (hydroxyalkanoates) from *Pseudomonads* Part 2: Process development and economic evaluation. *Bioprocess Engineering*, 17(1), 15-21.

Fei T., Cazeneuve S., Wen Z., Wu L., and Wang T., Effective recovery of poly-β-hydroxybutyrate (PHB) biopolymer from *Cupriavidus necator* using a novel and environmentally friendly solvent system, *Biotechnoloogy Progress*, vol. 32, no. 3, pp. 678–685, 2016.

Fiorese M. L., Freitas F., Pais J., Ramos A. M., De Aragão G. M. F., and Reis M. A. M., Recovery of polyhydroxybutyrate (PHB) from *Cupriavidus necator* biomass by solvent extraction with 1,2-propylene carbonate, *Engineering in Life Science*., vol. 9, no. 6, pp. 454–461, 2009.

Kahar, P., Agus, J., Kikkawa, Y., Taguchi, K., Doi, Y., & Tsuge, T. (2005). Effective production and kinetic characterization of ultra-high-molecular-weight poly [(R)-3-hydroxybutyrate] in recombinant *Escherichia coli*. *Polymer degradation and stability*, 87(1), 161-169.

Lauzier, C., Revol, J. F., & Marchessault, R. H. (1992). Topotactic crystallization of isolated poly (β-hydroxybutyrate) granules from *Alcaligenes eutrophus*. *FEMS microbiology reviews*, 9(2-4), 299-310.

Lee, S. Y., & Chang, H. N. (1995). Production of poly (hydroxyalkanoic acid). In *Microbial and enzymatic bioproducts* (pp. 27-58). Springer, Berlin, Heidelberg.

Lee, S. Y., Lee, K. M., Chan, H. N., & Steinbüchel, A. (1994). Comparison of recombinant *Escherichia coli* strains for synthesis and accumulation of poly-(3-hydroxybutyric acid) and morphological changes. *Biotechnology and bioengineering*, 44(11), 1337-1347.

Li, R., Zhang, H., & Qi, Q. (2007). The production of polyhydroxyalkanoates in recombinant *Escherichia coli*. *Bioresource technology*, 98(12), 2313-2320.

Liu, F., Li, W., Ridgway, D., Gu, T., & Shen, Z. (1998). Production of poly-β-hydroxybutyrate on molasses by recombinant *Escherichia coli*. *Biotechnology Letters*, 20(4), 345-348.

Manangan, T., & Shawaphun, S. (2010). Quantitative extraction and determination of polyhydroxyalkanoate accumulated in *Alcaligenes latus* dry cells. *Science Asia*, 36, 199-203.

Martínez, V., Herencias, C., Jurkevitch, E., & Prieto, M. A. (2016). Engineering a predatory bacterium as a proficient killer agent for intracellular bio-products recovery: The case of the polyhydroxyalkanoates. *Scientific reports*, 6, 24381.

McChalicher, C. W., Srienc, F., & Rouse, D. P. (2010). Solubility and degradation of polyhydroxyalkanoate biopolymers in propylene carbonate. *AIChE journal*, 56(6), 1616-1625.

Porter, M., & Yu, J. (2011). Crystallization kinetics of poly (3-hydroxybutyrate) granules in different environmental conditions. *Journal of Biomaterials and Nanobiotechnology*, 2(03), 301.

Samorì, C., Basaglia, M., Casella, S., Favaro, L., Galletti, P., Giorgini, L., ... & Tagliavini, E. (2015). Dimethyl carbonate and switchable anionic surfactants: two effective tools for the extraction of polyhydroxyalkanoates from microbial biomass. *Green chemistry*, 17(2), 1047-1056.

Yu, H., Yin, J., Li, H., Yang, S., & Shen, Z. (2000). Construction and selection of the novel recombinant *Escherichia coli* strain for poly (β-hydroxybutyrate) production. *Journal of bioscience and bioengineering*, 89(4), 307-311.

Zhang, H., Obias, V., Gonyer, K., & Dennis, D. (1994). Production of polyhydroxyalkanoates in sucrose-utilizing recombinant *Escherichia coli* and *Klebsiella strains*. *Applied and Environmental Microbiolology*, 60(4), 1198-1205.

Chapter 6

Conclusion and future perspectives on PHB production processes

This work aimed to investigate the biotechnological PHB production, challenging several steps related to poly-3-hydroxybutyrate fermentation and extraction.

The investigation of PHB production started by the observation of the effects of carbon monoxide as the primary substrate for *Rhodospirillum rubrum*. Even if carbon monoxide is toxic for the majority of living beings, the strain gained an energetic advantage from this industrial waste. As a consequence, the investigation showed up how the *R. rubrum* specific growth rate and lag phase depend on the CO concentrations, which are influenced by the pre-adaptation conditions in turn. Therefore, a pre-adaptation was necessary for improving the growth yield.

The exposition to CO did not only generate a metabolically active population but on the other side, *R. rubrum* showed up a phenotypical adaptive evolution, under repetitive CO-based fermentations. Thus, it acquired the capacity to grow faster, reducing the experimental repeatability at the same time. However, such limitations could be overcome by the application of mixotrophic pre-adaptation conditions, in which CO and fructose co-feeding guaranteed higher biomass accumulation with an equal CO adaptation efficiency.

By this study, *R. rubrum* was tested for the first time under pressure into a dedicated bioreactor. The pressure improvement up to a value of 8 atm did not influence the bacteria growth rate. However, the PHB accumulation rose from 13% of a standard pressure condition to 37% under pressure, probably due to a higher solubility of the produced CO_2. Indeed, the increased solubility of carbon dioxide could be correlated with an improvement of carboxylation reactions, which could indirectly influence the net biopolymer production.

The role of the gas diffusion was not only critical for those PHB producing strains which based their lifecycle on waste gasses but also for highly productive species as the aerobic *Azotobacter vinelandii*.

Into aerobic species fed by sugar, the gas transfer rate became an investigation instrument for identifying the PHB production trend. And, using *A. vinelandii* OP, the presence of an opposite relation between an increase in biomass accumulation and a reduced PHB production under growing gas transfer rate was established. Thus, the optimal PHB volumetric productivity in *A. vinelandii* OP came out at a k_La value of 100 h^{-1} with a final Q_{PHB} of 0.51 g L^{-1} h^{-1}.

Finally, an experimental campaign dedicated to the purification of the biopolymer with the application of the green-based dimethyl carbonate was explored. The dimethyl carbonate was tested avoiding cell disruption pre-treatment steps, and the influence of extraction time on the final purification yield and purity of the extracted PHB were quantified for wet and dried biomass.

Tests demonstrated that DMC is a valid alternative to the standard chlorinated solvents application. It ensured at least a PHB extraction yield of 73% with 100% of purity independently from the extraction time and biomass pre-treatment.

Different routes for closing the gap between our knowledge and the mechanisms applied by nature to recycle carbon were traced by this work. On the base of gas-based fermentation technology, results outlined the importance of CO_2 as an indirect substrate for enhancing PHB production. However, the limitations caused by sole CO feeding suggests the development of other fermentation strategies, as the application of high-density fermentations, for instance. Besides, once reached a high PHB yield, further investigation should address a PHB biosynthesis coming from the recycling of industrial or household wastes. In this way, a decrease in the production costs of PHB process could be feasible, allowing to enter PHB into a wider and more sustainable production.

Abbreviations

μ	Specific growth rate
CBB	Calvin-Benson-Bahassam cycle
CODH	Carbon monoxide dehydrogenase
DMC	Dimethyl carbonate
DOT	Dissolved oxygen tension
k_La	Gas mass transfer constant
k_m	Michaelis-Menten constant
NPCM	Non-polymer cell mass
OCR	Oxygen Consumption rate
OD_{660}	Optical density at 660 nm
OTR	Oxygen Transfer Rate
pCO	CO partial pressure
PHA	Poly-hydroxyalkanoate
PHB	Poly-3-hydroxyalanoate
PHV	Poly-3-hydroxyvalerate
Q_{PHB}	PHB Columetric Productivity
SCR	Substrate consumption rate
$Y_{PHB/S}$	PHB yield on substrate
$Y_{X/S}$	Biomass yield on substrate
η	Kolmogorov's scale

Appendix

Schematic bioreactor set-up for CO-based fermentation

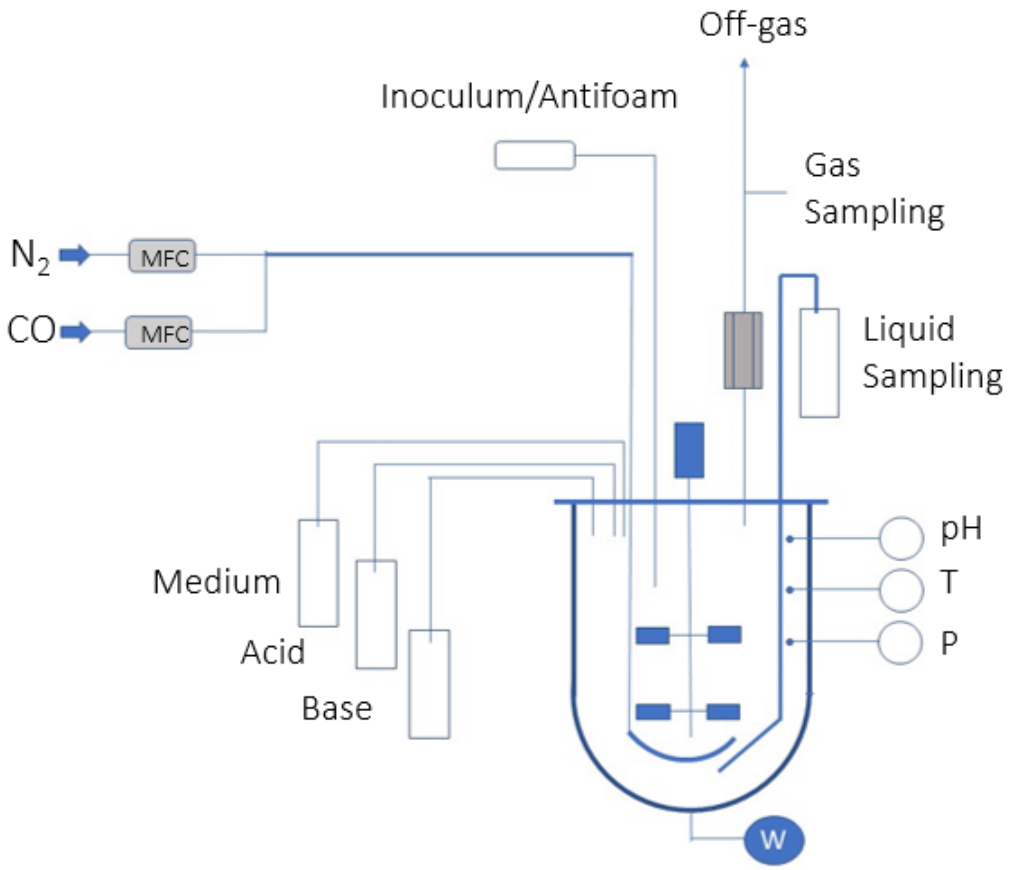

Figure A. Schematic bioreactor set-up designed for the investigation of the effects of pressure in the CO-based fermentation of *R. rubrum*.

Figure A reports the scheme of the reactor designed for set-up a CO-based fermentation under pressure. This instrument, designed for reaching a maximum operating pressure of 10 atm, was equipped with pumps, probes, piping, valves, flow controls devises and fittings able to work within the desired medium-high pressure.

The 2L stainless steel vessel was equipped with a motor based on the magnetic coupling for the internal stirring ensured by Rushton impellers. The reactor was provided with a heating jacket allowing a temperature variation between -35 and 300 °C, that not only maintained the desired temperature during the fermentation but also guaranteed an *in situ* sterilization.

The equipment was connected to external vessels for automatic feeding of liquids, like the fermentation medium, acids and base solutions, which were equipped with HPLC pumps able to operate within the desired pressure.

A suitable inoculum port was supplied for seeding the vessel under sterile conditions. While for the sampling of headspace gas or liquids, two dedicated lines were provided.

During the process pH, pressure, and temperature (pH, T, and P, respectively in Figure A) were monitored and recorded using suitable sensor devices. As well as, dedicated mass flow controllers (MFC in Figure A) for CO and N_2 and an off-gas line were constantly monitored. Therefore, fermentations were followed by a process control software.

For the cleaning of the reactor, a waste valve was added at the bottom of the vessel and a complete vessel emptying was ensured.

Burk's medium

Recipe of final concentration

Burk's medium		
	Reagent	**Final concentration** (g/L)
1	Sucrose	30
	K_2HPO_4	0.66
	$KH_2\ PO_4$	0.16
2	$CaSO_4 \cdot 2H_2O$	0.056
3	$MgSO_4 \cdot 7H_2O$	0.2
	$Na_2MoO_4 \cdot 2H_2O$	0.0029
	$FeSO_4 \cdot 7H_2O$	0.027
	NaCl	0.2

The recipe for the preparation of the Burk's medium is composed by three main parts, here presented by the numbers 1,2 and 3, which have to be sterilized separately for preventing caramelization of the phosphates with the sugar or precipitations.

Take care that the salts solution is prepared with a concentration of 100X:

Salt solution	
Reagent	($g\ L^{-1}$)
$MgSO_4 \cdot 7H_2O$	20
$Na_2MoO_4 \cdot 2H_2O$	0.29
$FeSO_4 \cdot 7H_2O$	2.7
NaCl	20

RRNCO Medium

RRNCO medium	
Reagent	g L^{-1}
$MgSO_4$ x $7H_2O$	0.25
$CaCl_2$ x $2H_2O$	0.132
NH_4Cl	1
MOPS	2.1
Yeast extract	1

Once mixed the listed reagents, the solution is added with 20µM $NiCl_2$ and by 10 mL of a chelated-iron solution.

Chelated Iron-Molybdenum Solution	
Reagent	(g L^{-1})
H_3BO_3	0.28
Na_2EDTA	2
Ferric citrate	0.4
Na_2MoO_4	0.1

After that, it is ready to be autoclaved.

Before starting the fermentation, the medium should be added by the following reagent previously separately sterilized: 2 µg L^{-1} biotin, 12.5 mM $NaHCO_3$, 9.5 mM Buffer Phosphate. The final pH should be around 7-7.2